Institute of Oceanology
Polish Academy of Sciences (IOPAN)

in collaboration with

International Environmental Doctoral School
University of Silesia in Katowice

Effects of Microplastic Pollution on Structure and Functioning of Pelagic Microbial Food Webs

Doctoral Thesis

Uroosa

PhD Candidate

This thesis was prepared under the supervision of

Dr. hab. Katarzyna Piwosz, prof. MIR-PIB

and

Dr. hab. Jozef Wiktor, prof. IO PAN

The research leading to this PhD thesis was conducted at

Department of Fisheries Oceanography and Marine Ecology
National Marine Fisheries Research Institute
Gdynia

Poland, 2026

Title: Effects of Microplastic Pollution on Structure and Functioning of Pelagic Microbial Food Webs

PhD Candidate: Uroosa

Supervisors: Dr. hab. Katarzyna Piwosz, prof. MIR-PIB

Dr.hab. Jozef Wiktor, prof. IO PAN

Wpływ zanieczyszczenia mikroplastikiem na strukturę i funkcjonowanie pelagicznych mikrobiologicznych sieci troficznych

Doktorantka: Uroosa

Promotorzy: Dr hab. Katarzyna Piwosz, prof. MIR-PIB

Dr hab. Józef Wiktor, prof. IO PAN

Oświadczenie Autora

Niniejszym oświadczam, że rozprawa doktorska stanowi wynik mojej oryginalnej pracy badawczej prowadzonej pod opieką dr hab. Katarzyny Piwosz, prof. MIR-PIB. Wszystkie badania przedstawione w niniejszej rozprawie zostały wykonane przeze mnie jako pierwszego autora i głównego wykonawcę. Byłam odpowiedzialna za realizację eksperymentów, analizę danych, interpretację wyników oraz przygotowanie manuskryptów wchodzących w skład rozprawy.

Żadna część niniejszej rozprawy nie zawiera wyników badań, których głównym autorem była inna osoba. Wszelkie wkłady współautorów i współpracowników zostały odpowiednio uwzględnione i opisane.

Oświadczam ponadto, że niniejsza rozprawa nie była wcześniej przedłożona, w całości ani w części, w celu uzyskania jakiegokolwiek stopnia lub tytułu naukowego.

Imię i nazwisko: UROOSA

Podpis: UROOSA

This thesis is part of the project based PhD program at the Institute of Oceanology Polish Academy of Sciences, conducted in collaboration with the International Environmental Doctoral School, University of Silesia Katowice. The research component of this work was conducted at Department of Fisheries Oceanography and Marine Ecology in National Marine Fisheries Research Institute, Gdynia.

Financial Support

This work was funded by the National Science Centre, Poland, project no. 2021/42/E/NZ8/00163 awarded to dr .hab. Katarzyna Piwosz, prof. MIR-PIB.

Acknowledgments

I dedicate this achievement to my mother, whose unconditional love, unwavering support, and belief in me have been my anchor throughout this journey.

I am deeply grateful to my supervisor, Dr. Katarzyna Piwosz, for her continuous guidance, encouragement, and invaluable mentorship throughout this research. Her profound scientific insight, patience, and constructive feedback not only shaped this thesis but also helped me grow immensely as an independent researcher.

I would also like to extend my sincere thanks to my colleagues, Sohrab Khan, Aleksandar Stanojković, Marcin Białowąs, Magdalena Jakubowska-Lehrmann, Barbara Urban-Malinga, and Cristian Villena Alemany, for their practical assistance and insightful advice.

Special thanks go to Ms. Regina Terlecka, Ms. Ksenia Pazdro, and Ms. Zuzanna Goik for their seamless administrative support and, above all, for their kindness and encouragement during challenging moments.

To my friends, Sohaib Khan, Shahzaib Khan, and Mahima Pai: thank you for being my emotional rock during this PhD. Your presence ensured I never felt alone in this process.

Thank you all for sharing this journey with me. This milestone belongs to all of you.

Abstrakt

Mikroplastik stał się permanentnym zanieczyszczeniem w ekosystemie morskim, jednak jego wpływ na organizmy znajdujące się u podstaw pelagicznych sieci troficznych pozostaje nadal niewystarczająco zbadany. Plastikowe śmieci ulegają fragmentacji na coraz mniejsze cząstki, osiągając nawet rozmiary bakterii czy innych mikroorganizmów stanowiących podstawę pokarmową w środowisku morskim. Nakładanie się zakresów wielkości ma istotne znaczenie ekologiczne, ponieważ mikroplastiki o rozmiarach zbliżonych do bakterii mogą funkcjonować nie tylko jako zanieczyszczenia obecne w toni wodnej, lecz również jako cząstki fizycznie napotykane przez bakterie i heterotroficzne wiciowce nanoplanktonowe (HNFs, heterotrophic nanoflagellates), odgrywające kluczową rolę w transferze energii i obiegu składników odżywczych w mikrobiologicznych sieciach troficznych. Nadal istnieją jednak dwie zasadnicze luki badawcze: niewielkie mikroplastiki są trudne do wiarygodnego wykrywania, a ich wpływ na naturalne zbiorowiska mikroorganizmów pozostaje słabo poznany.

Celem niniejszej rozprawy było zbadanie wpływu mikroplastików o rozmiarach zbliżonych do bakterii na strukturę i funkcjonowanie pelagicznych mikrobiologicznych sieci troficznych w strefie przybrzeżnej Morza Bałtyckiego. Praca łączy rozwój metod analitycznych z eksperymentami prowadzonymi na poziomie całych zbiorowisk mikroorganizmów, integrując zagadnienia detekcji cząstek, liczebności mikroorganizmów, respiracji, składu gatunkowego oraz interakcji troficznych pomiędzy bakteriami a heterotroficznymi wiciowcami nanoplanktonowymi. W pierwszym badaniu opracowano i zoptymalizowano protokół wykrywania cząstek mikroplastiku o średnicy równej lub mniejszej niż 2 µm za pomocą barwienia czerwienią Nilu (Nile Red). Zoptymalizowana metoda zapewniała silną i powtarzalną fluorescencję dla polistyrenowych cząstek o średnicy 1 i 2 µm oraz polietylenowych cząstek o średnicy 2 µm, podczas gdy kontrole nieorganiczne i utrwalony materiał biologiczny nie generowały sygnałów o porównywalnej intesynwności. Dodatkowo

utrwalanie próbek formaliną poprawiało jakość sygnału bez utraty selektywności metody, co wskazuje na możliwość jej stosowania w analizie zakonserwowanych próbek morskich oraz potencjalną użyteczność w laboratoriach o ograniczonym dostępie do bardziej kosztownych technik spektroskopowych.

Drugie badanie dotyczyło zależnego od stężenia wpływu polistyrenowych cząstek o średnicy 1,1 μm na naturalne zbiorowiska mikroorganizmów Morza Bałtyckiego. Jako kontrolę dla fizycznej obecności cząstek o rozmiarach odpowiadających potencjalnej ofierze pokarmowej zastosowano szklane cząstki o tej samej średnicy. Wraz ze wzrostem stężenia cząstek obserwowano spadek liczebności i tempa wzrostu wiciowców nanoplanktonowych, a podobne reakcje w wariantach z polistyrenem i szkłem wskazywały, że efekt ten był przede wszystkim wynikiem fizycznych zakłóceń procesu żerowania, a nie toksyczności specyficznej dla danego polimeru. Nie wykazano natomiast wpływu na liczebność bakterii oraz tempo respiracji. Sugeruje to, że ograniczenie wzrostu wiciowców nanoplanktonowych nie wynikało wyłącznie ze zmniejszonej dostępności pokarmu. Wyniki te wskazują, że cząstki o rozmiarach bakterii mogą zaburzać funkcjonowanie bakteriożernych wiciowców ze względu na ich niską wartość odżywczą lub też jako fizyczne czynniki zakłócające wydajność żerowania.

W trzecim badaniu rozszerzono to podejście poprzez porównanie wpływu cząstek polistyrenu, polietylenu oraz szkła stosowanych w podobnych stężeniach i zakresie wielkości odpowiadającym bakteriom. Celem eksperymentu było określenie, czy rodzaj polimeru wywołuje odrębną odpowiedź na poziomie zbiorowisk mikroorganizmów wykraczające poza ogólny efekt fizycznej obecności zawieszonych cząstek. Łącząc pomiary liczebności organizmów, respiracji oraz analizy molekularne, oceniono, czy bakterie i mikroorganizmy eukariotyczne reagują odmiennie na obecność różnych cząstek plastikowych i obojętnych. Uzyskane wyniki wskazują, że odpowiedź zbiorowisk tych organizmów zależy od kontekstu środowiskowego, a zmiany w składzie mogły zachodzić nawet w sytuacjach, gdy całkowita

liczebność i aktywność mikroorganizmów wykazywały jedynie słabe, niekierunkowe reakcje na zastosowane warianty eksperymentalne.

Podsumowując, przeprowadzone badania wskazują, że mikroplastiki o rozmiarach zbliżonych do bakterii należy postrzegać zarówno jako istotny cel analiz środowiskowych, jak i jako cząstki ekologicznie aktywne, zdolne do modyfikowania interakcji zachodzących w zbiorowiskach mikroorganizmów. Ich oddziaływanie może wynikać zarówno ze specyficznych właściwości poszczególnych polimerów, jak i z samej obecności licznych cząstek o niskiej wartości odżywczej w zakresie wielkości naturalnej ofiary bakteryjnej. Poprzez połączenie rozwoju metod detekcji z doświadczeniami na naturalnych zbiorowiskach mikroorganizmów z Morza Bałtyckiego, niniejsza rozprawa wnosi wkład w mechanistyczne zrozumienie sposobu, w jaki małe cząstki mikroplastiku mogą wpływać na interakcje pomiędzy bakteriami i heterotroficznymi wiciowcami nanoplanktonowymi, skład zbiorowisk mikroorganizmów oraz przepływ węgla i energii w pelagicznych mikrobiologicznych sieciach troficznych.

Słowa kluczowe: mikroplastiki; cząstki o rozmiarach bakterii; czerwień Nilu (Nile Red); heterotroficzne wiciowce nanoplanktonowe (HNFs); mikrobiologiczna sieć troficzna; Morze Bałtyckie; polistyren; polietylen.

Abstract

Microplastic pollution has become a persistent pressure in marine ecosystems, yet its effects at the base of pelagic food webs remain insufficiently understood. As larger plastic items fragment, they generate increasingly small particles that can overlap in size with bacteria and other microbial prey. This size overlap is ecologically important because bacteria-sized microplastics may not only be toxic contaminants in the water column, but also physical particles encountered by bacteria and heterotrophic nanoflagellates (HNFs), the key organisms responsible for energy transfer and nutrient cycling in microbial food webs. However, two major gaps remain: small microplastics are difficult to detect reliably, and their effects on natural microbial communities are still poorly resolved.

This thesis investigated how bacteria-sized microplastics affect the structure and functioning of pelagic microbial food webs in the coastal Baltic Sea. It combines methodological development with whole-community experiments to connect particle detection, microbial abundance, respiration, community composition, and trophic interactions between bacteria and HNFs. The first study developed and optimized a Nile Red staining protocol for the detection of small microplastics, with particular emphasis on particles at or below 2 micrometres. The optimized protocol produced strong and consistent fluorescence for 1 and 2 micrometre polystyrene particles and 2 micrometre polyethylene particles, while inorganic controls and fixed biological material did not produce comparable signals. Formalin fixation further improved signal quality without reducing selectivity, showing that the method can be applied to preserved marine samples and may be useful for laboratories with limited access to more expensive spectroscopic techniques.

The second study examined the concentration-dependent effects of 1.1 micrometre polystyrene particles on natural Baltic microbial communities, using glass spheres as an inert control for the physical presence of prey-sized particles. HNFs growth declined with increasing particle

concentration, and similar responses in polystyrene and glass treatments indicated that the effect was mainly driven by physical interference rather than polymer-specific toxicity. Bacterial abundance and respiration were comparatively less affected, suggesting that reduced HNFs growth was not simply caused by prey limitation. These findings show that bacteria-sized particles can disrupt microbial grazers by acting as non-nutritive prey analogues or physical interferents in the feeding environment.

The third study extended this approach by comparing the effects of polystyrene, polyethylene, and glass particles at similar bacteria-sized concentrations. This experiment tested whether polymer identity produced distinguishable microbial responses beyond the general physical effect of suspended particles. By combining abundance measurements and molecular community analyses, the study evaluated whether bacterial and eukaryotic microbial communities responded differently to plastic and inert particles. The results indicated that no distinct changes in microbial community composition were observed.

Together, these studies demonstrated that bacteria-sized microplastics should be considered both as analytical targets and as ecological particles capable of modifying microbial interactions. Their effects may arise through polymer-specific properties, but also through the physical presence of abundant, non-nutritive particles within the bacterial prey-size range. By linking detection methods with experimental microbial ecology, this thesis contributes to a mechanistic understanding of how small microplastics may alter bacteria-HNFs interactions, microbial community structure, and the transfer of carbon and energy through pelagic microbial food webs.

Keywords: microplastics; bacteria-sized particles; Nile Red; heterotrophic nanoflagellates; microbial food web; Baltic Sea; polystyrene; polyethylene

Table of Contents

Introduction

Introduction

Plastic pollution has become one of the defining environmental pressures of the modern ocean. Since large-scale production began in the mid-twentieth century, plastics have shifted from useful and durable materials to persistent contaminants that enter terrestrial, freshwater, coastal, and open-ocean ecosystems. Global plastic production reached 430.9 million tonnes in 2024, according to preliminary data from PlasticsEurope (PlasticsEurope, 2025). It is projected to exceed 600 million tonnes by 2050 (Cornwall, 2021). Global analyses of plastic production and waste fate show that only a minor fraction of all plastic waste has been recycled or incinerated, whereas the majority has accumulated in landfills or the natural environment (Geyer et al., 2017). Annual inputs of plastic waste into the ocean are also substantial, with land-based sources alone estimated to contribute millions of tonnes per year (Jambeck et al., 2015).

Because plastics are resistant to biodegradation, they can persist for decades to centuries while fragmenting into progressively smaller particles, including microplastics (MPs) and nanoplastics (MacLeod et al., 2021; Dawson et al., 2018; Khoaele et al., 2023). These particles are now recognized as ubiquitous contaminants in marine ecosystems worldwide. They have been detected in large ocean gyres, including the Pacific, Atlantic, and Indian Oceans (Law and Thompson, 2014; Eriksen et al., 2013; Cozar et al., 2017; Reddy et al., 2006), as well as in polar regions, near the equator, around densely populated coasts and remote islands, and from beaches to the deep sea (Yang et al., 2021).

1.1 Plastic Pollution as a Global Marine Problem and in the Baltic Sea

Marine plastics occur across a wide size range, from large floating debris to microscopic particles. Early observations of plastic particles on the Sargasso Sea surface already showed that the open ocean was receiving persistent synthetic debris (Carpenter and Smith, 1972). More recent surveys

and modelling have demonstrated major accumulation zones, such as the Great Pacific Garbage Patch, where plastics persist in surface waters and become fragmented into smaller particles over time (Lebreton et al., 2018).

The Baltic Sea is especially relevant in this context because it is a semi-enclosed, densely used, and relatively shallow sea with restricted water exchange. Such conditions can enhance the residence time of contaminants and increase the likelihood that plastic particles interact with planktonic organisms. Surface-water monitoring in the eastern Baltic Sea has reported widespread microplastic occurrence and spatial-temporal variability, supporting the view that Baltic microbial and planktonic communities are chronically exposed to plastic particles (Mishra et al., 2022).

In addition, the Baltic region is densely populated and highly industrialized, with approximately 85 million people living within its drainage basin, where intensive urbanization, industrial activities, maritime transport, tourism, fisheries, and agricultural runoff substantially contribute to the introduction of plastic waste into the marine environment (Graca et al., 2017). Recent studies have identified multiple sources of microplastics in the Baltic Sea, including wastewater treatment plant effluents, synthetic textile fibers, tire wear particles, fishing gear degradation, shipping activities, and urban stormwater runoff (Eerkes-Medrano et al., 2015). Although wastewater treatment plants are capable of removing a significant proportion of microplastics, considerable quantities of microscopic particles still enter aquatic ecosystems because of incomplete filtration processes. Synthetic microfibers released during domestic laundering have become one of the dominant forms of microplastics detected in Baltic Sea waters, while fishing and shipping activities contribute to the release of ropes, nets, paint particles, and plastic fragments into the marine ecosystem (Graca et al., 2017). Microplastics have been detected throughout the Baltic Sea environment, including surface waters, water columns, sediments, beaches, and marine organisms,

with their distribution strongly influenced by hydrodynamic conditions, salinity gradients, and water stratification processes characteristic of the Baltic Sea (Uurasjärvi et al., 2020). Research has demonstrated that microplastics can accumulate not only at the sea surface but also within stratified water layers and bottom sediments, which function as long-term sinks for plastic particles. Coastal and urbanized areas generally show higher concentrations of microplastics because of their proximity to pollution sources. Furthermore, microplastics can adsorb and transport hazardous pollutants such as persistent organic pollutants (POPs), heavy metals, and polycyclic aromatic hydrocarbons (PAHs), thereby increasing toxicological risks within marine food chains (Gewert et al., 2017). Since the Baltic Sea ecosystem is already affected by eutrophication, hypoxia, overfishing, and chemical contamination, microplastic pollution represents an additional environmental stressor that may further compromise ecosystem stability and biodiversity. Despite increasing scientific attention, the assessment of microplastic pollution in the Baltic Sea remains challenging because of methodological inconsistencies among studies, including differences in sampling techniques, particle size ranges, analytical procedures, and reporting units, which often limit direct comparison of results (Eerkes-Medrano et al., 2015).

1.2 From Large to Bacteria-Sized Particles

Most environmental microplastic studies have historically focused on particles collected by nets or sieves with mesh sizes designed for larger planktonic material (Lindeque et al., 2020). This approach has generated valuable data, but it strongly biases observations toward larger particles. Comparisons of sampling methods show that grab samples and smaller mesh sizes can recover much higher particle concentrations than conventional neuston tows, indicating that small particles are frequently underestimated (Barrows et al., 2017; Lindeque et al., 2020). The implication is

straightforward: the smaller the target particle size, the more incomplete abundance estimates become.

This sampling bias matters because fragmentation increases particle number as plastic items break into smaller pieces. Even if total plastic mass remains similar, the ecological interface between plastic and organisms changes dramatically as surface area and particle number increase. Small fragments may remain suspended, be transported through the water column, or become available to organisms that cannot ingest larger particles. Observational work on buoyant plastics indicates that wind-driven mixing and water-column processes can distribute plastic particles below the immediate surface layer, increasing the potential exposure of pelagic organisms (Kukulka et al., 2012; Reisser et al., 2015). Recent measurements of nanoplastics across the North Atlantic further suggest that the smallest plastic fraction may be widespread throughout the water column (ten Hietbrink et al., 2025).

Microplastics are typically defined as particles ranging from 1 micrometre to 5 mm in size, of either primary or secondary manufacturing origin (Frias and Nash, 2019). Plankton-sized microplastics have already been reported in shelf waters, supporting the idea that plastic particles can occur in the same physical space and size spectrum as natural planktonic food items (Di Mauro et al., 2017). Once plastic particles approach bacterial size, they are no longer simply pollutants suspended in water; they can become potential prey analogues, physical interferents, or non-nutritive particles encountered by microbial grazers.

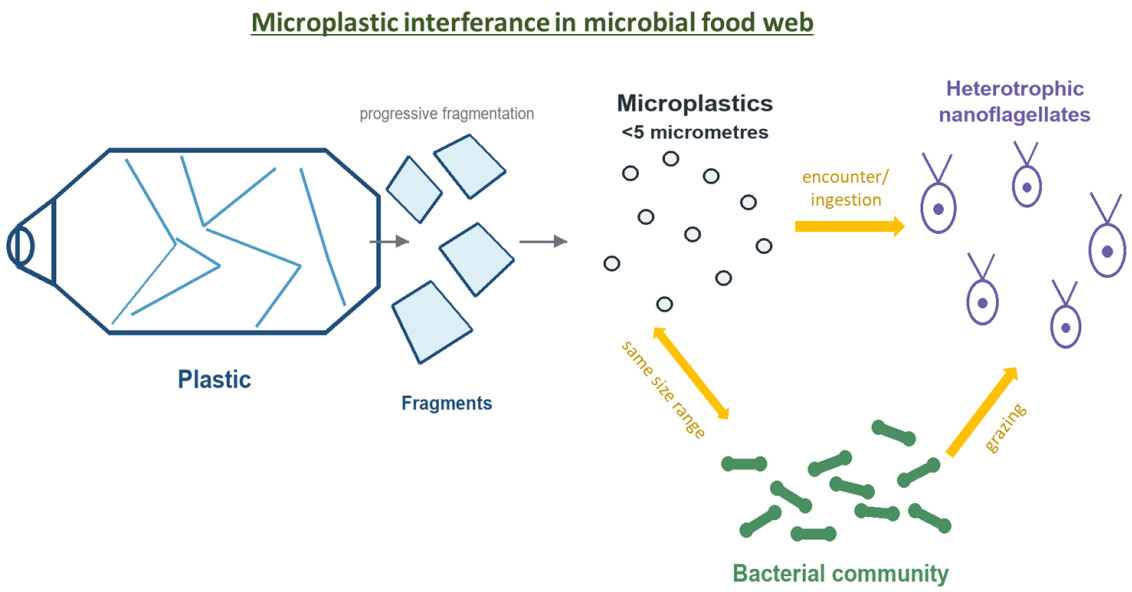

Figure 1. Bacteria-sized microplastic interference in the microbial food web. Plastic debris fragments into microplastics smaller than 5 micrometres, which overlap with bacterial prey size and may interact with bacteria and heterotrophic nanoflagellates, potentially affecting grazing interactions and microbial food-web functioning.

1.3 Methodological Challenge: Detecting Small Microplastics

The ecological importance of small microplastics cannot be evaluated without reliable detection methods. This is one of the central methodological challenges in microplastic research. Spectroscopic techniques such as Fourier-transform infrared spectroscopy and Raman spectroscopy provide chemical identification of polymers and are often treated as reference methods. However, their application to very small particles can be limited by cost, instrument availability, sample preparation requirements, acquisition time, spectral interference, and decreasing sensitivity at small particle sizes. These constraints are especially important for routine analyses of environmental samples and for laboratories with limited resources.

Fluorescence-based approaches using Nile Red have emerged as practical alternatives for screening microplastics because Nile Red preferentially stains hydrophobic polymer matrices and allows rapid visualization under fluorescence microscopy. The method has been applied to the identification and quantification of microplastics in controlled and environmental samples (Shim et al., 2016; Erni-Cassola et al., 2017; Maes et al., 2017). Further method development has incorporated automated image analysis, flow cytometry, and machine-learning classification to increase throughput and reduce subjectivity (Prata et al., 2019; Kaile et al., 2020; Meyers et al., 2022). Nevertheless, many existing protocols were developed for particles larger than the smallest bacteria-sized fraction, leaving a methodological gap for particles close to 1-2 micrometres.

Our optimized protocol (explained in Chapter 1) showed strong and consistent fluorescence for 1 and 2 micrometre polystyrene and 2 micrometre polyethylene particles, while inorganic controls and fixed biological material did not produce comparable signals (Uroosa and Piwosz, 2026).

Reliable detection of bacteria-sized microplastics is therefore not only a methodological problem, but also a prerequisite for understanding their ecological relevance. Once particles enter the same size range as bacterial prey, they may interact directly with the organisms and processes that structure pelagic microbial food webs.

1.4 Pelagic Microbial Food Webs and Why They Matter

Pelagic microbial food webs are central to the functioning of aquatic ecosystems. The microbial loop concept established that dissolved organic matter released by phytoplankton and other sources can be taken up by heterotrophic bacteria, which are then consumed by protists and transferred to larger planktonic consumers (Azam et al., 1983). This pathway redirects carbon and nutrients that would otherwise be inaccessible to metazoan grazers and links dissolved organic matter to higher trophic levels. In many aquatic environments, a substantial fraction of primary production can pass

through microbial pathways, making microbial food webs essential components of carbon and nutrient cycling (Fouilland and Mostajir, 2010).

Heterotrophic nanoflagellates are particularly important in this process. They are among the main grazers of bacteria and small microbial prey, and their feeding activity influences bacterial abundance, bacterial community composition, nutrient regeneration, and carbon transfer. In coastal Baltic waters, planktonic nanoflagellates show strong seasonal dynamics and diverse trophic roles, including bacterivory and mixotrophy (Piwosz and Pernthaler, 2010). More recent observations from the Baltic Proper further support the ecological importance and taxonomic diversity of heterotrophic nanoflagellates in regional microbial food webs (Piwosz et al., 2025, Khan et al., 2025).

Microbial grazing is not a simple bulk process in which all particles of the same size are equivalent. Feeding by phagotrophic zooflagellates depends on hydrodynamic forces, surface interactions, prey size, prey motility and grazer behaviour (Monger and Landry, 1990).

Food quality is another key factor. Bacterial prey differ in their nutritional value, digestibility, morphology, and susceptibility to grazing. Experimental work has shown that heterotrophic flagellate communities can respond differently to bacterial food quality that affects HNFs' growth and community structure (Simek et al., 2013). If natural bacterial prey already vary in quality, and if protists respond to such variation, then non-nutritive plastic particles of bacterial size may alter feeding efficiency, growth rates, and community composition even in the absence of acute chemical toxicity.

1.5 Direct Effects on Bacteria and Heterotrophic Nanoflagellates

Microplastics can affect bacteria both as suspended particles and as surfaces that modify the local chemical and physical environment. Bacteria are among the first organisms to encounter small plastic particles in seawater, and their responses can include attachment, biofilm formation, changes in extracellular polymeric substances, altered metabolism, and shifts in community composition (Montoya et al., 2024). Some studies have reported direct toxicity of polystyrene nano- and microplastics to marine bacteria, including growth inhibition, oxidative stress, and changes in nitrogen-transformation processes under high exposure levels (Sun et al., 2018). Other studies have shown that polystyrene particles can alter microbial community balance and predicted function in surrounding seawater (Ye et al., 2021), while community experiments reported weak or context-dependent responses to conventional and biodegradable microplastics (Lora et al., 2024). This mixed evidence is important because it suggests that bacterial responses are not controlled by polymer identity alone, but by particle size, concentration, exposure time, surface properties, associated organic matter, and the composition of the resident microbial community.

Bacterial responses are central to pelagic food-web functioning because they are not an isolated endpoint in the system. They are prey for heterotrophic nanoflagellates (HNFs) and other protists, and changes in bacterial abundance, cell size, physiology, or taxonomic composition alter the amount and quality of food available to protistan grazers (Rodríguez-Martínez et al., 2022). HNFs are major bacterial consumers in aquatic systems, thus they are responsible for transferring bacterial carbon toward larger protists and metazoan food webs (Azam et al. 1983). Their grazing also regulates bacterial population size and can shape bacterial community composition through selective removal of more vulnerable prey (Ivanković et al., 2023). Therefore, any microplastic-

driven change in bacterial communities has the potential to affect HNFs growth, community composition, and carbon transfer through the microbial loop.

The relationship between bacteria and HNFs is strongly influenced by prey quality. HNFs respond not only to the number of bacterial cells present; they also respond to bacterial identity, digestibility, morphology, and nutritional value (Rodríguez-Martínez et al., 2022, Ivanković et al., 2023) . Experimental work has shown that distinct bacterial strains can support different flagellate growth responses and can restructure natural HNFs communities (Simek et al., 2013). This matters for microplastic pollution because small plastic particles may affect the bacteria-HNFs link through at least two routes. First, microplastics may change the bacterial prey field by altering bacterial activity or community composition. Second, bacteria-sized microplastics may enter the same encounter and ingestion pathway as bacterial prey while providing little or no nutritional value.

For HNFs, the size overlap between bacteria and the smallest microplastics is particularly important. Feeding by nanoflagellates depends on microscale hydrodynamics, surface interactions, and prey-particle encounter processes (Monger and Landry, 1990). Plastic microspheres and fluorescently labelled particles have long been used as analogues in grazing studies, demonstrating that protists can capture and ingest particles in the bacterial size range (Tranvik et al., 1989). However, ingestion does not mean that all particles are equivalent as food. Studies of bacterivorous nanoflagellates show that inert particles can be ingested but may be processed, retained, or egested differently from living bacteria, and that these responses vary among taxa (Boenigk et al., 2001). Thus, microplastics may behave as misleading prey: they are physically available to grazers but nutritionally poor.

This creates several possible mechanisms by which microplastics can affect HNFs communities. At high particle concentrations, plastic particles may reduce effective encounter rates between HNFs and bacterial prey by increasing the number of non-food particles in the feeding environment. If some HNFs taxa are better able to reject or rapidly egest inert particles, while others ingest and retain them, microplastics could also shift HNFs community composition. In this way, the same exposure can have both functional consequences, such as reduced growth or carbon transfer, and structural consequences, such as changes in the relative abundance of HNFs lineages.

1.6 Polymer Type, Microbial Community Composition, and Functional Potential

In addition to particle size and concentration, polymer type can influence how microplastics interact with microorganisms. Polystyrene (PS) and polyethylene (PE) are both common plastic polymers, but they differ in density, hydrophobicity, surface properties, ageing behaviour, and potential additive or oligomer profiles (Salehi et al., 2024). These material differences can affect microbial attachment, biofilm formation, sorption of organic compounds, and the way particles interact with bacterial cells and protistan grazers (Fulfer and Menden-Deuer, 2021). At the same time, polymer effects are difficult to separate from general particle effects, because any abundant, prey-sized, non-nutritive particle can alter the physical environment in which bacteria and heterotrophic nanoflagellates interact.

Published plastisphere studies show that plastic particles are not biologically neutral surfaces. Microbial assemblages on plastic debris can differ from those in surrounding seawater, and may include heterotrophic bacteria, phototrophs, predators, symbionts, and potential pathogens (Zettler et al., 2013). In marine colonization experiments, substrate type, season, and geography influenced the composition of microbial communities growing on plastic debris, indicating that both material properties and environmental context shape microbial responses (Oberbeckmann et al., 2016). In

the North and Baltic Seas, potentially pathogenic *Vibrio* spp. were detected on polyethylene, polypropylene, and polystyrene particles, further demonstrating that polymer particles can act as selective microbial habitats (Kirstein et al., 2016).

Microplastics can also affect free-living bacterial communities in the surrounding water. Exposure to PS particles has been associated with microbial dysbiosis and functional shifts in seawater communities, suggesting that particle presence can modify bacterial community structure beyond the particle surface itself (Ye et al., 2021). However, the strength and direction of these effects are not always consistent. For example, experiments comparing conventional and biodegradable microplastics reported only weak effects on some marine microbial communities (Lora et al., 2024). Such contrasting results indicate that bacterial responses to microplastics are context dependent and may vary with polymer type, particle size, particle concentration, exposure time, and the initial composition of the microbial community.

Responses of bacterial communities to microplastic presence are important because bacteria form the prey base for heterotrophic nanoflagellates. As discussed above, HNFs are selective grazers; they respond to prey size, digestibility, morphology, physiology, and taxonomic identity. Experimental evidence shows that differences in bacterial food quality can alter the growth and composition of flagellate communities (Obiol et al., 2023). Therefore, if PS or PE particles shift bacterial community composition or functional traits, they may indirectly influence HNFs communities by changing the quality of available prey. This pathway is especially relevant in pelagic microbial food webs, where bacterial growth and protistan grazing are tightly coupled (Rodríguez-Martínez et al., 2022).

The few available studies on protistan ingestion of microplastics support this concern. Microplastics can be ingested by microzooplankton and may affect microbial-loop interactions

(Geng et al., 2021). Heterotrophic dinoflagellates exposed to polystyrene microspheres showed reduced grazing and growth in some cases, indicating that prey-sized plastic particles can interfere with protistan feeding processes (Fulfer and Menden-Deuer, 2021). Ciliated protozoa have also been shown to take up nano- and small microplastics under experimental conditions (Nalecz-Jawecki et al., 2021). Together, these studies suggest that microplastic particles can enter protistan food vacuoles and affect microbial grazers through particle ingestion, prey dilution, or handling costs.

The available literature therefore points to a key unresolved question: are microbial responses to bacteria-sized microplastics mainly driven by polymer-specific properties, or by the physical presence of non-nutritive particles in the bacterial prey-size range? PS and PE may differ in how they interact with bacteria and protists, but inert particles of similar size can also interfere with microbial grazing simply by increasing the number of non-food particles in suspension.

1.7 Aims and Findings

The overall aim of this thesis was to investigate how bacteria-sized microplastics affect the structure and functioning of pelagic microbial food webs. Structure is considered here in terms of microbial community composition and the abundance of key trophic groups, especially bacteria and heterotrophic nanoflagellates. Functioning is considered in terms of microbial growth, respiration, community functional potential, and possible consequences for bacteria-HNF carbon transfer. The thesis combines methodological development with whole-community manipulation experiments to connect particle detection, microbial ecology and food-web functioning.

Specifically, the thesis addresses three connected objectives. First, it develops and evaluates a Nile Red-based protocol for detecting small microplastics in preserved samples, with emphasis on particles at or below 2 micrometres. Second, it tests whether bacteria-sized polystyrene particles

affect bacteria-HNF dynamics in a concentration-dependent manner, and whether these effects are better explained by polymer identity or by the physical presence of prey-sized particles. Third, it compares polystyrene and polyethylene to examine whether different particle types produce distinct effects on bacterial abundance, HNFs abundance, respiration, microbial community composition and potential functional change in bacterial community using metagenomics .

Together, these studies contribute to a mechanistic understanding of microplastic pollution at the base of pelagic food webs. They ask whether the smallest plastic particles represent not only contaminants to be detected, but also ecological particles that can alter microbial interactions. By focusing on bacteria-sized particles, natural Baltic Sea microbial communities, and the balance between polymer-specific and physical-particle effects, this thesis addresses an emerging question in marine microbial ecology: how will persistent, non-nutritive particles affect the flow of carbon and energy through the microbial food web?

Study	Core question	Role in the thesis argument
Chapter 1	How can small microplastics at or below 2 micrometres be reliably detected in preserved samples?	Provides the methodological foundation for studying the smallest, ecologically relevant plastic particles.
Chapter 2	Do bacteria-sized polystyrene particles affect bacteria-HNFs food-web structure and function, and are effects caused by polymer chemistry or particle presence?	Tests concentration-dependent effects and distinguishes physical-particle effects from polystyrene-specific effects using glass controls.
Chapter 3	Do polystyrene and polyethylene particles differ in their effects on bacteria, HNFs, respiration, and microbial community composition compared with inert glass particles?	Extends the mechanism by comparing polymer type at a bacteria:particle ratio of approximately 1:1.

Chapter I

frontiers in Marine Science

TYPE Methods
PUBLISHED 23 April 2026
DOI 10.3389/fmars.2026.1818345

OPEN ACCESS

EDITED BY
Xinchen Gu,
South China University of Technology, China

REVIEWED BY
Surya Singh,
ICMR-National Institute for Research in Environmental Health, India
Delor Jestin Florence,
Université Clermont Auvergne, France

*CORRESPONDENCE
Uroosa
uroosayousafzai1@gmail.com

RECEIVED 26 February 2026
REVISED 25 March 2026
ACCEPTED 01 April 2026
PUBLISHED 23 April 2026

CITATION
Uroosa and Piwosz K (2026) Systematic optimization of Nile Red staining parameters for the reliable detection of microplastics ≤ 2 µm.
Front. Mar. Sci. 13:1818345.
doi: 10.3389/fmars.2026.1818345

Systematic optimization of Nile Red staining parameters for the reliable detection of microplastics ≤ 2 µm

Uroosa[1,2]* and Kasia Piwosz[1]

[1]National Marine Fisheries Research Institute, Gdynia, Poland, [2]Institute of Oceanology, Polish Academy of Sciences, Sopot, Poland

Detection of small microplastics remains analytically challenging despite their growing environmental and biological relevance. Nile Red staining offers an affordable alternative to state-of-the-art techniques, such as Fourier-transform infrared (FTIR) and Raman spectroscopy. However, it has been mainly used for larger particles, typically > 20 µm. This study presents an optimized filtration and Nile Red (NR) staining protocol for the reliable detection of microplastics smaller than 5 µm, with particular emphasis on particles ≤ 2 µm. Filtration conditions and staining parameters, including NR concentration and incubation time, were systematically optimized to enhance detection efficiency. Under these conditions, polystyrene (1 µm and 2 µm) and polyethylene (2 µm) particles exhibited strong and consistent signals, while inorganic controls showed no staining, confirming dye specificity. Formalin fixation, a treatment often applied to conserve environmental samples for later analyses, further improved particle brightness and signal-to-noise ratio without compromising selectivity, as no fluorescence was observed in fixed biological material. Our simple, cost-effective protocol can be applied in labs with lower resources and also for initial screening of particles in natural samples for further analyses.

KEYWORDS
formalin fixed samples, microplastics, Nile red, optimization, staining protocol

1 Introduction

Plastic debris, both large and small, has become pervasive across the world's oceans. Under the influence of ultraviolet (UV) radiation, oxidation, and physical abrasion, plastic items gradually fragment into ever-smaller pieces of microplastic less than 5 mm in size (Barnes et al., 2009; Cole et al., 2011). Using Raman spectroscopy for polymer identification, previous studies have reported the detection of microplastic particles in surface water samples, under analytical conditions capable of resolving particles below 20 µm. The average detectable particle size is approximately 2.5 µm for polystyrene (Christina et al., 2020).

The accurate detection and quantification of microplastics (MPs) in environmental samples remains a significant analytical challenge, particularly for particles at the lower end of the microplastic size range (Duis and Coors, 2016; Meyers et al., 2022). Although gold-standard techniques such as Fourier-transform infrared (FTIR) and Raman spectroscopy offer definitive chemical characterization, and thus identification of plastic polymers, their implementation is hindered by high capital costs and the requirement for specialized

technical expertise (Araujo et al., 2018; Cowger et al., 2024). These barriers often render such methods impractical for resource-limited settings. Furthermore, spectroscopic analysis is frequently constrained by protracted acquisition times and a significant loss of sensitivity for particles below 20 µm, complicating the detection of the smallest microplastic fractions (Primpke et al., 2017).

In response, fluorescence staining using the lipophilic dye Nile Red (NR) has emerged as a rapid, cost-effective alternative. NR preferentially partitions into the hydrophobic plastic matrix, producing a strong, visible fluorescence signal under blue-light excitation (Maes et al., 2017; Bakir et al., 2020; de Witte et al., 2022). This approach is particularly valuable for visualizing and quantifying micron-sized particles (Erni-Cassola et al., 2017), for which NR staining offers significant advantages in accessibility and practicality compared to other analyses.

A significant challenge in marine research is the preservation of samples collected during field expeditions. Chemical fixatives, specifically formalin, are routinely used to stabilize marine biological cultures and environmental samples to prevent metabolic degradation (Leischner et al., 2010). The role of formalin fixation, a staple in marine histology, remains under-addressed in the context of microplastic quantification. There is a critical need to understand how these preservation methods influence the optical properties of target plastics and whether they can hinder the process or be leveraged to improve detection limits.

The successful application of NR staining to small particles requires careful optimization, because this technique was used for particles above 5 µm sized particles till now. This study presents an optimized Nile Red staining protocol tailored for marine environmental samples, focusing on microparticles with a minimum size of 1 µm. By systematically evaluating the interaction between formalin fixation and staining parameters, we demonstrate a significant enhancement in fluorescence intensity of MPs particles. Crucially, our findings show that this enhancement does not compromise selectivity against marine organic backgrounds. This protocol provides a robust, standardized tool for monitoring the smallest, most elusive microplastics in preserved marine samples.

2 Materials and methods

2.1 Materials and data collection

The protocol was optimized on unstained, clear microspheres made of commonly used plastic polymers: Polystyrene (PS) beads of size 1.1 µm (Polyscience, CAT. 19518500) and 2 µm (CAT. 1981415), and Polyethylene (PE) beads of size 1-4 µm (Cospheric, CPMS-0.96). Silica microspheres of similar size (1-4 µm, Bangs Laboratories, Inc., CAT. SSD5000) were used as a negative control. The dry powder was resuspended in sterile MilliQ water one week before the experiment to a final concentration of PS 1.1 µm (4.43×10^9 PS spheres mL^{-1}), PS 2µm (5.34×10^9 PS spheres mL^{-1}), PE 2µm (5.54×10^9 PS spheres mL^{-1}), and Silica (2.47×10^{10} Silica spheres mL^{-1}). For the optimization procedure, we used 50µl of microsphere solutions in 100 mL of MQ water.

Nile Red fluorescent dye (AURA, Cat-PA-03-2331-T, Poland) was dissolved in HPLC-grade Acetone (POCH, Poland, Cat-102480151) to form a stock solution of 200 µg mL^{-1}, which was stored in the dark to prevent photodegradation. We used 100% acetone because NR is more soluble in it compared to other solvents (Shim et al., 2016). Working solution of 100 µg mL^{-1} was later prepared by adding 1ml of 100% acetone.

Formaldehyde solution 40% (CHEMPUR, CAT. 114321733, Poland) was used to fix samples. Formalin-fixed samples, including algal culture (*Chlamydomonas vectensis*, strain no. NIVA-CHL 174, The Norwegian Culture Collection of Algae: NORCCA), were stained to assess the effect of the NR stain on organic matter as well as the effect of the presence of formalin on microplastics NR staining method.

A filtration setup with multiple filtration units and a pump was used for filtration. PBS-T buffer (1 mL of Triton-X from sigma-aldrich in 1 L of 1× PBS) was used for cleaning the filtration unit vessels to prevent particle carry-over of microspheres between samples. PBS-T was also used to rinse the sample bottle after filtration to remove any remaining residues; the rinse solution could then be filtered to ensure complete particle recovery for plastic quantification. The filters were then air-dried and mounted on microscopic slides using immersion oil (Figure 1).

Epifluorescence microscopy was used for quantification and visualization of microplastic spheres, employing a Nikon Eclipse 80i upright microscope at 1000× magnification.

2.2 Solvent test and filter selection

A trial was conducted to determine the acetone concentration that would be compatible with the protocol and cause no damage to the filters. Two types of filters that retain particles on their surface: Whatman Polycarbonate Nuclepore Filter (PC; 25 mm, 0.2 µm pore size) and Anodisc (Whatman Anodisc alumina membrane filters, 0.2 µm pore size) were tested. A few drops of stock solution with 100% acetone were added directly onto the filter. However, this damaged the PC filter, and further processing was not possible. Therefore, a series of acetone concentrations (10%, 5%, 2%, and 1%) was assessed to evaluate their effects on both PC and Anodisc filters. The incubation times were 2 h, 4 h, 24 h, and 48 h.

2.3 Incubation and NR stain optimization

Samples were incubated with Nile Red for 2 h, 4 h, 24 h, and 48 h, as the previously reported incubation time of 15 min (Camilleri et al., 2025) was not sufficient for staining smaller plastic particles, which showed no detectable fluorescence under those conditions. Nile Red concentrations of 1 µg mL^{-1} (Leischner et al., 2010) and 10 µg mL^{-1}, which have previously been recommended (Primpke et al., 2017), were tested to determine an appropriate concentration for staining smaller microplastics (< 5 µm). The optimized protocol was further tested on samples with particle-free formalin added to a final concentration of 0.4%.

3 Results

Polycarbonate (PC) filters were damaged when exposed to the two highest concentrations of acetone (100% and 10%) at all tested time points, including the shortest incubation period of 2 h.

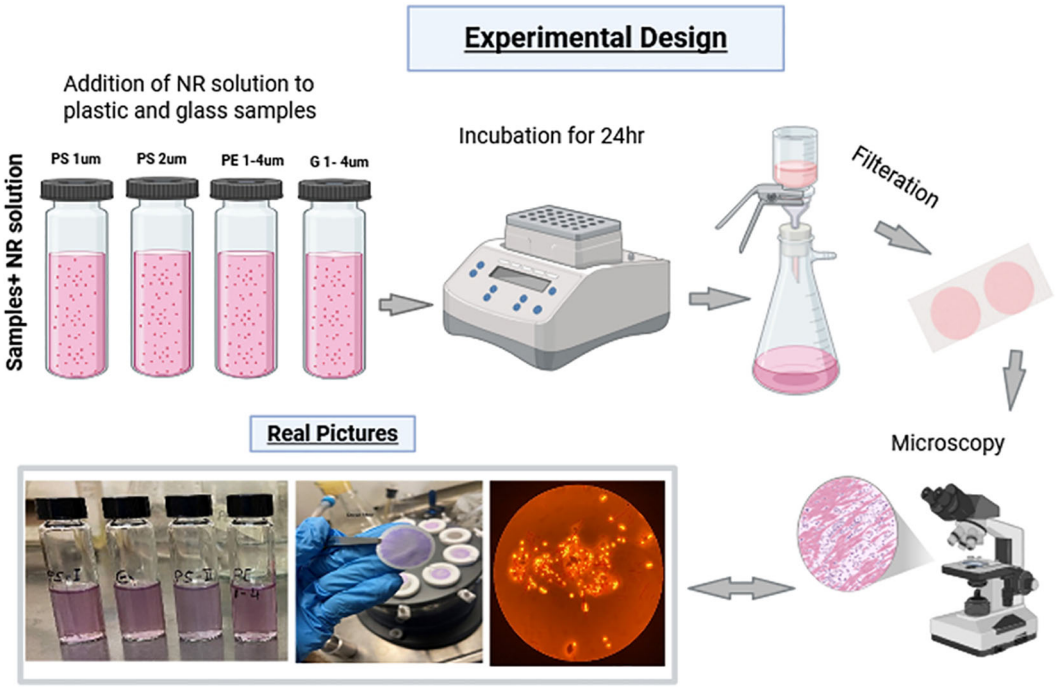

FIGURE 1
Experimental framework for optimizing Nile Red staining protocols including control (Glass) and plastic treatments of polystyrene (PS 1 µm, PS 2 µm) and polyethylene (PE 2 µm).

However, Anodisc filters showed no damage even at the highest concentration. Both PC and Anodisc filters demonstrated excellent compatibility with 5% diluted acetone following incubation for 2 h and 24 h, with no observable structural damage (Supplementary Figure 1). Although Anodisc filters exhibited superior solvent resistance compared to PC filters, optimization of the acetone concentration resulted in comparable performance between the two filter types.

Incubation time was evaluated at multiple time points (2 h, 4 h, 24 h, and 48 h) to determine an optimal balance between sufficient dye uptake and minimal background interference. Extending the incubation period to 24 h resulted in consistent and reproducible staining (Supplementary Figure 2) and was therefore selected for subsequent experiments. In contrast, incubation for 2 and 4 h showed no dye uptake by the plastic particles and no visible signal, whereas incubation for 48 h resulted in maximum background interference, which blocked the particle image (Supplementary Figure 2).

Initial staining attempts using 1 µg mL^{-1} Nile Red (final concentration in the samples) did not produce visible fluorescence signals for small polymer particles (1 µm and 2 µm). Increasing the final dye concentration to 10 µg mL^{-1} significantly enhanced fluorescence intensity and signal strength, enabling clear visualization and reliable identification of smaller microplastic particles. The final acetone concentration in stained samples was 5%, allowing application of PC filters, which is a much cheaper alternative. Polystyrene (PS) microspheres with sizes of 1 µm and 2 µm, and polyethylene (PE) particles with a size of 2 µm were readily detectable under an epifluorescence microscope (Figures 2A–C). In contrast, silica spheres used as negative controls showed no fluorescence signals (Figure 2D), confirming the specificity of the dye. Moreover, the addition of formalin markedly enhanced fluorescence intensity, producing brighter and more clearly defined particles that were easier to identify and quantify (Figures 2E, F). Formalin-fixed samples of the green algal culture were used to assess whether NR stains natural microorganisms, potentially obscuring microplastic detection. The trial concluded that cultures that were fixed only with formalin remained easily detectable under standard imaging due to chlorophyll autofluorescence (Figure 2G), however no staining occurred in the cultures in the presence of the NR stain (Figure 2H). However, the. Lack of autofluorescence signals after the NR staining had been caused by acetone, which is routinely used for chlorophyll extraction as it effectively breaks down and solubilizes pigments.

Contamination control was identified as a critical factor in the analytical workflow. Standard cleaning procedure using only MilliQ water was insufficient, as residual plastic particles were detected both on PC and Anodisc filters upon subsequent filtration (Figure 3). To address this, after removal of the first filter, a new filter was inserted, and the vessel was cleaned with 10 mL of PBS-T, followed by 20 rinses with MilliQ water. This cleaning procedure was repeated between each subsequent filter, for a total of four cycles. All four filters were examined microscopically, and the fourth filter showed negligible residual contamination. This optimized cleaning protocol effectively eliminated carry-over contamination between samples, particularly when processing a large number of samples simultaneously.

The final recommended protocol is available as Supplementary File S1:

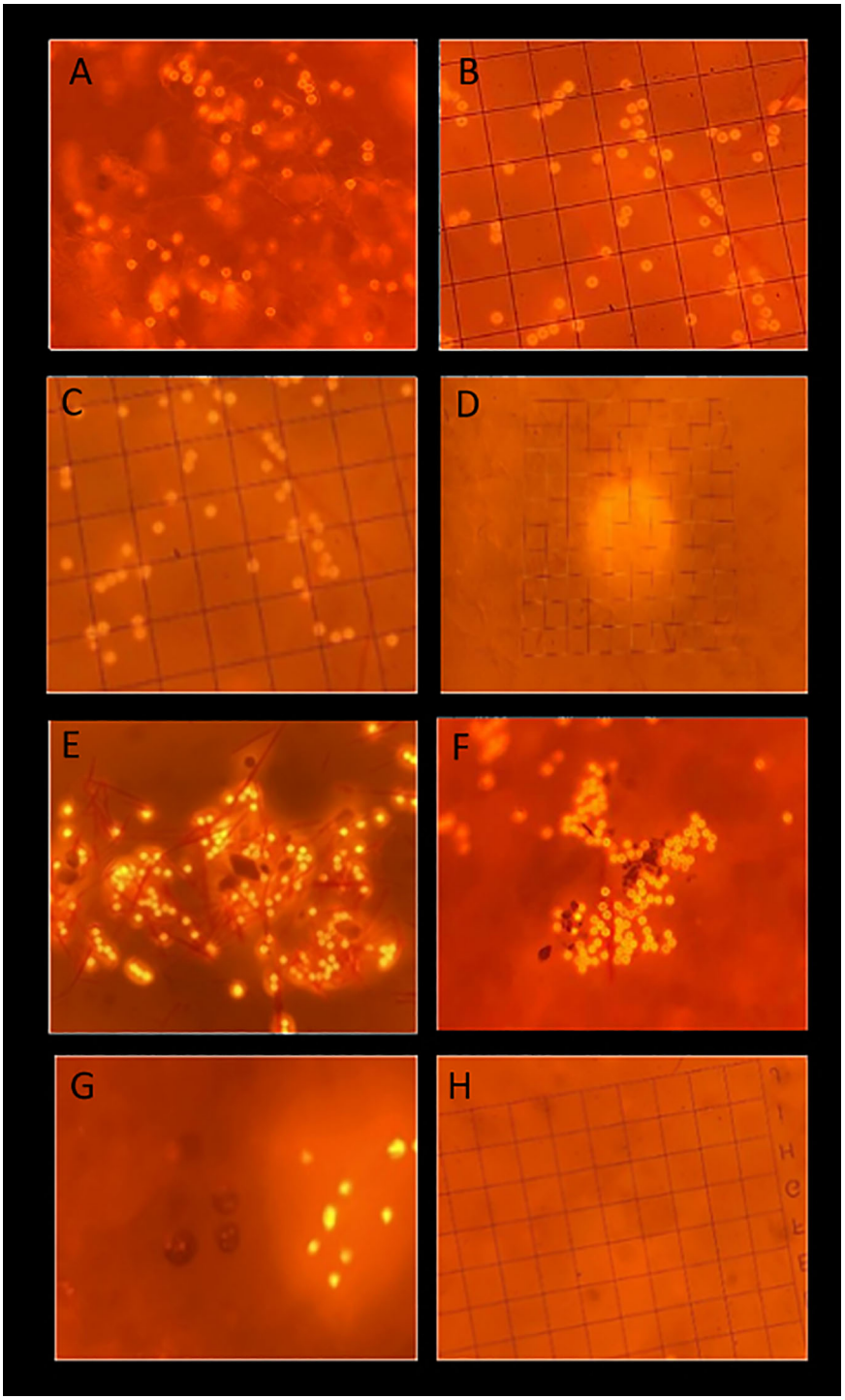

FIGURE 2
Validation and optimization of Nile Red (NR) staining for microplastic identification. **(A, B)** PS particles (1 µm and 2 µm, respectively) exhibiting fluorescence. **(C)** PE particles (2 µm) successfully stained and visualized. **(D)** Glass sphere negative control showing no dye uptake, confirming NR specificity. **(E, F)** Enhanced fluorescence intensity and particle definition following formalin fixation. **(G)** Visualization of cultures fixed with formalin without NR stain, showing clear detectability under standard imaging. **(H)** Lack of staining in cultures treated with NR alone.

4 Discussion

The present study demonstrates the effectiveness of an optimized filtration and Nile Red staining protocol for the detection of microplastics smaller than 5 µm, addressing a critical analytical challenge in microplastic research. Particles in this size range are increasingly recognized for their potential ecological and biological impacts (Zhi et al., 2025), yet they remain difficult to reliably detect due to methodological limitations. The filtration strategy applied here proved valuable for retaining and visualizing < 5 µm plastic particles, supporting its suitability for studies targeting small microplastics and, potentially, even nanoplastics (< 1µm).

A staining protocol developed here (Supplementary File S1, Figure 1) enables the visualization of micro and nanoparticles of size 2μm and 1 μm. After optimizing the incubation time and NR concentration, the staining results were highly effective, and clear microscopic images of stained plastic particles (PS 1 μm, PS 2 μm, and PE 2 μm) were obtained (Figures 2A–C). Optimization of the staining protocol was essential for achieving reliable detection of small plastic particles, as previously published protocols underperformed for such small microspheres (Leischner et al., 2010). By carefully adjusting Nile Red concentration and incubation time, strong and consistent fluorescence signals were obtained for both polystyrene and polyethylene particles. Insufficient dye concentrations or shorter incubation times are known to result in weak fluorescence, particularly for small particles with limited surface area (Kuruma et al., 2025). The optimized conditions used in this study enhanced particle visibility while maintaining staining specificity, enabling clear discrimination of plastic particles under fluorescence microscopy. These findings highlight the importance of protocol standardization when targeting small microplastics, as minor variations in staining parameters can substantially influence detection efficiency.

Increasing the final concentration of Nile Red (NR) stain led to a higher acetone concentration in the samples, which caused damage to the polycarbonate (PC) filters. Although optimization of the acetone concentration allowed the protocol to function properly for both filter types, there remains a risk that PC filters, being plastic, may become stained and contribute to increased background interference. In contrast, Anodisc filters are resistant to staining and generate less background interference, making them the preferred option.

The effect of chemical fixation on microplastic detection quality was evaluated. Formaldehyde fixation is widely used because it is cheap and the fixation is permanent (Leischner et al., 2010), therefore widely used to preserve environmental and biological samples by stabilizing morphology and preventing metabolic degradation. However, its influence on Nile Red staining efficiency for microplastics has not been systematically addressed. Our results demonstrate that, while Nile Red staining is effective without fixation, the presence of formalin enhances signal intensity, improving the signal-to-noise ratio and overall detection performance (Figures 2E, F). Importantly, this finding enables Nile Red staining of samples previously preserved for biological analyses, allowing microplastic detection from the same material. This integrated approach is particularly advantageous for large-scale laboratory studies, as it reduces additional sample handling and preparation time.

These observations support the assumption that during the staining process, the NR selectively targets and identifies only plastic particles within the sample matrix. Importantly, Nile Red did not stain biological material in fixed samples (Figure 2H), indicating that formalin fixation did not compromise staining selectivity (Maes et al., 2017). This finding supports the compatibility of Nile Red staining with commonly used fixation procedures and suggests that formalin may improve fluorescence outcomes when analyzing preserved environmental samples.

Long term exposure of plastic polymers to environmental conditions may cause changes in polymer particles surface chemistry, and thus the reactivity with NR. Unfortunately, we have no means to test our protocol on real environmental samples, as this would require a dedicated large-scale sampling. Thus, we tested our optimized protocol on marine water samples with added PS microspheres that had been stored for a year. The results were consistent, indicating no observable effect from changes in surface chemistry (Supplementary Figure 3).

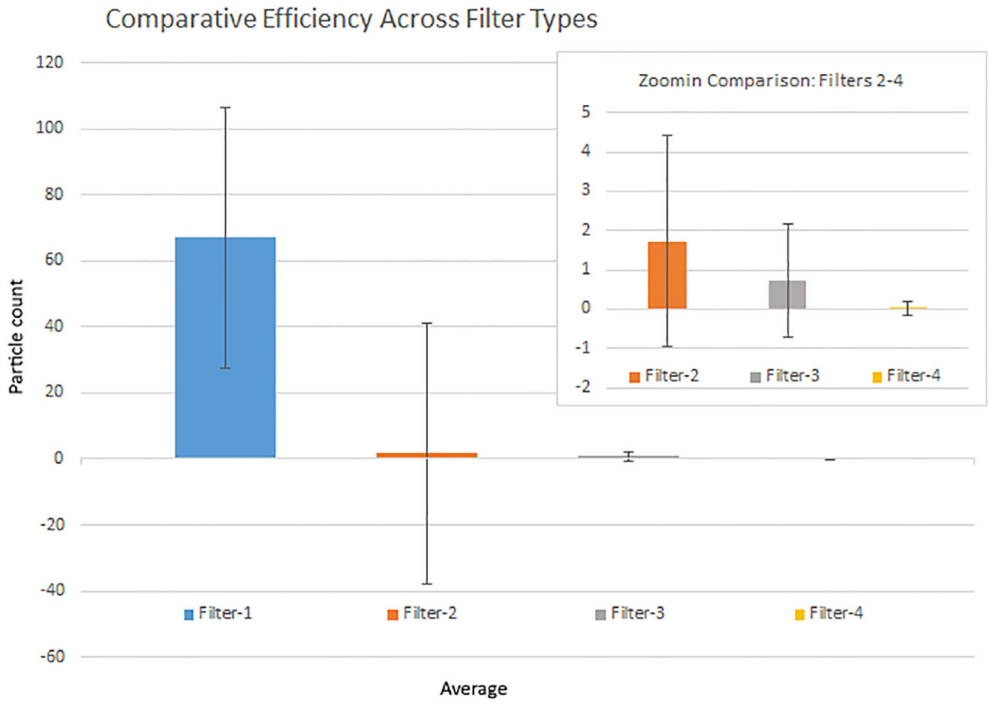

FIGURE 3
Efficiency of contamination control measures. Average particle counts across four sequential filtration stages. The marked reduction from Filter-1 (Avg=67.1) to Filter-4 (Avg=0.03) validates the effectiveness of the cleaning protocol in preventing cross-contamination between samples.

The main limitation of this study is that only microspheres from two polymer types at small particle sizes were tested. This was caused by the fact that microspheres of size < 4 μm made of other plastic polymers are not available commercially. This also applies to different shapes that could be a constraint for the proposed protocol.

This study advances the development of reliable methodologies for the detection of small microplastics by optimizing filtration, staining conditions, fixation compatibility, and contamination control. Still, further work may be needed to validate the method across a wider range of polymer types, shapes, and sizes, as well as in real environmental samples.

5 Conclusion

This study establishes an optimized filtration and Nile Red staining protocol for the reliable detection of microplastics smaller than 2 μm. Our optimized protocol enabled specific visualization of polystyrene and polyethylene particles while excluding inorganic and biological material. Importantly, formalin fixation enhanced fluorescence intensity without compromising staining selectivity, allowing microplastic detection in preserved samples. Together with rigorous contamination control, this approach provides a robust and practical framework for standardized detection of small microplastics in environmental and biological studies that offers an affordable alternative to state-of-the-art techniques, such as Fourier-transform infrared (FTIR) or Raman spectroscopy.

Data availability statement

The original contributions presented in the study are included in the article/Supplementary Material. Further inquiries can be directed to the corresponding author.

Author contributions

U: Conceptualization, Data curation, Formal Analysis, Investigation, Validation, Visualization, Writing – original draft. KP: Funding acquisition, Supervision, Writing – review & editing.

Funding

The author(s) declared that financial support was received for this work and/or its publication. National Science Centre, Poland, project no. 2021/42/E/NZ8/00163 awarded to KP.

Conflict of interest

The author(s) declared that this work was conducted in the absence of any commercial or financial relationships that could be construed as a potential conflict of interest.

Generative AI statement

The author(s) declared that generative AI was not used in the creation of this manuscript.

Any alternative text (alt text) provided alongside figures in this article has been generated by Frontiers with the support of artificial intelligence and reasonable efforts have been made to ensure accuracy, including review by the authors wherever possible. If you identify any issues, please contact us.

Publisher's note

Supplementary material

The Supplementary Material for this article can be found online at: https://www.frontiersin.org/articles/10.3389/fmars.2026.1818345/full#supplementary-material

References

Araujo, C. F., Nolasco, M. M., Ribeiro, A. M., and Ribeiro-Claro, P. J. (2018). Identification of microplastics using Raman spectroscopy: Latest developments and future prospects. *Water Res.* 142, 426–440. doi: 10.1016/j.watres.2018.05.060

Bakir, A., Desender, M., Wilkinson, T., van Hoytema, N., Amos, R., Airahui, S., et al. (2020). Occurrence and abundance of meso and microplastics in sediment, surface waters, and marine biota from the South Pacific region. *Mar. pollut. Bull.* 160, 111572. doi: 10.1016/j.marpolbul.2020.111572

Barnes, D. K., Galgani, F., Thompson, R. C., and Barlaz, M. (2009). Accumulation and fragmentation of plastic debris in global environments. *Philos. Trans. R. Soc Lond. B. Biol. Sci.* 364, 1985–1998. doi: 10.1098/rstb.2008.0205

Camilleri, J., Agius Anastasi, A., and Briffa, S. M. (2025). Detection, quantification, and characterisation of microplastics in maltese bottled water. *Microplastics* 4, 88. doi: 10.3390/microplastics4040088

Christina, R., Domna, G. K., and Nic Chormaic, S. (2020). In-situ analysis of small microplastics in coastal surface water samples of the subtropical island of Okinawa, Japan. doi: 10.48550/arXiv.2008.08259

Cole, M., Lindeque, P., Halsband, C., and Galloway, T. S. (2011). Microplastics as contaminants in the marine environment: A review. *Mar. pollut. Bull.* 62, 2588–2597. doi: 10.1016/j.marpolbul.2011.09.025

Cowger, W., Roscher, L., Jebens, H., Chamas, A., Maurer, B. D., Gehrke, L., et al. (2024). Generation of macro- and microplastic databases by high-throughput FTIR analysis with microplate readers. *Anal. Bioanal Chem.* 416, 1311–1320. doi: 10.1007/s00216-024-05127-w

de Witte, B., Catarino, A. I., Vandecasteele, L., Dekimpe, M., Meyers, N., Deloof, D., et al. (2022). Feasibility study on biomonitoring of microplastics in fish gastrointestinal tracts. *Front. Mar. Sci.* 8. doi: 10.3389/fmars.2021.794636

Duis, K., and Coors, A. (2016). Microplastics in the aquatic and terrestrial environment: sources (with a specific focus on personal care products), fate and effects. *Environ. Sci. Eur.* 28, 2. doi: 10.1186/s12302-015-0069-y

Erni-Cassola, G., Gibson, M. I., Thompson, R. C., and Christie-Oleza, J. A. (2017). Lost, but Found with Nile Red: A Novel Method for Detecting and Quantifying Small Microplastics (1 mm to 20 µm) in Environmental Samples. *Environ. Sci. Technol.* 51, 13641–13648. doi: 10.1021/acs.est.7b04512

Kuruma, Y., Sakurai, H., and Okuda, T. (2025). Highly efficient Nile red staining for the rapid quantification of microplastic number concentrations using flow cytometry. *Anal. Methods* 17, 9381. doi: 10.1039/D5AY01093D

Leischner, U., Schierloh, A., Zieglgänsberger, W., and Dodt, H. U. (2010). Formalin-induced fluorescence reveals cell shape and morphology in biological tissue samples. *PloS One* 5, e10391. doi: 10.1371/journal.pone.0010391

Maes, T., Jessop, R., Wellner, N., Haupt, K., and Mayes, A. G. (2017). A rapid-screening approach to detect and quantify microplastics based on fluorescent tagging with Nile Red. *Sci. Rep.* 7, 44501. doi: 10.1038/srep44501

Meyers, N., Catarino, A. I., Declercq, A. M., Brenan, A., Devriese, L., Vandegehuchte, M., et al. (2022). Microplastic detection and identification by Nile red staining: Towards a semi-automated, cost- and time-effective technique. *Sci. Total Environ.* 823, 153441. doi: 10.1016/j.scitotenv.2022.153441

Primpke, S., Lorenz, C., Rascher-Friesenhausen, R., and Gerdts, G. (2017). An automated approach for microplastics analysis using focal plane array (FPA) FTIR microscopy and image analysis. *Anal. Methods* 9, 1499–1511. doi: 10.1039/C6AY02476A

Shim, W. J., Song, Y. K., Hong, S. H., and Jang, M. (2016). Identification and quantification of microplastics using Nile Red staining. *Mar. pollut. Bull.* 113, 469–476. doi: 10.1016/j.marpolbul.2016.10.049

Zhi, L., Li, R., Li, Z., Su, Z., Chen, F., Qin, Q., et al. (2025). Micro/nanoplastics in aquatic ecosystems: Analytical challenges, ecological impacts, and mitigation strategies. *Environ. Chem. Ecotoxicol* 7. doi: 10.1016/j.enceco.2025.07.009

Supplementary Material

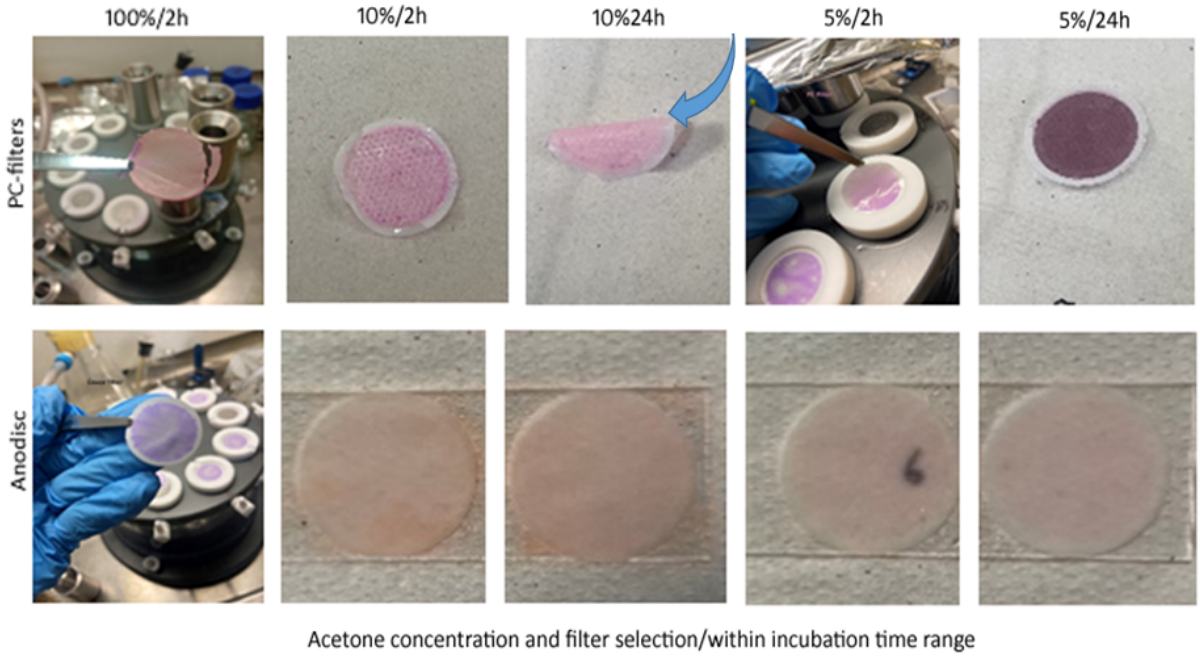

Supplementary Figure 1. Evaluation of filter compatibility and solvent resistance for Nile Red (NR) staining. Polycarbonate (PC) filters exhibited structural damage when exposed to 100% acetone and showed deformation at 10% acetone, particularly after 24 h incubation. In contrast, no visible structural damage was observed with 5% acetone at either 2 h or 24 h incubation. Anodisc alumina filters remained structurally intact across all tested acetone concentrations and incubation times.

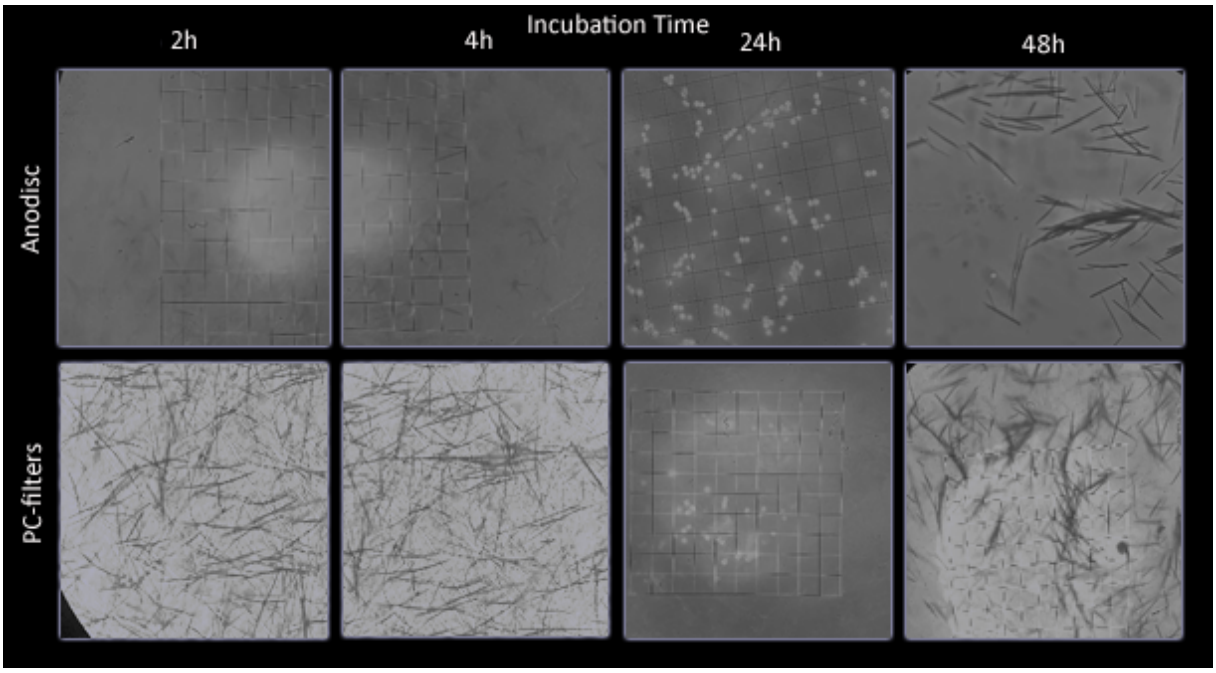

Supplementary Figure 2 In this figure incubation times of 2 h, 4 h, 24 h, and 48 h were evaluated to identify the optimal balance between dye uptake and background fluorescence. Shorter incubations (2 h and 4 h) produced weaker staining, whereas 48 h increased background signal. A 24 h incubation yielded consistent, reproducible fluorescence with minimal background and was therefore selected for subsequent experiments.

Supplementary File 1

Nile red protocol for microplastic detection

Consumables

1. 5 ml tubes (can be washed and reused)
2. 0.2 µm pore, diameter 25 mm, PC filters and/OR 0.2 µm pore, diameter 25 mm Anodisc, (Whatman Anodisc alumina membrane filters)
3. 1.2 µm MCE filters (support filters for PC)
4. Filtration tower
5. Pump
6. Nile Red
7. Microscopic slides
8. Cover glass 25x50-60 mm
9. Permanent markers for labelling
10. Paper towels

Solutions and reagents

1. 36-40% particle-free formalin, prefiltered through 0.2 µm filter
2. Nile red stock solution (conc. 200 µg mL^{-1})
   a. 1 ml of acetone (HPLC grade)
   b. 200 µg of nile red stain
   c. Mix, keep in dark etc

Preparation

1. Label 5 ml tubes
2. Add 50 µl of formalin into each tube (final concentration: 0.4%)
3. Prepare and label microscopic slides
4. Set up the filtration tower and the pump

Staining the samples

1. Take 4.45 ml of the plastic sample using 5 ml pipette and pour it into the labelled 5 ml tubes with formalin 50ul
2. Add 0.5 ml of Nile Red stock solution (final conc. 20 µl mL^{-1})
3. Mix by gently rotating the tube 10x
4. Incubate for 24 hours, at 60^0C in dark.

Filtration and preparing the slides

5. Add a few drops of MQ water onto the filtration plate and fix the support cellulose filter (for PC filteration)
6. Add a drop of MQ water onto the support filter and fix the 0.2 µm white PC filter. Make sure the shiny side of the filter is up
7. For Anodisc filters add a few drops of MQ water onto the filtration plate and fix the filter directly

8. Close the filtration tower. Take care not to disturb or move the filters
9. Add 2 ml of fresh MQ water
10. Add 5ml whole sample and filter it
11. Add 10 mL of PBS-T, followed by 20 rinses with MilliQ water. Repeat this procedure 4 times, to rinse the walls of the funnel
12. Gently remove the filtration funnel and slightly rise a filter on one side while the pump is ON
13. Switch off the pump
14. Remove the filter and let it air dry for 1-2 minutes in the dark on a paper towel

Preparing the slides (place two samples on one slide

15. Place a drop of emersion oil on a clean microscopic slide
16. Place a filter onto the drop.
17. Place 1 drop of emulsion on top of the filter and cover gently with a cover slip. Do not press
18. Keep the slides in the dark until they can be counted on the epifluorescent microscope

Chapter II

Concentration-Dependent Effects of Polystyrene Microplastics on Bacterial and Protistan Communities: Evidence for Physical Stressors

Uroosa[1,2], Sohrab Khan[1], Marcin Białowąs[1], Magdalena Jakubowska-Lehrmann[1], Barbara Urban-Malinga[1], Cristian Villena Alemany[3,4], Kasia Piwosz[1*].

1 National Marine Fisheries Research Institute, ul. Kołłątaja 1, 81-332 Gdynia, Poland.

2 Institute of Oceanology, Polish Academy of Sciences, Powstańców Warszawy 55, 81-712 Sopot, Poland

3 Institute of Microbiology of the Czech Academy of Sciences, Třeboň, 37901, Czechia.

4 Leibniz Institute of Freshwater Ecology and Inland Fisheries, Stechlin, Germany.

* Corresponding author: kpiwosz@mir.gdynia.pl

Abstract

Microplastics (MPs) are pervasive pollutants in marine ecosystems, yet their impacts on microbial food webs remain poorly understood. We investigated the effects of bacteria-sized (1.1 μm) polystyrene (PS) particles on heterotrophic nanoflagellates (HNFs) and their bacterial prey in a 5-day microcosm experiment with 24-hour sampling intervals. Treatments included three PS particle concentrations (low, medium, high), inert glass spheres at the same concentrations as a control for the physical effect of particles, and a particle-free control. HNF growth declined in a concentration-dependent manner, with comparable suppression in PS and glass treatments, indicating that the response was driven by physical interference. Bacterial abundance, respiration, and community composition were unaffected, excluding prey limitation as a mechanism for HNF decline. HNF community changes were driven by incubation time rather than particle type, with a decrease in the contribution of mixotrophic Haptophyta and an increase in heterotrophs, including the genus *Neobodo*. These findings demonstrate that the physical presence of micro-sized particles alone can impair HNFs' growth, potentially disrupting microbial-mediated carbon transfer and nutrient cycling. Our results underscore that particle pollution, even in the absence of chemical toxicity, can exert rapid and concentration-dependent effects on key microbial predators, highlighting a critical mechanism by which MPs may alter marine microbial ecosystem function.

Keywords

Microplastic, Polystyrene, Heterotrophic nanoflagellates, Plastic pollution, Microbial Community, Microbial food webs

1. Introduction

The annual global plastic production increases 10% per year since the 1950s (Hammer et al., 2012) and is predicted to reach 600 million tonnes by 2050 (Cornwall et al., 2021). Recent studies indicates that global plastic production reached 430.9 million tonnes in 2024, according to preliminary data from PlasticsEurope (PlasticsEurope, 2025). Around 0.5% of the world's plastic waste ends up in the oceans (Hannah, 2023), and consequently the influx of plastics into marine environments, both directly and via riverine inputs, is also rising, with an estimated 4.7 to 12.8 million tonnes of plastic entering the oceans each year (Agamuthu et al., 2019). Thus, microplastics pollution poses a widespread and enduring danger to the global environment, significantly influencing marine ecosystems (Sun et al., 2018, Viel et al., 2023). Microplastics pollution is notably severe in the Baltic Sea, with reported concentrations ranging from 0.07 to 3,300 particles per m^3 (Narloch et al., 2022), compared to 0.001 to 440 particles per m^3 in the Great Pacific Garbage Patch (Lebreton et al., 2018).

Although there is no universally accepted definition, microplastics (MPs) are generally described as plastic polymer particles ranging from 1 μm to 1 or 5 mm (Frias and Nash, 2019, Hartmann et al., 2019). They serve as ecological niches for microorganisms, enabling the spread of harmful pathogens (Bellas et al., 2016, Huang et al., 2021, Wright et al., 2020). For example, bacteria were found on polyethylene (PE), polypropylene (PP), and polystyrene (PS) particles in the North and Baltic Seas (Kirstein et al., 2016). Moreover, the bacteria-sized nanoplastics (< 1 μm) - the smallest particles that form the largest fraction of the marine plastic mass - were reported to be ubiquitous in the water column from the temperate to subtropical North Atlantic (Ten Hietbrink et al., 2025). It is predicted that their concentrations will increase as larger plastic particles degrade (Granek et al., 2020).

PS is the third most abundant plastic material by contribution to the carbon pool (9%, Stubbins et al. 2021) that has been found in the ocean already for over half a century (Carpenter and Smith, 1972). This thermoplastic polymer is known for its extreme resistance to biodegradation (Mor and Sivan, 2008). Thus, it poses persistent threats to marine organisms and disrupts ecological balance by interacting with marine contaminants (Okeke et al., 2022; Song et al., 2025). For instance, PS particles have been shown to cause cell aggregation, lower cellular chlorophyll concentrations, inhibit photosynthesis, and ultimately reduce the growth rate of various algal species (Zhang et al., 2017, Wu et al., 2019). These effects depend on the concentration of MPs and occur at levels exceeding those currently observed in the environment. Nonetheless, MPs can disrupt population regulation mechanisms by reducing nutrient availability or absorption and decreasing predator species populations (Prata et al.,2019). Protistan predators, such as copepods and the heterotrophic dinoflagellate *Oxyrrhis marina*, ingest PS particles at the expense of microalgae consumption (A ter Halle et al.,2016).

Microorganisms play a key role in the functioning of the aquatic ecosystem. It is estimated that up to 50% of primary production enters microbial food webs (Fouilland et al.,2010). Therefore, any changes in their functioning will profoundly impact the entire ecosystem. Effects of microplastics pollution have been intensively studied in aquatic animals (Sun et al., 2018, Naji et al., 2018, Provencher et al.,2018, Duncan et al., 2019, Hossain et al. 2019, Lusher et al., 2018, Urban-Malinga et al.,2022), while consequences for pelagic microbial communities composition and function still represent an important knowledge gap (Saborimanesh, 2026). It can be assumed that increasing concentrations of bacteria-sized MPs may have both direct and indirect effects on pelagic food webs. It is well known that bacterial grazers, such as ciliates and heterotrophic nanoflagellates (HNFs), ingest microplastics, and fluorescently labelled plastic microspheres have

been successfully used to estimate grazing rates on bacteria (Monger et al., 1990; Tranvik et al.,1989, Geng et al., 2021). However, MPs likely represent low-quality food for HNFs, catching and ingestion of which may lower their growth rates. Moreover, as MPs accumulate in the environment, HNFs will be faced with the increasing challenge of accurately discriminating between high-quality bacterial food and detrimental plastic pieces (Santos et al.,2021). These may further induce substantial changes at the base of the microbial food webs by affecting community composition, activity, and growth rates. However, this phenomenon has not yet been considered in the context of MPs pollution and its potential effect on key elements of the carbon cycle, specifically pelagic microbial food webs. Also, the ecosystem-level consequences of MPs-induced changes in microbial communities and trophic interactions remain poorly understood.

This study investigates the immediate effects of bacteria-sized polystyrene (PS) microspheres on the activity, growth, and community composition of bacteria and their predators, small (3–5 μm) HNFs. We hypothesize that MPs represent lower-quality food for HNFs than bacteria, thereby reducing their growth rates and altering community composition, with stronger effects at higher MP concentrations. To test this, we conducted a 5-day laboratory experiment with 24-hour sampling intervals using a natural microbial community from the coastal Baltic Sea. Changes in abundance were analyzed alongside 16S and 18S amplicon sequencing data to assess bacterial and eukaryotic community responses to PS microsphere exposure.

2. Materials and Methods

2.1 Experimental design

We used commercially available PS spheres from Polysciences (Polybeads microspheres, Cat. No. 19518-500) and glass spheres from Bangs Laboratories, Inc. (Silica microspheres, dry, Cat. No.

SSD40000) in the size range 1.1 µm. The dry powder was resuspended in sterile MilliQ water one week before the experiment to a final concentration of 4.43×10^{9} PS spheres ml^{-1} and 2.47×10^{10} glass spheres ml^{-1}.

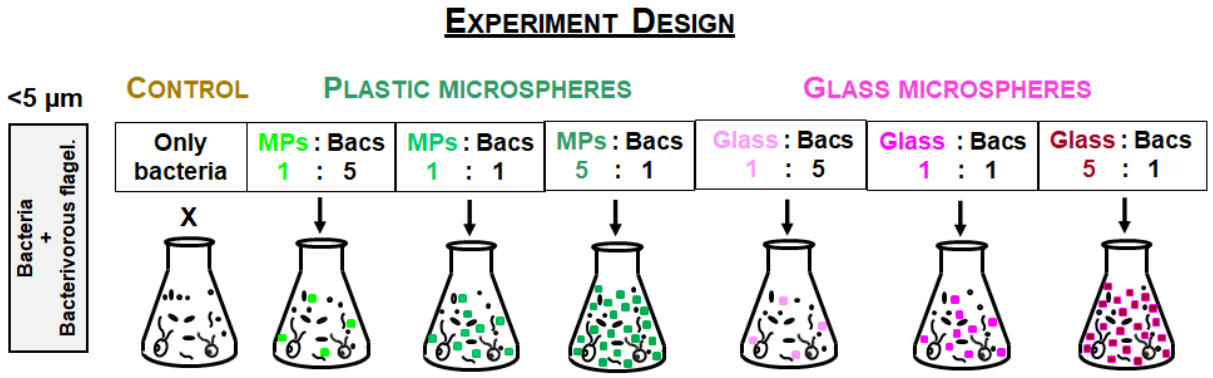

Figure 1: Schematic representation of the experimental design, including the control and treatment concentrations (1:5-Low, 1:1-Medium, and 5:1-High) of polystyrene (PS) and glass (G) microspheres used to assess their effects on microbial communities.

The experiment involved 7 treatments: two sphere types (PS and glass) and the control without any spheres (Fig.1). PS treatments included PS-Low (targeted PS:bacteria abundance ratio 1:5), PS-Medium (targeted PS:bacteria abundance ratio 1:1), and PS-High (targeted PS:bacteria abundance ratio 5:1). The same ratios were used for the glass treatments, which were used as a control for the physical effects of the presence of particles of the same size and their increased concentration: Glass-Low (targeted Glass:bacteria abundance ratio 1:5), Glass-Medium (targeted Glass:bacteria abundance ratio 1:1), Glass-High (targeted Glass:bacteria abundance ratio 5:1). All PS and Glass treatments were done in triplicates, while control was done in duplicates. The number

of PS and glass microspheres added to the experimental variants was calculated based on bacterial abundance in the prefiltered samples (Table 1), determined as described below.

Table 1. Abundance of bacteria in collected seawater, number of PS and glass particles added to experimental treatments, and final bacteria:particles ratios in the treatments. Number of cells or spheres per ml are the concentrations in the treatments at T0. Stock added is the volume of stock solutions added to triplicated bottles in each treatment. Stock solutions contained 4.43×10^{9} PS spheres ml^{-1} and 2.47×10^{10} glass spheres ml^{-1}.

PARTICLE TYPE	**LOW CONC.**	**MEDIUM CONC**	**HIGH CONC**
BACTERIA (CELLS ML^{-1})	3.26×10^{6}	3.26×10^{6}	3.26×10^{6}
PS STOCK ADDED (ML)	0.5	2.5	12
PS (SPHERES ML^{-1})	4.43×10^{5}	2.21×10^{6}	1.06×10^{7}
BACTERIA:PS RATIO	7.36:1	1.47:1	1:3.26
GLASS STOCK ADDED (ML)	0.1	0.5	2.5
GLASS (SPHERES ML^{-1})	4.95×10^{5}	2.47×10^{6}	1.24×10^{7}
BACTERIA:GLASS RATIO	6.59:1	1.32:1	1:3.80

2.2 Setting up the experiment

Two hundred liters of surface seawater were collected from a coastal station (54°31'05.2'' N; 18°33'21.5''E) in the Gulf of Gdańsk (southern Baltic Sea, Poland) into containers thoroughly cleaned with sanitizing detergent, 10% bleach, and MilliQ water, and rinsed three times with the sampled water. The water was prefiltered on-site through a 10 μm mesh plankton net and transported to the laboratory within 30 minutes. Further fractionation through 5 μm polycarbonate filters (diameter 142 mm, Millipore) was done using an autoclaved gravity filtration apparatus made of stainless steel (Sartorius) that was sterilized with boiling MilliQ water each time the filter was exchanged. One hundred twenty liters of filtered water were distributed into twenty 10-litre glass bottles (six liters per bottle). Afterwards, the bottles were closed with silica plugs and put into the water bath at *in situ* temperature (±15°C, room temperature). Bottles were incubated in the dark. The content of each bottle was continuously aerated to maintain water movement and prevent sedimentation of microspheres. The air was delivered via sterile 0.2 μm syringe filters and autoclaved aeration stones that were exchanged after each sampling.

The filtered water was used for the analysis of the total bacterial and HNFs abundance, as well as microbial community composition at time 0h, as described below. Subsequent samples were collected from the experimental bottles into sterile glass bottles under a fume hood every 24 h for a total time of 106 h. This time has been found optimal to measure microbial responses both at single species (Geng et al. 2021) and community level (Šimek et al., 2013).

2.3 Abundance of Bacteria and Heterotrophic Nanoflagellates

Three ml of water sampled for bacterial abundance was fixed with 150 μl of prefiltered 40% formalin (Final concentration: fc = 2%). The fixed samples were then filtered onto black-stained polycarbonate filters (PC; 25 mm, 0.2 μm) and stained with 4'-6-diamidino-2-phenylindole

(DAPI; 1 μg ml^{-1}). For HNF, 25 ml of sample water was fixed with neutral Lugol solution (fc = 1%), particle-free formalin (fc = 2%), and followed by decolorization with 3% $Na_2S_2O_3$ (Sherr BF et al., 1987). The fixed samples were then filtered onto black-stained polycarbonate filters (PC; 25 mm, 0.8 μm) that were then air-dried and stained with 4'-6-diamidino-2-phenylindole (DAPI; 1 μg ml^{-1})

The filters were analyzed at 1000× magnification using epifluorescence microscopy (Nikon upright microscope Eclipse 80i) equipped with Hg-lamp with UV/blue light filter for DAPI.

2.4 Control of contamination

We took necessary precautions to prevent any contamination during the experiment and analyses. Processes were performed under a fume hood when needed, to lessen cross-contamination, particularly to avoid the air-borne plastic particles. No plastic materials were used in the filtration set-up and other laboratory procedures. Working surfaces and necessary equipment were continually rinsed with MilliQ, followed by 70% alcohol and additionally decontamination solution (1% NaOCl, 1% NaOH, 1% detergent) in case of DNA extraction. In addition, the fume hood used for DNA extraction was sterilized using a UV lamp. To control for contamination during the sample collection and processing, blank controls consisting of filtered sterile MilliQ water were collected alongside the samples for DNA extraction. Although no DNA was detected, these blank controls were included in library preparation and sequencing, where amplification failed, confirming the absence of contamination during biomass collection and DNA extraction (Khan et al., 2025).

2.5 Respiration

20 ml water sampled from each replicate was collected at time 0 into calibrated 20 ml sensor vials with integrated optical sensor for temperature and oxygen (cat. no. TOVIAL20, PyroScience GmbH, Aachen, Germany) with fasten adapter ring (ADVIAL20T, PyroScience). In addition, three killed negative controls from the autoclaved Baltic Sea water were prepared to account for abiotic processes and control for contamination of the samples. Oxygen concentration and compensation temperature were measured using bare optical fibers (SPFIB-BARE, PyroScience) and the FireSting-O2 device (FSO2-C2, PyroScience) in the Pyro Workbench software (version V1.4.7.2305, PyroScience) every 24 hours during the whole experiment.

Raw data were imported into R software (version 4.4.1) for further analysis (R Core Team, 2024). Respiration rate in μM O_2 day^{-1} in each replicate was calculated from the slope of O_2 concentration (in μM) vs. time (Fig. S1), fitted with a linear regression (lm function). Differences in the respiration rate between the treatments were tested using Kruskall-Wallis test.

2.6 DNA sample collection, extraction, and sequencing

A liter of water was collected into sterile glass bottles. Two half-liter water samples were filtered onto mixed-cellulose-esters filters (47 mm, 0.2 μm, Millipore, Darmstadt, Germany), placed into sterile 2 ml cryotubes, flash-frozen in liquid nitrogen and stored at -80°C. DNA was extracted using our custom, optimized protocol combining the GeneMATRIX Soil DNA Purification Kit (Eurx, Gdansk, Poland) and GeneMAGNET PCR Clean-Up Beads (Eurx, Cat. ES3401). The extracted DNA samples were stored at -80°C. The quality and concentration of the extracted DNA were assessed with gel electrophoresis, NanoDrop One (Thermo Scientific), and QubitFlex Flourometer (Invitrogen, CAT.Q33327) using Qubit™ 1X dsDNA High Sensitivity (HS) Assay Kit.

Extracted DNA samples were sent to Novogene (Cambridge, UK) for sequencing on the NovaSeq platform (2x250 bp). The V3-V4 regions of 16S rRNA genes were amplified for bacterial community (Bolyen E et al., 2019; Fadeev Eduard et al., 2021), and the V6-V8 fragment of 18S rRNA gene was sequenced for eukaryotic community (Meike et al., 2022).

2.7 Sequence analysis

Demultiplexed sequence data underwent quality control and pre-processing using the DADA2 pipeline within the R environment, version 4.3.2 (Callahan BJ et al.,2016). The initial dataset comprised an average of 50,739 ± 3458 reads per sample for 16S and 55,590 ± 6179 reads per sample for 18S. These reads were then filtered and trimmed using the filterAndTrim function with parameters set to maxN = 0, maxEE = c(2,2), and truncQ = 2, as implemented in the DADA2 package (v1.12.1) within the R/Bioconductor framework. Amplicon sequence variants (ASVs) were then inferred, and chimeric sequences were removed using the 'consensus' method (Callahan BJ et al., 2017). The final dataset included an average of 47,615 ± 4364 reads per sample for 16S and 37,889 ± 6233 reads per sample for 18S.

Taxonomic assignment of the ASVs was carried out using the *assignTaxonomy* function in DADA2, leveraging curated, reference databases: SILVA version 138.1 for bacterial 16S rRNA gene sequences (Pruesse E et al.,2007, Quast C et al.,2012) and PR2 version 5.0.0 for 18S rRNA gene sequences (Guillou, et al. 2012). Community composition bar plots were generated using ggplot2 v3.4.3 (Ginestet C, 2011).

2.8 Data analysis

Amplicon data were analyzed using phyloseq v1.46.0 (McMurdie PJ et al.,2013). Non-eukaryotic/non-bacterial ASVs and those unclassified at subdivision level were filtered out, retaining only eukaryotic and bacterial data.

To account for differences in sequencing depth, samples were rarefied 1000 times to the read count 15050 using rrarify function in vegan package. This procedure removed 9 samples with less than 10000 reads. The resulting abundance tables were averaged to generate a representative abundance matrix. Taxa were aggregated at the genus level (using tax_glom) to facilitate diversity comparisons. Sequences unassigned at the genus level were grouped based on the phylogenetic analysis as described above. Final data was visualized using ggplot2 v3.4.3 (Ginestet C, 2011).

All multivariate statistical analyses were conducted using PRIMER (v7.1.17) software (Clarke and Gorley, 2015) along with the PERMANOVA+ add-on (v1.0.7) with 9999 permutations (Anderson et al., 2008). nMDS based on Bray-Curtis similarities from fourth root-transformed Eukaryotic/Bacterial ASV relative abundance data was used to visualise changes in community composition across time points and treatment concentrations. (Clarke and Gorley, 2015). The effects of the factors 'Time' (whole data) and 'Concentration' (PS and Glass separately) on microbial community composition were tested using PERMANOVA, with significance set at $p = 0.005$. For significantly different treatments, we conducted differential abundance analysis of microbiome data with bias correction in ANCOMBC v2.4.0 (Lin and Peddada, 2020) and plotted using ggplot2 v3.4.3 (Ginestet C, 2011). PS-Low and Glass-Low treatments were excluded from this analysis because Glass-Low replicates showed very high dispersion, and one replicate was not sequenced successfully.

Differences in respiration and growth rates were assessed with Kruskall-Wallis test at a significance level alpha = 0.05. Post-hoc Dunn's test with Benjamini-Hochberg correction for multiple testing was conducted to identify differences between the treatments. For this analysis, a significance level of alpha = 0.1 was assumed.

2.9 Data availability

Illumina sequencing data were deposited in the EMBL database under BioProject PRJEB107429. Other data are available at Zenodo (DOI: 10.5281/zenodo.18450021) and will be released upon acceptance of the manuscript (link for reviewers): https://zenodo.org/records/18450021?preview=1&token=eyJhbGciOiJIUzUxMiJ9.eyJpZCI6IjI1ZmU1MTY4LTc2NWQtNGI3OC1iODRmLTllNmU2ZmI2Yzg2MiIsImRhdGEiOnt9LCJyYW5kb20iOiJhYWFmZmE1NDVkYTIyMTM3MDUyZmQzYTNmOWIyYmNmZSJ9.s_VagkKduXKAyLuN0Uo30Jz9HTklY_ZXH_WjGmzwDk9zjWCbtKh7t38PNITQGCLYhgnsyc96eHNSD8tmoPOHeQ) .

3. Results

3.1 Microbial community growth and respiration

Respiration rates varied from the lowest values of 7.5± 0.622 µM O_2 day^{-1} (average ± standard deviation) in Glass Low to the highest values of 10.5± 0.55 µM O_2 day^{-1} in Control (Fig. 2). There were no significant differences between the treatments ($p = 0.15$). Killed control showed no oxygen decrease (Fig. S1).

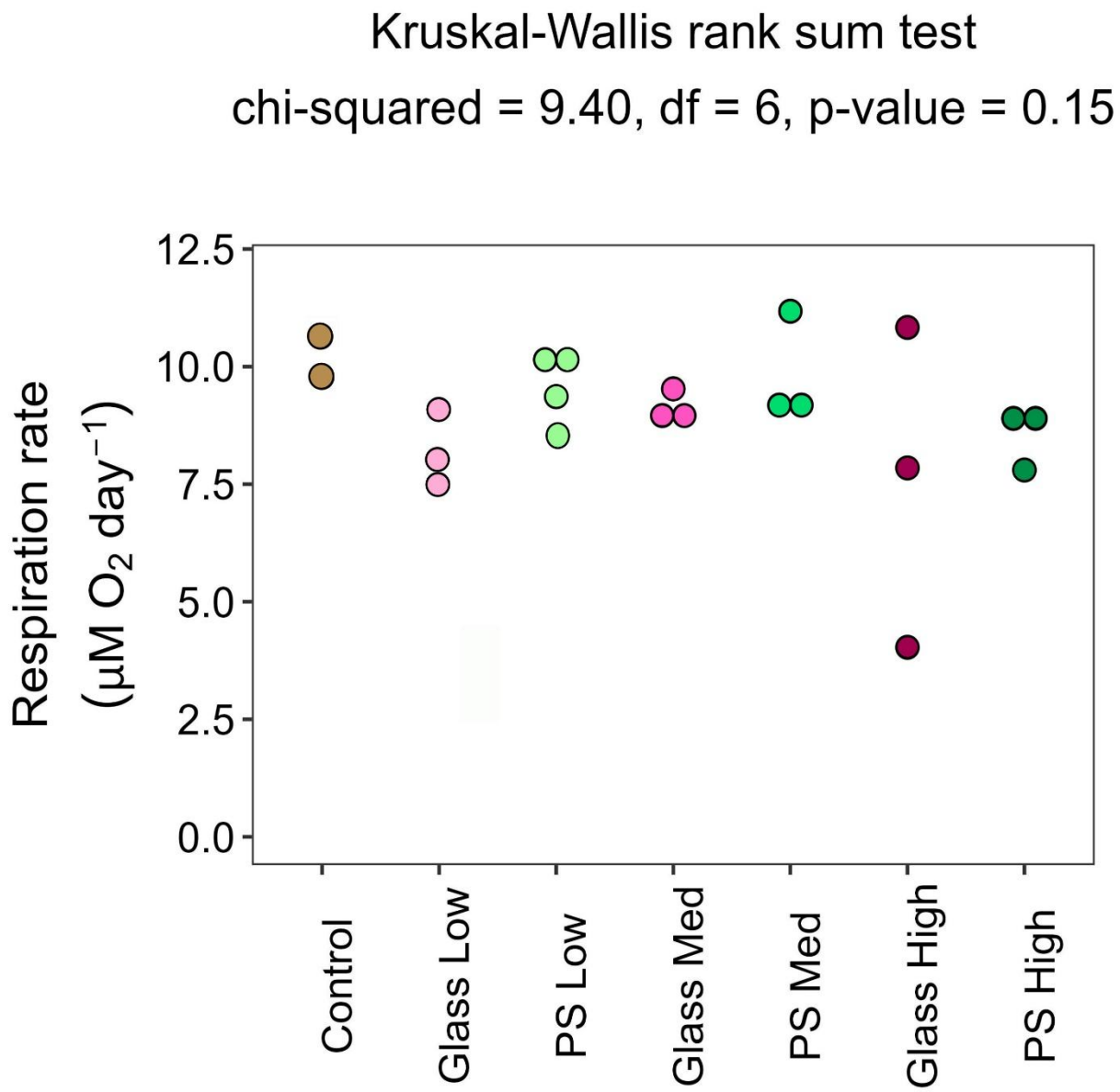

Figure 2 : Respiration rates of the microbial communities in the control, polystyrene (PS-Low, PS-Medium, PS-High), and glass (Glass-Low, Glass-Medium, Glass-High) treatments, with the results of the Kruskal-Wallis rank-sum test.

The abundance of HNF showed different dynamics among treatments. There was an initial increase in the abundance in control between 0hrs and 58hrs, followed by a gradual decrease until

the end of the experiment (Fig. 3a). Based on these results, we defined two growth phases: Phase 1 (growth rate in the control μ = 0.1 day^{-1}) and Phase 2 (μ = -0.3 day^{-1}) (Fig. S2). The presence of particles significantly decreased the growth rate in Phase1 in the concentration dependent manner (Kruskal–Wallis, p = 0.028, with significantly lower rates in PS-High and Glass-High compared to the control treatment (Dunn test, p-value < 0.1).

HNF growth in Phase 2 was negative in all treatments, and although Kruskal–Wallis test indicated the differences between the treatments (p = 0.04), the Dunn test was not significant. Moreover, the rates were similar between the treatments with equivalent concentrations of PS and Glass spheres, that is: PS-Low vs Glass-Low, PS-Medium vs. Glass-Medium and PS-High vs. Glass-High.

Bacterial abundance initially declined from 0 h to 58 h in the control and all treatments (Fig. 3b). This was followed by an irregular pattern of increase or decrease in a treatment-dependent manner. Based on these patterns, we defined three growth phases: Phase 1 (0h-58h, growth rate in the control: μ = -0.5), Phase 2 (58h-82h, μ = 0.4), and Phase 3 (82h-106h, μ = -0.5) (Fig. S3). The presence of particles did not affect the growth rate in Phase 1 significantly (p = 0.1). In Phase 2, a significant difference between the growth rates was observed (p = 0.02), with an increase in growth rate and abundance in the control and all PS and glass treatments except for Glass-Low and PS-High (Fig.3b, Fig. S3).

Growth rates in Phase 2 showed no significant differences between most of the treatments, except for PS-Low vs. Glass-Low (Dunn Test, p = 0.04). In Phase 3, almost all treatments showed a decrease in abundance, with the exception of Glass-Low and Glass-Medium, which exhibited a clear increase. In Growth Phase 3, comparison of the control relative to PS and glass concentrations showed significance only for Control vs. Glass-Low (Dunn Test p = 0.07).

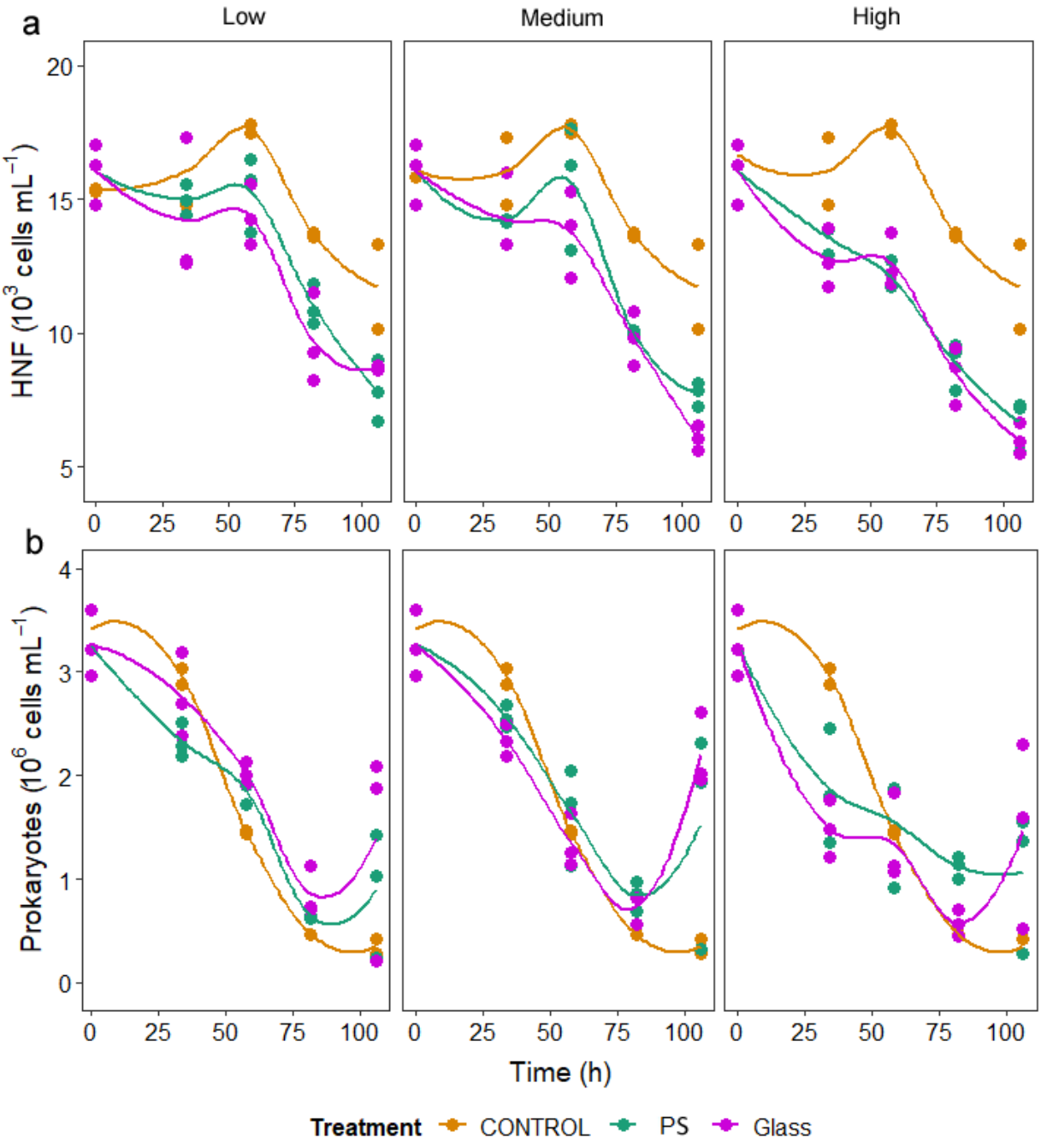

Figure 3: Temporal dynamics of the abundance of (a) Heterotrophic Nanoflagellates (HNF) and (b) Bacterial Communities under varying concentrations of polystyrene (PS) and glass/in various experimental treatments.

3.2 Changes in eukaryotic community composition

There was a significant temporal shift in the eukaryotic community composition, analysed using amplicon sequencing of the V6-V8 fragment of 18S rRNA gene over the course of the experiment (PERMANOVA, p-value < 0.005).

Initially, Haptophyta, Stramenopiles and Telonemia dominated the eukaryotic community in all treatments (Fig.4a), while Discoba showed a higher contribution to the HNF community at the end of the exposure.

Haptophytes contributed almost 60% to all reads at 0h, and dropped to <5% after in different concentrations of PS and Glass (Fig.4a). C*hrysochromulina* contributed 50-60% to haptophytes reads in all treatments, with an increasing pattern from 58 h to 106 h, while both *Haptolina* and *Prymnesium* showed decreasing trends with time in all treatments (Fig.4a).

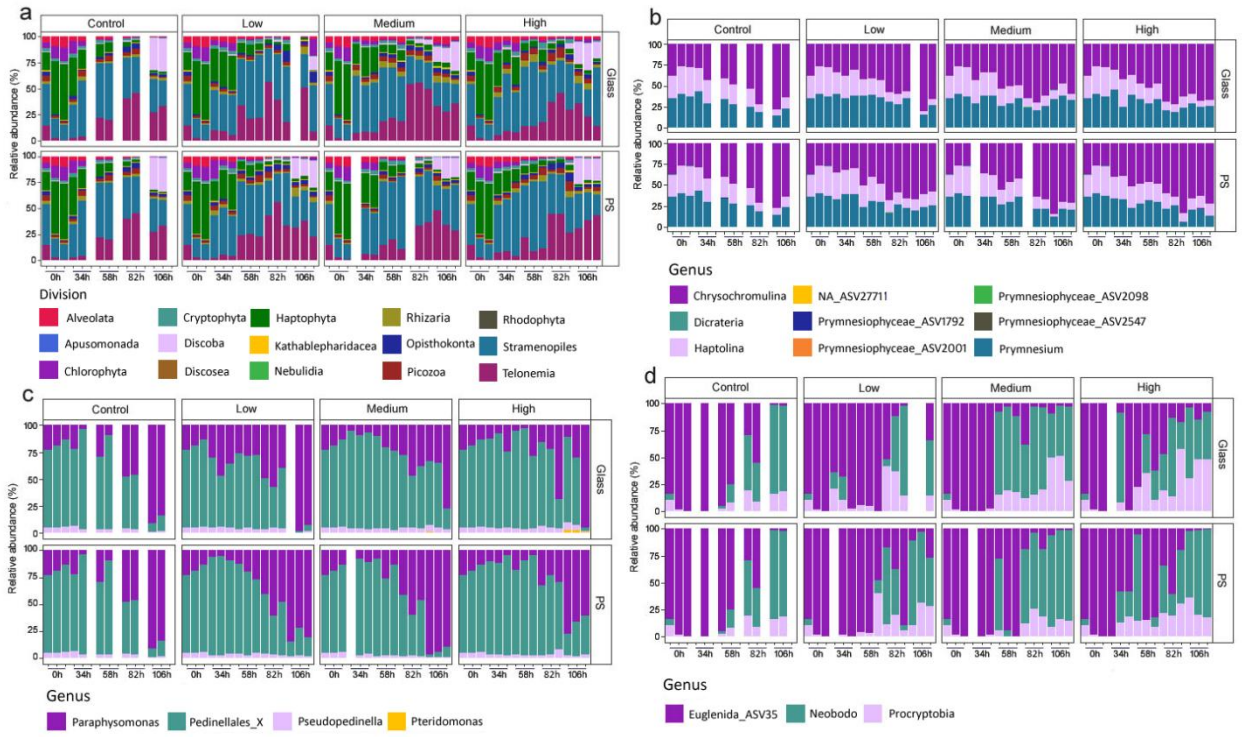

Figure 4: Relative abundance of the Heterotrophic Nanoflagellate (HNF) community based on 18S rRNA gene sequences. (a) Whole community composition at the Division level, and the most abundant genera within the dominant divisions: (b) Haptophyta, (c) Stramenopiles, and (d) Discoba.

Telonemids started to increase in relative abundance at 58h and were dominant at 84h, constituting about 50-60% of total reads (Fig. 4a). Telonemia group-1 contributed almost 95% of telonemid reads in all treatments over the whole course of the experiment (Fig. S4).

Stramenopiles stayed consistently one of the major divisions. Unknown *Pedinellales*, represented initially up to 85% of the stramenopile reads, but towards the end of the experiment, it was replaced by *Paraphysomonas* that became dominant in control, PS-Low, PS-Medium, PS-High and Glass-Low (Fig.4c).

Phylum Discoba showed an increase in relative abundance at 106h in all treatments. *Euglenida_ASV35, Neobodo* and *Procryptobia* were the dominant genera (Fig.4d). *Euglenida_ASV35* completely dominated Discoba in the first half of the experiment, contributing 90-95% to Discoba reads. They were replaced by *Neobodo*, which made up about. 75% of their

reads already at 84h in PS-Medium and Glass-Medium, and at 106h in control, PS-Low, PS-Medium, PS-High and Glass-Low, Glass-Medium, Glass-High. *Procryptobia* showed an increasing trend with time and was found more abundant at 84h and 106h in Glass-Medium and Glass-High, with a contribution of up to 50% of Discoba reads.

The effect of treatments was detectable only on the last sampling point (106 h), at which protistan communities exposed to PS and Glass microspheres were significantly different (PERMANOVA,

p-value < 0.005, Table S1). However, pairwise significant differences among treatment concentrations were only detected between control vs PS-High and control vs Glass-

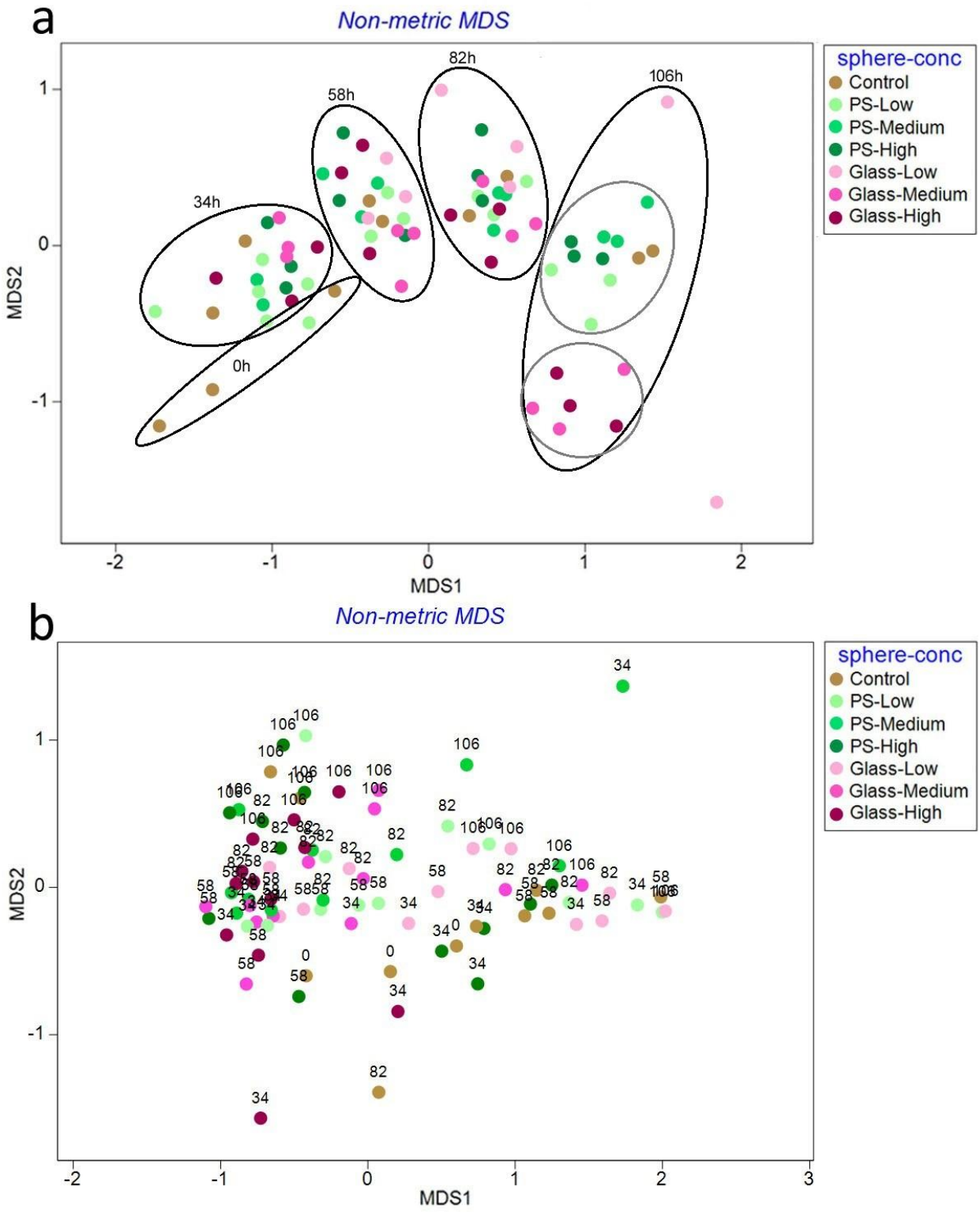

Figure 5: Non-metric multidimensional scaling (nMDS) based on relative abundance data from amplicon sequencing, of (a) Heterotrophic Nanoflagellates (HNF) and (b) Bacterial communities in the control, polystyrene (PS-Low, PS-Medium, PS-High), and glass (Glass-Low, Glass-Medium, Glass-High) treatments, at five time points (0, 34, 58, 84, and 106 hours). The grey circles represents grouping of the treatments PS and Glass.

Medium (Table S1, Fig. 5a). Therefore, the ANCOM-BC analysis, conducted to detect the ASVs differentially abundant in the PS vs Glass treatments, was performed on pooled PS-High + PS-Medium vs Glass-High + Glass-Medium data.

The ANCOM-BC results showed several genera to have negative LFC (Log Fold Change) values in the PS treatments (Fig. 6), indicating that some groups were specifically affected by particle type.

They included ciliates *Pelagodinium* and *Urotricha*, cryptophyte *Teleaulax*, eustigmatophyte *Nannochloropsis*, stramenopile from MAST-6 lineage, and diatoms *Chaetoceros* and *Cyclotella*. In addition, numerous low-abundance (<0.06% of reads) ASVs and the genera *Azadinium*, *Cymbomonas*, *Biecheleriopsis* and unknown Dinoflagellata were detected only in the glass treatments (Fig. S5).

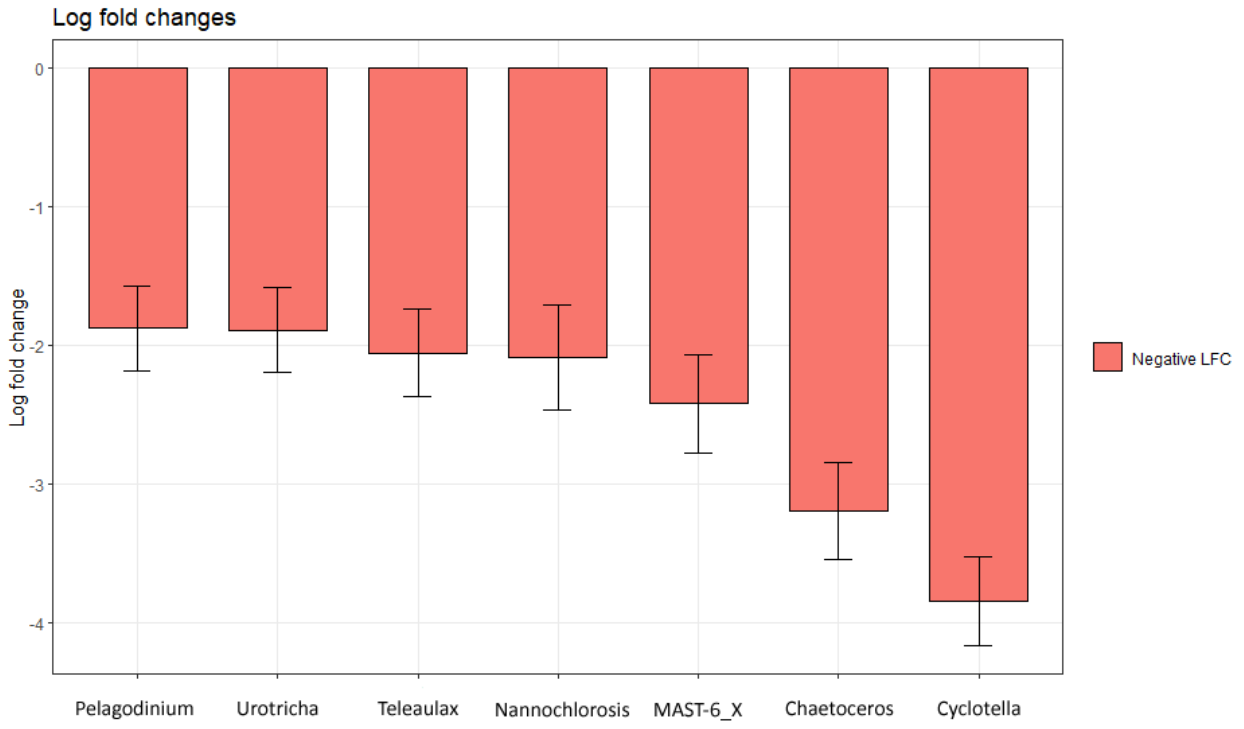

Figure 6: Analysis of composition of microbiomes showing log fold change (LFC) values at genus level between protistan communities at 106 h in PS and Glass treatments (pooled data for PS-Medium + PS High vs Glass-Madium+ Glass High). Nagative values indicates lower relative abundance in the PS treatments. Error bars represent standard error.

3.3 Changes in bacterial community composition

In contrast to the protistan community, no significant differences were found in bacterial community composition among time points (PERMANOVA, p-value > 0.005, Table S2). Pairwise significance among treatment concentrations was only detected in control vs Glass-High and Glass-Low vs Glass-High (p = 0.005). Similarly, no consistent pattern of community shift was found in bacterial community composition across time and treatment concentration (Fig.5b)

Phyla Pseudomonadota Bacteroidota and Actinomycetota, contributed about 90% to the bacterial reads across all the treatments (Fig. 7a). Despite the lack of significant differences, there were some changes in the relative abundances of these dominant phyla with time.

Actinomycetota followed a decreasing trend with time in control and all PS treatments, while remaining consistent in all glass treatments. Sporichthyaceae and Microbacteriaceae were dominant families, contributing around 80-90% to the total actinobacterial reads. Sporichthyaceae dominated at 0h in control, PS, and Glass treatments with almost 60% Actinomycetota reads. However, at 106h, Microbacteriaceae dominated with 60-65% of reads, except for the Glass-High variant, dominated by Sporichthyaceae (Fig. 7b).

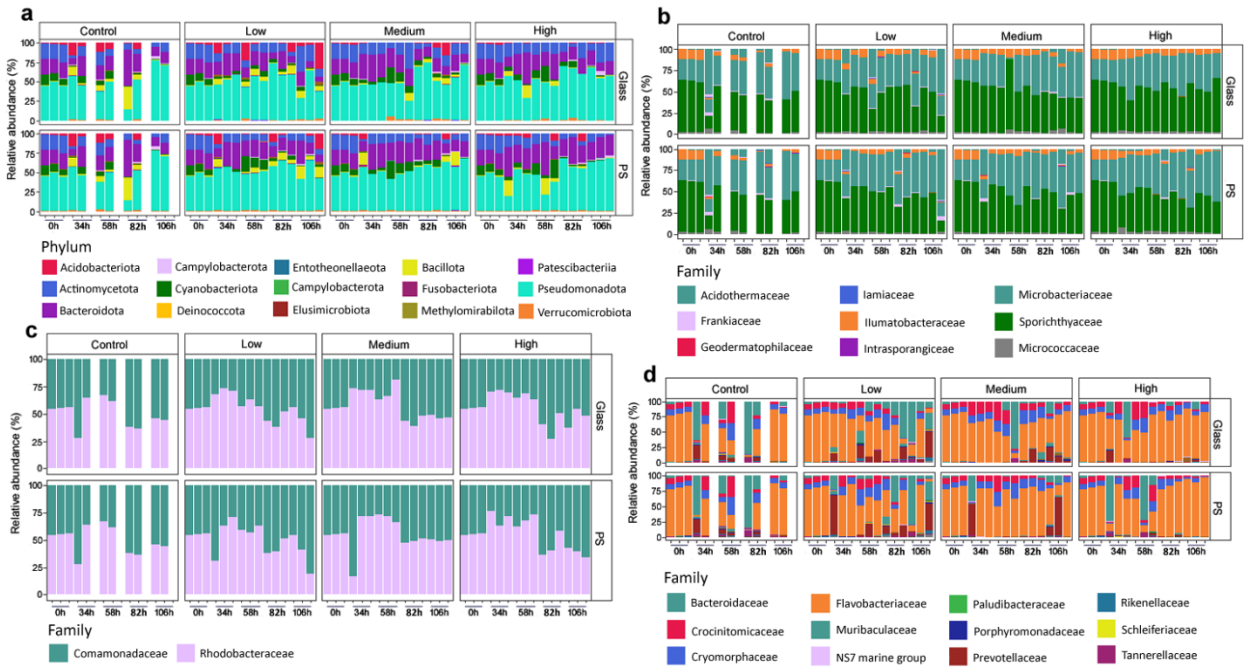

Figure 7: Bacterial community composition based on 16S rRNA gene amplicons. (a) Whole community composition at the Phylum level, and the most abundant families within the three most abundant phyla (b) Actinomycetota, (c) Pseudomonadota, and (d) Bacteroidota.

Pseudomonadota, being one of the main contributing phyla, showed an opposite trend to Actinomycetota in control, PS (PS-Medium and PS-High), and glass (Glass-Medium and Glass-High). Comamonadaceae and Rhodobacteraceae were the most contributing families to Proteobacteria reads, with little variability over the experiment (Fig.7c).

Concentrations of Bacteroidota slightly increased over the course of the experiment. Flavobacteriaceae was the dominant family most of the time in all treatments, especially in PS-High and Glass-High. Bacteroidaceae showed some relative increase at 84h in control, Glass-Low, and PS-Low (Fig.7d). Moreover, in single replicates, Prevotellaceae showed short-term dominance in PS-Low and PS-Medium treatments.

4. Discussion

Our study provides two main advances in understanding microplastic (MP) impacts on marine ecosystems. First, while previous research had focused on its toxicity on specific species (Zhang et al., 2017, Sun et al., 2021, Geng et al. 2021), we examined the effects of bacteria-sized microplastic particles at the microbial community level. While there is little information about concentrations of such particles in the water, they seem to much more numerous than larger particles (Wiggin and Holland, 2019). Second, by including particle control using inert glass spheres, we were able to demonstrate, for the first time, that the physical presence of particles may be a driver of MP-induced changes in microbial communities. Negative effects on microbial biomass emerged only at the highest concentrations, suggesting resilience of microbial assemblages to current and near future concentration (ten Hietbrink et al. 2025). However, given increasing pollution levels, durability and the fact that MPs already exceed zooplankton biomass

and may comprise over 50% of particulate organic matter in parts of the Pacific Ocean (Di Mauro et al.,2017), such concentrations are not implausible.

While our work is among the first to study the effect of microplastics on natural pelagic microbial communities, it has some restrictions that resulted from the obstacles when working with such small particles. First, we were limited by the obtainability of commercial products of desired dimensions to pure PS spheres, because other polymers or shapes are not available. Moreover, the aging treatment of such small particles is also hampered, as they are difficult to qualitatively retrieve afterwards. Finally, the fact that we used pure polymer might have affected the outcome of our experiments, as a substantial part of microplastic toxicity is caused by leaking oligomers and additives (Jin et al., 2022, Huang et al., 2024, Kwon et al 2015). However, they leak out within days (Kwon et al., 2015). Since the main source of such small particles is degradation (Granek et al., 2020), they should not contain many additives anymore, making the use of pure polymer adequate to the expected environmental conditions. Taking together, despite these limitations, our results provide an important, novel insight into the response of planktonic microorganisms to PS pollution at the community level.

HNF growth rates declined with increasing particle concentration, with the strongest suppression observed at high levels of both PS and glass (Fig.3a). This concentration-dependent pattern suggests that the response was linked to particle abundance rather than particle composition, pointing toward a physical interference mechanism. This conclusion is also supported by the observation that respiration rates showed no significant differences among treatments (Fig.2). Physical disturbance by suspended particles is known to affect microbial grazers by disrupting feeding currents, reducing prey encounter rates, or occupying ingestion vacuoles without providing nutritional value (Boenigk & Arndt, 2002; Azam & Malfatti, 2007; Victoria and Sussane et

al,.2021), which could explain the observed particle-concentration-dependent decline in abundance despite stable bacterial populations (Fig.3). The similar HNF community responses to PS and glass treatments support this interpretation (Fig.3a), implying that during the initial exposure phase (limited to 5 days in this study), MPs act primarily as inert physical stressors for protistan communities. Similar concentration-dependent negative effect of PS spheres was observed for a bacterivorous ciliate *Strombidium sulcatum*, but due to lack of inert particle controls, it was not possible to investigate the mechanisms (Geng et al. 2021). Our results indicate the negative dominant effect of the particle presence on the growth and abundances of HNFs, regardless of the particle type. Since bacteria were not significantly affected across treatments (Fig.3b), it is unlikely that prey availability drove the observed protistan responses. Given the central role of HNFs as primary bacterial grazers within aquatic microbial food webs, their suppression can disrupt carbon transfer and nutrient regeneration processes (Azam & Malfatti, 2007).

Multivariate analyses showed a clear separation of eukaryotic communities between glass and PS treatments only at time 106 h (Table S1). Moreover, PS treatments grouped with particle free controls at that time (Fig. 5a), indicating that the community difference had not resulted from the PS-related toxicity. While toxicity was not measured here, it is often considered a key factor responsible for the adverse effects of microplastics on biota (Hsieh et al., 2023; Natarajan et al., 2022; Hwang et al., 2020). The significant positive correlation between 5-day exposure to glass and the contribution of diverse microbial taxa, including primary producers (*Chaetoceros, Cyclotella, Nannochloropsis*) and grazers (*Urotricha*, MAST-6_X), indicates an unexpected effect inert particles may pose to microbial eukaryotes, and thus potentially to the microbial loop. A very interesting result was the enhancement of silicifying diatoms *Chaetoceros* and *Cyclotella* that

require silica to build their frustules. While we do not have direct proof, it is plausible that they used glass particles as a source of this nutrient (Penna et al., 2003). The increased contribution of algae could also explain the increase of algivorous HNFs from MAST-6 (Piwosz and Pernthaler, 2010) and the ciliate genus *Urotricha* (Asghar et al., 2025).

In contrast to eukaryotes, bacterial community composition remained stable throughout the experiment, even at the highest concentrations on MPs and Glass microspheres (Fig.5b). While this result strongly contrasts with the observation on pure cultures and soil communities (Lai et al., 2025, Che et al.,2024, Sun et al .,2021, Kim et al., 2022), it agrees with the observation from aquatic environments. The dominant effect of time over experimental treatment is not unusual (Vanharanta et al., 2024), and such resilience of bacterial assemblages to short-term microplastic exposure has also been reported in previous studies (Lora et al., 2024). Overall, pelagic bacterial communities exhibited no major time or treatment-induced compositional shifts, indicating their high resilience to short-term exposure to high concentrations of small particles.

The mechanisms underlying the observed decrease in HNFs cannot be firmly determined from our results. We hypothetised that the reduced prey quality and availability, caused by particle presence, would require HNF to increase efforts to obtain good quality food, due to, for instance, longer time required to catch and ingest a suitable prey (Boenigk et al., 2001) or additional physical effects, such as interference with feeding or altered microscale flow (Azam & Malfatti, 2007). Consequently, they would not have enough resource for growth. If that had been the case, bacterial abundance would have increased in the particle treatments due to decreased grazing pressure. Such pattern was observed only between the last two time points in the treatments with both PS and Glass particles (Fig. 3b). While metatranscriptomics could have provided valuable information on active metabolic pathways and stress responses of protistan communities under particle exposure,

these communities were dominated by poorly characterized taxa that lack sufficient genomic and transcriptomic reference data (Keeling et al., 2014), thus limiting the ability of this approach to provide mechanistic insights at present.

Overall, our results suggest that there is still a window of opportunity to mitigate plastic pollution before critical microbial components of marine ecosystems are irreversibly affected, a message underscored by the recent failure to finalize the UN plastics treaty (Peter and Jen, 2025). Future studies, incorporating functional assays, imaging, and longer-term (chronic) exposures could help to clarify the drivers of HNF decline and their ecosystem implications.

Acknowledgment

We would like to thank Mariusz Zalewski for his valuable assistance with water sampling.

Supplementary Figures

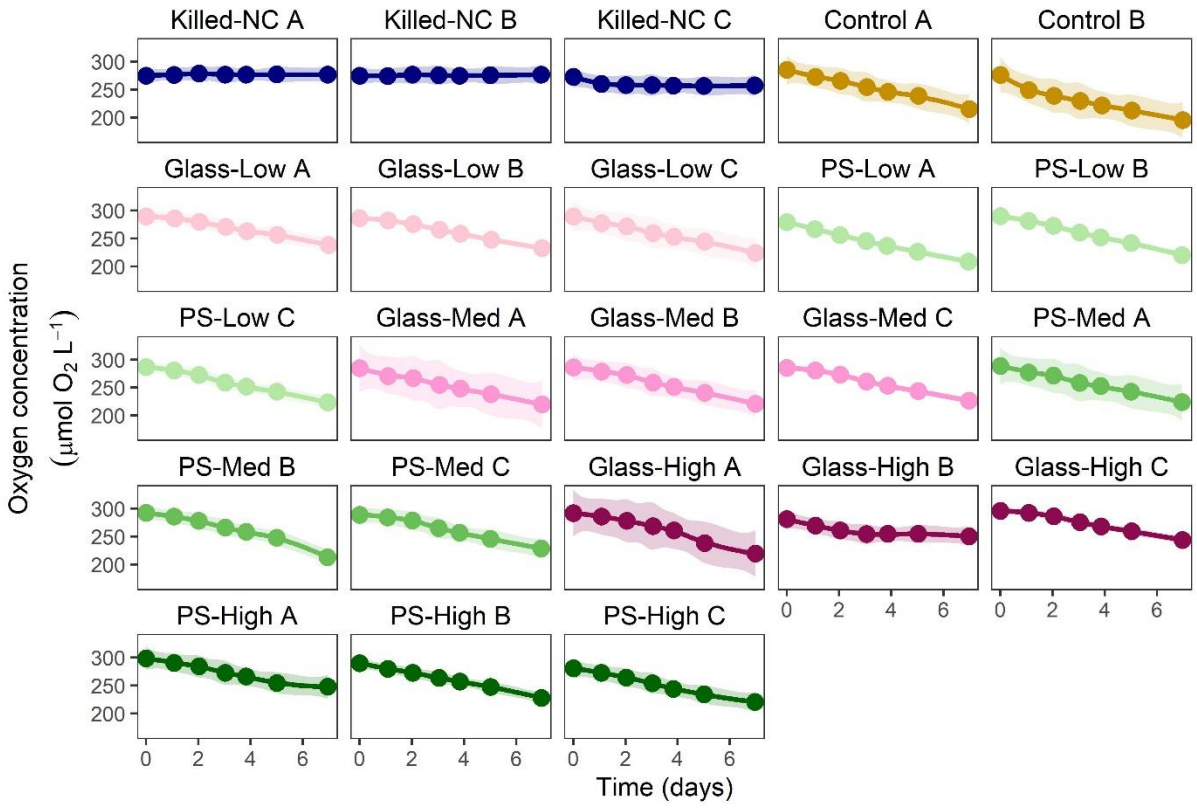

Supplementary figure 1: *Changes in oxygen concentrations over the duration of the experiment in individual replicates. Points show the measured values; lines represent linear fitting to the data. Respiration rates shown in Fig. 1 were calculated from the slopes of linear regression. Killed-NC: killed negative controls prepared from the autoclaved Baltic Sea water prepared to account for abiotic processes and exclude contamination of the samples.*

Growth Phase-1 (P-value = 0.02)

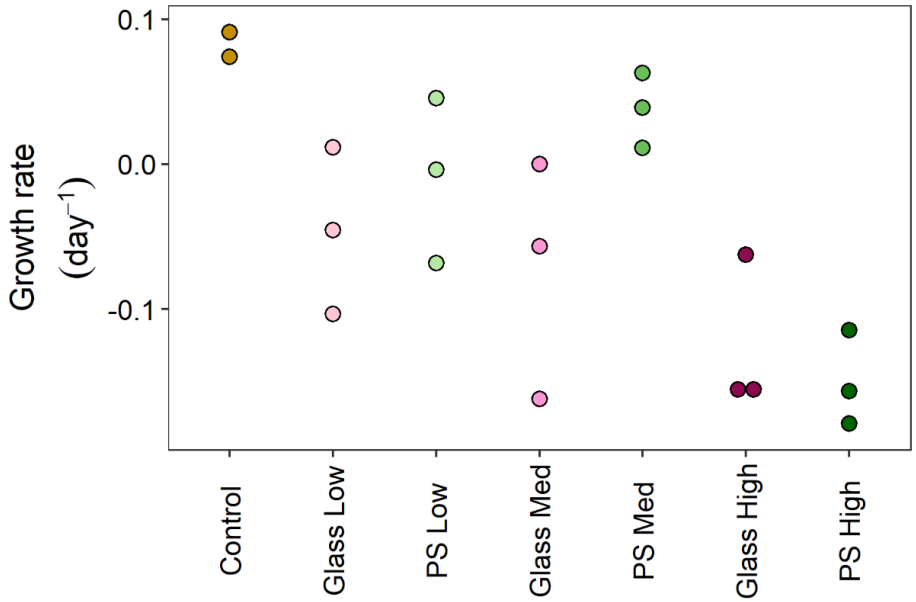

Growth Phase-2 (p-value= 0.04)

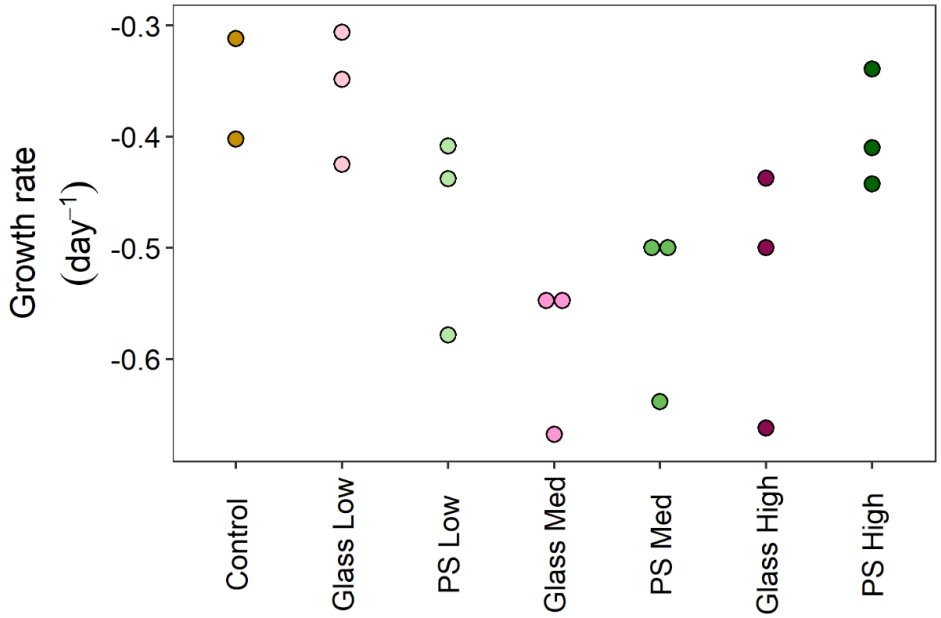

Supplementary fig.2: *Growth rate of Heterotrophic Nanoflagellate (HNF) communities analyzed using the Kruskal-Wallis test. Comparison of growth rates in control, polystyrene (PSLow, PS-Medium, PS-High), and glass (Glass-Low, Glass-Medium, Glass-High) treatments during two growth phases: Growth Phase 1 (0-58 h) and Growth Phase 2 (58-84 h).*

Growth Phase-1 (p-value = 0.15)

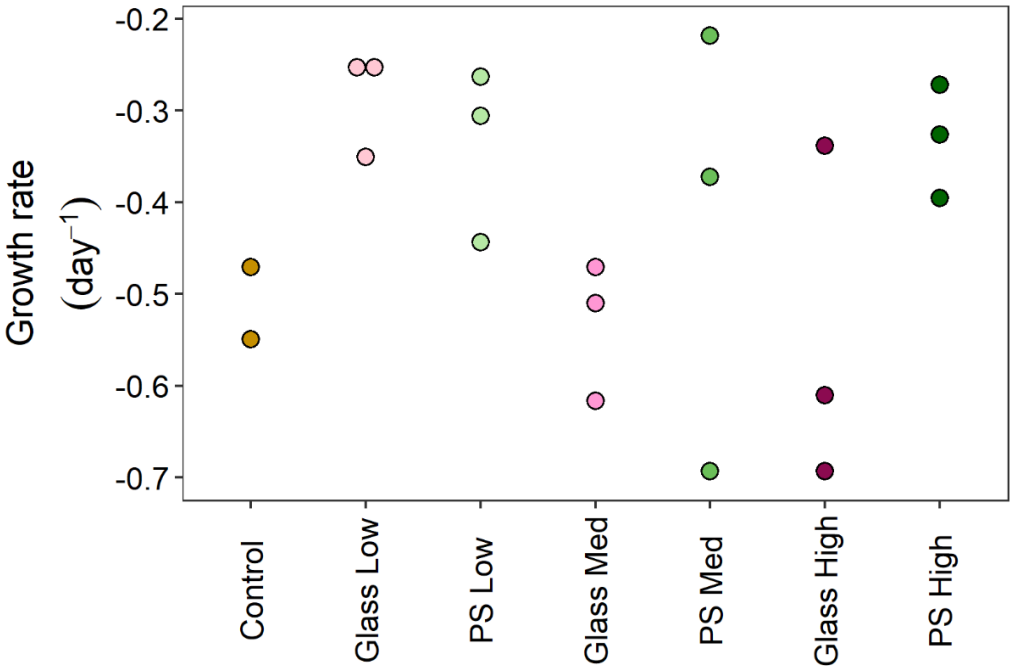

Growth Phase-2 (p-value = 0.02)

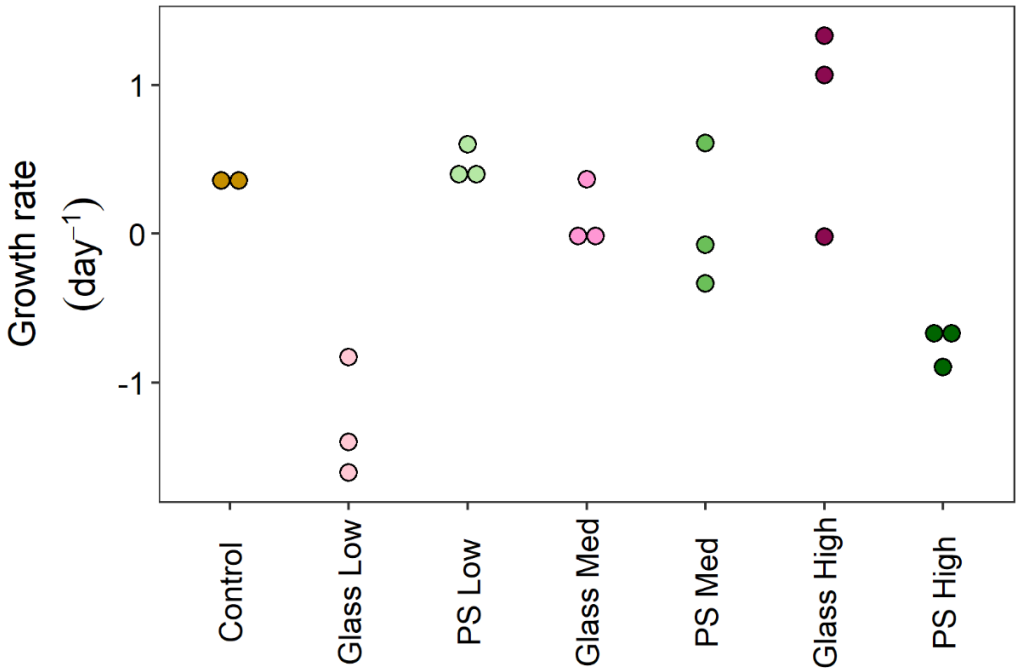

Growth Phase-3 (p-value = 0.03)

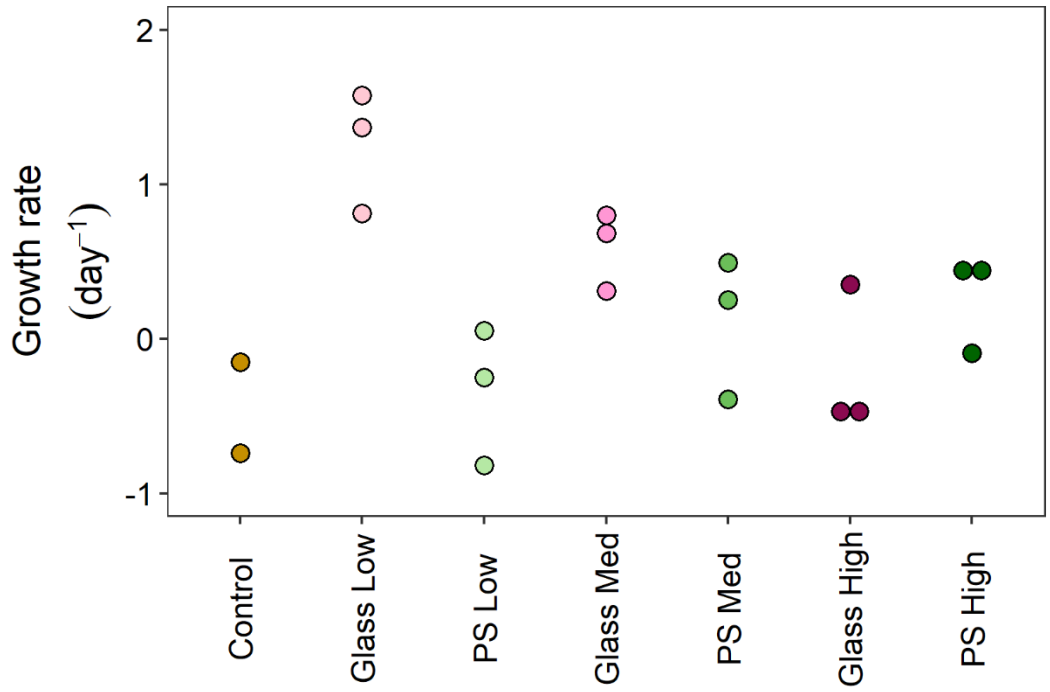

Supplementary figure 3: *Growth rates of bacterial communities assessed using the Kruskal–Wallis test. Growth rate comparisons were conducted among control, polystyrene (PS-Low, PS-Medium, PS-High), and glass (Glass-Low, Glass-Medium, Glass-High) treatments across three growth phases: Phase 1 (0–58 h), Phase 2 (58–84 h), and Phase 3 (84–106 h).*

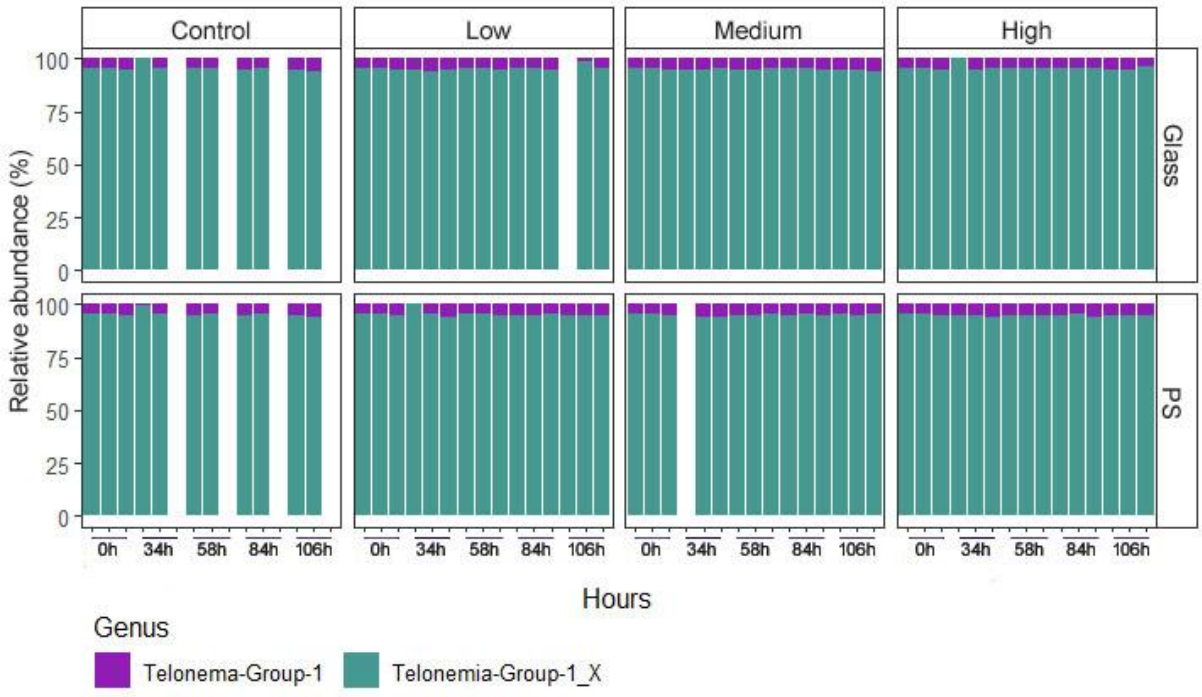

Supplementary figure 4: *Relative abundance of Telonemia, one of the dominant divisions, at the genus level. Two uncultured genera from Telonemia-Group-1 dominated (Telonemia group-1_X and Telonemia group-1) across control, polystyrene (PS-Low, PS-Medium, PSHigh), and glass (Glass-Low, Glass-Medium, Glass-High) treatments. The abundance of both genera remained constant across all five time points (0, 34, 58, 84, and 106 hours).*

Supplementary Table 1. *PERMANOVA (pairwise) results for 18S ASV data comparing polystyrene (PS- Time, PS- Concentration) and glass (Glass-Time, Glass-Concentrations) across time points and different concentrations*

Microspheres at Highest Time point

106HRS			
Groups	t	P(perm)	perms
CONTROL, Polystyrene	1.154	0.1463	28
CONTROL, Glass	2.4597	0.035	28
Polystyrene, Glass	3.184	0.0021	462

Pairwise PS-TIME

Groups	t	P(perm)	perms
0, 34	1.5512	0.0042	165
0, 58	2.6208	0.0049	220
0, 82	3.6301	0.0037	220
0, 106	3.9588	0.0035	220
34, 58	2.2492	0.0001	8146
34, 82	3.7061	0.0002	8145

34, 106	4.3073	0.0001	8163
48, 72	2.4781	0.0001	8088
48, 96	3.5852	0.0002	8155
72, 96	2.1535	0.0001	8156

Pairwise comparison between PS-Concentrations and Control

Groups	t	P(perm)	perms
Low, Control	1.9413	0.0099	455
Low, Medium	0.88631	0.5484	9888
Low, High	0.89418	0.5583	9898
Control, Medium	2.2351	0.0078	364
Control, High	2.2968	0.0028	455
Medium, High	0.82819	0.6405	9862

Glass-time

Groups	t	P(perm)	perms
0, 24	1.6828	0.0096	220

0, 48	2.7403	0.0045	220
0, 72	3.5638	0.0057	220
0, 96	2.3971	0.0062	165
24, 48	2.0663	0.0001	8116
24, 72	3.3822	0.0001	8120
24, 96	3.2683	0.0001	8177
48, 72	2.0773	0.0001	8109
48, 96	3.1455	0.0001	8166
72, 96	2.8437	0.0001	8169

GLASS-Concentrations and Control

Groups	t	P(perm)	perms
High, Low	1.0502	0.325	9872
High, Control	1.907	0.0054	455
High, Medium	0.7867	0.7636	9868
Low, Control	1.8153	0.0103	364
Low, Medium	1.2582	0.1201	9880

Control, Medium	2.0262	0.0044	455

Supplementary Table 2. *PERMANOVA (pairwise) results for 16S ASV data comparing Polystyrene (PS- Time, PS- Concentration) and glass (Glass-Time, Glass-Concentrations) treatments across time points and different concentrations.*

PS-Time

Groups	t	P(perm)	perms
0, 34	0.87874	0.5014	364
0, 58	1.2688	0.1369	364
0, 82	1.4982	0.0208	363
0, 106	1.6923	0.028	364
34, 58	1.2246	0.1553	9767
34, 82	1.2595	0.1224	9771
34, 106	1.6578	0.0291	9795
58, 82	1.2996	0.1171	9770
58, 106	1.8739	0.0133	9783
82, 106	1.1404	0.219	9786

Pairwise comparison of PS Concentrations and control

Groups	t	P(perm)	perms
Control, Medium	1.5383	0.0268	9876
Control, High	1.2197	0.1621	9904
Control, Low	0.75507	0.742	9893
Medium, High	0.90626	0.5747	9868
Medium, Low	1.2942	0.1122	9870
High, Low	1.0391	0.3121	9877

Glass-Time

Groups	t	P(perm)	perms
0, 34	0.99096	0.3692	364
0, 58	1.1961	0.2098	364
0, 82	1.3048	0.0868	364
0, 106	1.6786	0.0275	364
34, 58	1.0298	0.3119	9770
34, 82	1.1909	0.1846	9798
34, 106	1.7737	0.0215	9783

58, 82	0.99047	0.3411	9782
58, 106	1.7308	0.0337	9782
82, 106	1.3196	0.117	9763

Pairwise comparison of Glass Concentrations and control

Groups	t	P(perm)	perms
Control, Low	0.60852	0.9716	9894
Control, Medium	1.5017	0.0542	9889
Control, High	2.2234	0.0003	9882
Low, Medium	1.6437	0.0462	9887
Low, High	2.431	0.0008	9881
Medium, High	1.2695	0.0825	9870

References

Agamuthu P, Mehran SB, Norkhairah A, Norkhairiyah A. Marine debris: A review of impacts and global initiatives. Waste Manag Res. 2019 Oct;37(10):987-1002. doi: 10.1177/0734242X19845041.

Anderson MJ, Gorley RN, Clarke KR, 2008. PERMANOVA+ for PRIMER Guide to Software and Statistical Methods. PRIMER-E Ltd, Plymouth, U.K.

Asghar U, Mukherjee I, Sonntag B, Pires de Paula CC, Kasalický V, Bulzu P-A, Singh AP, Shabarova T, Piwosz K, Šimek K. Morphological and molecular analyses of season-specific responses of freshwater ciliate communities to top-down and bottom-up experimental manipulations. mSystems. 2025 Sep 23;10(9):e0030425. doi: 10.1128/msystems.00304-25. Epub 2025 Aug 15. PMID: 40815464; PMCID: PMC12455964.

Azam F, Malfatti F. Microbial structuring of marine ecosystems. Nat Rev Microbiol. 2007 Oct;5(10):782-91. doi: 10.1038/nrmicro1747. Erratum in: Nat Rev Microbiol. 2007 Dec;5(12):966.

Bellas J, Martínez-Armental J, Martínez-Cámara A, Besada V, Martínez-Gómez C. Ingestion of microplastics by demersal fish from the Spanish Atlantic and Mediterranean coasts. Mar Pollut Bull. 2016 Aug 15;109(1):55-60. doi: 10.1016/j.marpolbul.2016.06.026.

Boenigk, J. Arndt, H. Cleven, Ernst-J. The problematic nature of fluorescently labeled bacteria (FLB) in Spumella feeding experiments - an explanation by using video microscopy. Archiv fur Hydrobiologie 2001 Vol. 152.329-338. DOI: 10.1127/archiv-hydrobiol/152/2001/329

Boenigk J, Arndt H. Bacterivory by heterotrophic flagellates: community structure and feeding strategies. Antonie Van Leeuwenhoek. 2002 Aug;81(1-4):465-80. doi: 10.1023/a:1020509305868. PMID: 12448743.

Bolyen E, Rideout JR, Dillon MR, Bokulich NA, Abnet CC, Al-Ghalith GA,et al. Reproducible, interactive, scalable and extensible microbiome datascience using QIIME 2. Nat Biotechnol. 2019;37(8):852–7. https://doi.org/10.1038/s41587-019-0252-6.

Callahan BJ, McMurdie PJ, Holmes SP. Exact sequence variants should replace operational taxonomic units in marker-gene data analysis. ISME J. 2017 Dec;11(12):2639-2643. doi: 10.1038/ismej.2017.119.

Callahan BJ, McMurdie PJ, Rosen MJ, Han AW, Johnson AJ, Holmes SP. DADA2: High-resolution sample inference from Illumina amplicon data. Nat Methods. 2016 Jul;13(7):581-3. doi: 10.1038/nmeth.3869.

Carpenter EJ, Smith KL Jr. Plastics on the Sargasso sea surface. Science. 1972 Mar 17;175(4027):1240-1. doi: 10.1126/science.175.4027.1240. PMID: 5061243.

Clarke KR, Gorley RN, 2015. PRIMER v7: User Manual/tutorial. PRIMER-E Ltd, Plymouth, 296p.

Cornwall W. The plastic eaters. Science. 2021 Jul 2;373(6550):36-39. doi: 10.1126/science.373.6550.36.

Di Mauro R, Kupchik MJ, Benfield MC. Abundant plankton-sized microplastic particles in shelf waters of the northern Gulf of Mexico. Environ Pollut. 2017 Nov;230:798-809. doi: 10.1016/j.envpol.2017.07.030. Epub 2017 Aug 10. PMID: 28734261.

Duncan EM, Broderick AC, Fuller WJ, Galloway TS, Godfrey MH, Hamann M, Limpus CJ, Lindeque PK, Mayes AG, Omeyer LCM, Santillo D, Snape RTE, Godley BJ. Microplastic ingestion ubiquitous in marine turtles. Glob Chang Biol. 2019 Feb;25(2):744-752. doi: 10.1111/gcb.14519.

Fouilland E, Mostajir B. Revisited phytoplanktonic carbon dependency of heterotrophic bacteria in freshwaters, transitional, coastal and oceanic waters. FEMS Microbiol Ecol. 2010 Sep;73(3):419-29. doi: 10.1111/j.1574-6941.2010.00896.x.

Frias JPGL, Nash R. Microplastics: Finding a consensus on the definition. Mar Pollut Bull. 2019 Jan;138:145-147. doi: 10.1016/j.marpolbul.2018.11.022. Epub 2018 Nov 22. PMID: 30660255.

Fadeev Eduard , Cardozo-Mino Magda G. , Rapp Josephine Z. , Bienhold Christina , Salter Ian , Salman-Carvalho Verena , Molari Massimiliano , Tegetmeyer Halina E. , Buttigieg Pier Luigi , Boetius Antje. Comparison of Two 16S rRNA Primers (V3–V4 and V4–V5) for Studies of Arctic Microbial Communities. Front. Microbiol., 16 February 2021 Sec. Aquatic Microbiology. https://doi.org/10.3389/fmicb.2021.637526

Geng X, Wang J, Zhang Y, Jiang Y. How do microplastics affect the marine microbial loop? Predation of microplastics by microzooplankton. Sci Total Environ. 2021;758:144030. doi: 10.1016/j.scitotenv.2020.144030.

Ginestet, C. (2011), ggplot2: Elegant Graphics for Data Analysis. Journal of the Royal Statistical Society: Series A (Statistics in Society), 174: 245-246. https://doi.org/10.1111/j.1467-985X.2010.00676_9.x

Granek, E.F., Brander, S.M. and Holland, E.B. (2020), Microplastics in aquatic organisms: Improving understanding and identifying research directions for the next decade. Limnol Oceanogr Lett, 5: 1-4. https://doi.org/10.1002/lol2.10145

Guillou L, Bachar D, Audic S, et al. The Protist Ribosomal Reference database (PR2): a catalog of ya taunicellular eukaryote small sub-unit rRNA sequences with curated taxonomy. Nucleic Acids Research 2012;41:D597-D604.

Hammer J, Kraak MH, Parsons JR. Plastics in the marine environment: the dark side of a modern gift. Rev Environ Contam Toxicol. 2012;220:1-44. doi: 10.1007/978-1-4614-3414-6_1.

Hannah Ritchie (2023) - “How much plastic waste ends up in the ocean?” Published online at OurWorldinData.org. Retrieved from: 'https://ourworldindata.org/how-much-plastic-waste-ends-up-in-the-ocean'.

Hartmann NB, Hüffer T, Thompson RC, Hassellöv M, Verschoor A, Daugaard AE, Rist S, Karlsson T, Brennholt N, Cole M, Herrling MP, Hess MC, Ivleva NP, Lusher AL, Wagner M. Are We Speaking the Same Language? Recommendations for a Definition and Categorization Framework for Plastic Debris. Environ Sci Technol. 2019 Feb 5;53(3):1039-1047. doi: 10.1021/acs.est.8b05297.

ten Hietbrink S, Materić D, Holzinger R, Groeskamp S, Niemann H. Nanoplastic concentrations across the North Atlantic. Nature 2025 Jul 01;643, 412-416. 10.1038/s41586-025-09218-1

Hossain MS, Sobhan F, Uddin MN, Sharifuzzaman SM, Chowdhury SR, Sarker S, Chowdhury MSN. Microplastics in fishes from the Northern Bay of Bengal. Sci Total Environ. 2019 Nov 10;690:821-830. doi: 10.1016/j.scitotenv.2019.07.065.

Huang D, Xu Y, Yu X, Ouyang Z, Guo X (2021) Effect of cadmium on the sorption of tylosin by polystyrene microplastics. Ecotoxicol Environ Saf 207:111255. https://doi.org/10.1016/j.ecoenv.2020.111255.

Huang M, Si C, Qiu C, & Wang G. (2024). Microplastics analysis: from qualitative to quantitative. Environmental Science: Advances, 3, 1652–1668. https://doi.org/10.1039/d4va00244j

Jin M, Liu J, Yu J, Zhou Q, Wu W, Fu L, Yin C, Fernandez C, Karimi-Maleh H. Current development and future challenges in microplastic detection techniques: A bibliometrics-based analysis and review. Sci Prog. 2022 Oct-Dec;105(4):368504221132151. doi: 10.1177/00368504221132151.

Jousset, A., Bienhold, C., Chatzinotas, A. et al. Where less may be more: how the rare biosphere pulls ecosystems strings. ISME J 11, 853–862 (2017). https://doi.org/10.1038/ismej.2016.174

Kara J. Wiggin, Erika B. Holland. Validation and application of cost and time effective methods for the detection of 3–500 μm sized microplastics in the urban marine and estuarine environments surrounding Long Beach, California, Marine Pollution Bulletin, Volume 143, 2019, Pages 152-162, ISSN 0025-326X, https://doi.org/10.1016/j.marpolbul.2019.03.060.

Keeling, P. J., Burki, F., Wilcox, H. M., Allam, B., Allen, E. E., Amaral-Zettler, L. A., ... & Worden, A. Z. (2014). The Marine Microbial Eukaryote Transcriptome Sequencing Project (MMETSP): Illuminating the functional diversity of eukaryotic life in the oceans. PLOS Biology, 12(6), e1001889.

Khan S, Klaudia W, Joanna C, Krzysztof R, Lidia N, Anetta A, Tanja S, Indarnil M, Karel S, Aneta J, Mariusz Z, Kasia P. High-Temporal Resolution of Microbial Food Web Dynamics and Structure

During Phytoplankton Blooms in the Baltic Sea." Environmental Microbiology 27, no. 11 (2025): e70190.

Kim Y S, Kim Y J, Lee S W, Lee E H, Interactions between bacteria and nano (micro)-sized polystyrene particles by bacterial responses and microscopy, Chemosphere, Volume 306, 2022, 135584, ISSN 0045-6535, https://doi.org/10.1016/j.chemosphere.2022.135584.

Kirstein IV, Kirmizi S, Wichels A, Garin-Fernandez A, Erler R, Löder M, Gerdts G. Dangerous Hitchhikers? Evidence for Potentially Pathogenic Vibrio Spp. on Microplastic Particles. Marine Environ. Res. 2016 Sep 1, 120, 1–8. DOI: 10.1016/j. marenvres.2016.07.004.

Kwon BG, Koizumi K, Chung SY, Kodera Y, Kim JO, Saido K. Global styrene oligomers monitoring as new chemical contamination from polystyrene plastic marine pollution. J Hazard Mater. 2015;300:359–367. doi: 10.1016/j.jhazmat.2015.07.039.

Lai S, Fan C, Yang P, Fang Y, Zhang L, Jian M, Dai G, Liu J, Yang H and Shen L (2025) Effects of different microplastics on the physicochemical properties and microbial diversity of rice rhizosphere soil. Front. Microbiol. 15:1513890. doi: 10.3389/fmicb.2024.1513890

Lebreton L, Slat B, Ferrari F, Sainte-Rose B, Aitken J, Marthouse R, Hajbane S, Cunsolo S, Schwarz A, Levivier A, Noble K, Debeljak P, Maral H, Schoeneich-Argent R, Brambini R, Reisser J. Evidence that the Great Pacific Garbage Patch is rapidly accumulating plastic. Sci Rep. 2018 Mar 22;8(1):4666. doi: 10.1038/s41598-018-22939-w. PMID: 29568057; PMCID: PMC5864935.

Lin H, Peddada SD. Analysis of compositions of microbiomes with bias correction. Nat Commun. 2020 Jul 14;11(1):3514. doi: 10.1038/s41467-020-17041-7.

Lora, U., Schenone, L., Forn, I., Peters, F., Piiparinen, J., Kaartokallio, H., Lehtiniemi, M., & Sala, M. M. (2024). Weak effects of conventional and biodegradable microplastics on marine microbial communities. Frontiers in Marine Science, 11. https://doi.org/10.3389/fmars.2024.1502825

Lusher AL, Hernandez-Milian G, Berrow S, Rogan E, O'Connor I. Incidence of marine debris in cetaceans stranded and bycaught in Ireland: Recent findings and a review of historical knowledge. Environ Pollut. 2018 Jan;232:467-476. doi: 10.1016/j.envpol.2017.09.070.

McMurdie PJ, Holmes S. phyloseq: an R package for reproducible inter-active analysis and graphics of microbiome census data. PLoS ONE.2013;8(4): e61217. https://doi.org/10.1371/journal.pone.0061217.

Monger BC, Landry MR. Direct-interception feeding by marine zooflagellates: the importance of surface and hydrodynamic forces. Mar. Ecol. Prog. Ser. 65, 123-140 (1990).

Meike A. C. Latz, Vesna Grujcic, Sonia Brugel, Jenny Lycken, Uwe John, Bengt Karlson, Agneta Andersson, Anders F. Andersson . Short- and long-read metabarcoding of the eukaryotic rRNA operon: Evaluation of primers and comparison to shotgun metagenomics sequencing https://doi.org/10.1111/1755-0998.13623.

Mor R, Sivan A. Biofilm formation and partial biodegradation of polystyrene by the actinomycete Rhodococcus ruber: biodegradation of polystyrene. Biodegradation. 2008 Nov;19(6):851-8. doi: 10.1007/s10532-008-9188-0.

Naji A, Nuri M, Vethaak AD. Microplastics contamination in molluscs from the northern part of the Persian Gulf. Environ Pollut. 2018 Apr;235:113-120. doi: 10.1016/j.envpol.2017.12.046.

Narloch I, Gackowska A, Wejnerowska G. Microplastic in the Baltic Sea: A review of distribution processes, sources, analysis methods and regulatory policies. Environ Pollut. 2022 Dec 15;315:120453. doi: 10.1016/j.envpol.2022.120453.

Natarajan L, Soupam D, Dey S, Chandrasekaran N, Kundu R, Paul S, Mukherjee A. Toxicity of polystyrene microplastics in freshwater algae Scenedesmus obliquus: Effects of particle size and surface charge. Toxicol Rep. 2022 Oct 25;9:1953-1961. doi: 10.1016/j.toxrep.2022.10.013. PMID: 36518415; PMCID: PMC9743658.

Nayereh Saborimanesh. Microplastics disrupt microbial functions in aquatic ecosystems, Heliyon, Volume 12, Issue 3, 2026, e44579, ISSN 2405-8440, https://doi.org/10.1016/j.heliyon.2026.e44579.

Newton RJ, Jones SE, Eiler A, McMahon KD, Bertilsson S. A guide to the natural history of freshwater lake bacteria. Microbiol Mol Biol Rev. 2011 Mar;75(1):14-49. doi: 10.1128/MMBR.00028-10.

Okeke ES, Okoye CO, Chidike Ezeorba TP, Mao G, Chen Y, Xu H, Song C, Feng W, Wu X. Emerging bio-dispersant and bioremediation technologies as environmentally friendly management responses toward marine oil spill: A comprehensive review. J Environ Manage. 2022 Nov 15;322:116123. doi: 10.1016/j.jenvman.2022.116123.

Penna, A., Magnani, M., Fenoglio, I., Fubini, B., Cerrano, C., Giovine, M., & Bavestrello, G. (2003). Marine diatom growth on different forms of particulate silica: evidence of cell/particle interaction. Aquatic microbial ecology, 32(3), 299-306.

Peter Dauvergne and Jen Iris Allan. UN politics won’t deliver an ambitious plastics treaty. Science 2025, Vol. 390, No. 6768. DOI: 10.1126/science.aec1353.

Piwosz K, Pernthaler J. Seasonal population dynamics and trophic role of planktonic nanoflagellates in coastal surface waters of the Southern Baltic Sea. Environ Microbiol. 2010 Feb;12(2):364-77. doi: 10.1111/j.1462-2920.2009.02074.x. Epub 2009 Oct 2. PMID: 19799618.

PlasticsEurope. (2025). Plastics the Fast Facts 2025: Global and European plastics production and economic indicators. PlasticsEurope AISBL.

Prata JC, da Costa JP, Lopes I, Duarte AC, Rocha-Santos T. Effects of microplastics on microalgae populations: A critical review. Sci Total Environ. 2019 May 15;665:400-405. doi: 10.1016/j.scitotenv.2019.02.132. Epub 2019 Feb 10. PMID: 30772570.

Provencher JF, Vermaire JC, Avery-Gomm S, Braune BM, Mallory ML. Garbage in guano? Microplastic debris found in faecal precursors of seabirds known to ingest plastics. Sci Total Environ. 2018 Dec 10;644:1477-1484. doi: 10.1016/j.scitotenv.2018.07.101.

Pruesse E, Quast C, Knittel K, Fuchs BM, Ludwig W, Peplies J, Glöckner FO. SILVA: a comprehensive online resource for quality checked and aligned ribosomal RNA sequence data compatible with ARB. Nucleic Acids Res. 2007;35(21):7188-96. doi: 10.1093/nar/gkm864. Epub 2007 Oct 18. PMID: 17947321; PMCID: PMC2175337.

Quast C, Pruesse E, Yilmaz P, Gerken J, Schweer T, Yarza P, et al. TheSILVA ribosomal RNA gene database project: improved data processingand web-based tools. Nucleic Acids Res. 2012;41(D1):D590–6. https://doi.org/10.1093/nar/gks1219

R Core Team. (2024). R: A Language and Environment for Statistical Computing. R Foundation for Statistical Computing. https://www.R-project.org/

Santos RG, Machovsky-Capuska GE, Andrades R. Plastic ingestion as an evolutionary trap: Toward a holistic understanding. Science. 2021 Jul 2;373(6550):56-60. doi: 10.1126/science.abh0945.

Shu-Ling Hsieh, Shuchen Hsieh, Ruo-Qi Xu, Ya-Ting Chen, Chiu-Wen Chen, Reeta Rani Singhania, Yi-Chun Chen, Tsai-Hui Tsai, Cheng-Di Dong. Toxicological effects of polystyrene nanoplastics on marine organisms, Environmental Technology & Innovation, Volume 30, 2023, 103073, ISSN 2352-1864, https://doi.org/10.1016/j.eti.2023.103073.

Šimek K, Kasalický V, Jezbera J, Horňák K, Nedoma J, Hahn MW, Bass D, Jost S, Boenigk J. Differential freshwater flagellate community response to bacterial food quality with a focus on Limnohabitans bacteria. ISME J. 2013 Aug;7(8):1519-30. doi: 10.1038/ismej.2013.57. Epub 2013 Apr 4. PMID: 23552621; PMCID: PMC3721123.

Song JX, Scales BS, Nguyen M, Westberg E, Witalis B, Urban-Malinga B, Oberbeckmann S. Close encounters on a micro scale: microplastic sorption of polycyclic aromatic hydrocarbons and their potential effects on associated biofilm communities. Environ Microbiome. 2025 Jul 8;20(1):84. doi: 10.1186/s40793-025-00747-w. PMID: 40629382; PMCID: PMC12239331.

Stubbins A, Law KL, Muñoz SE, Bianchi TS, Zhu L. Plastics in the Earth system. Science. 2021 Jul 2;373(6550):51-55. doi: 10.1126/science.abb0354. PMID: 34210876.

Sun X, Liu T, Zhu M, Liang J, Zhao Y, Zhang B. Retention and characteristics of microplastics in natural zooplankton taxa from the East China Sea. Sci Total Environ. 2018 Nov 1;640-641:232-242. doi: 10.1016/j.scitotenv.2018.05.308.

Sun, R., Xu, K., Yu, L., Pu, Y., Xiong, F., He, Y., et al., 2021. Preliminary study on impacts of polystyrene microplastics on the hematological system and gene expression in bone marrow

cells of mice. Ecotoxicol. Environ. Saf. 218, 112296.

Sun Y, Duan C, Cao N, Li X, Li X, Chen Y, Huang Y, Wang J, Effects of microplastics on soil microbiome: The impacts of polymer type, shape, and concentration, Science of The Total Environment, Volume 806, Part 2, 2022, 150516, ISSN 0048-9697, https://doi.org/10.1016/j.scitotenv.2021.150516.

Ten Hietbrink S, Materić D, Holzinger R, Groeskamp S, Niemann H. Nanoplastic concentrations across the North Atlantic. Nature. 2025 Jul;643(8071):412-416. doi: 10.1038/s41586-025-09218-1. Epub 2025 Jul 9.

Ter Halle A, Ladirat L, Gendre X, Goudouneche D, Pusineri C, Routaboul C, Tenailleau C, Duployer B, Perez E. Understanding the Fragmentation Pattern of Marine Plastic Debris. Environ Sci Technol. 2016 Jun 7;50(11):5668-75. doi: 10.1021/acs.est.6b00594.

Tranvik LJ, Porter KG, Sieburth JM. Occurrence of bacterivory in Cryptomonas, a common freshwater phytoplankter. Oecologia. 1989 Mar;78(4):473-476. doi: 10.1007/BF00378736.

Viel T, Manfra L, Zupo V, Libralato G, Cocca M, Costantini M. Biodegradation of Plastics Induced by Marine Organisms: Future Perspectives for Bioremediation Approaches. Polymers (Basel). 2023 Jun 14;15(12):2673. doi: 10.3390/polym15122673.

Urban-Malinga B, Jakubowska-Lehrmann M, Białowąs M, Hallmann A. Microplastics cause neurotoxicity and decline of enzymatic activities in important bioturbator Hediste diversicolor. Mar Environ Res. 2022 Jul;179:105660. doi: 10.1016/j.marenvres.2022.105660. Epub 2022 May 25. PMID: 35690022.

Wright RJ, Erni-Cassola G, Zadjelovic V, Latva M, Christie-Oleza JA (2020) Marine Plastic Debris: A New Surface for Microbial Colonization. Environ Sci Technol 54:11657–11672. https://doi.org/10.1021/acs.est.0c02305.

Vanharanta M, Santoro M, Villena-Alemany C, Piiparinen J, Piwosz K, Grossart HP, Labrenz M, Spilling K. Microbial remineralization processes during postspring-bloom with excess phosphate available in the northern Baltic Sea. FEMS Microbiol Ecol. 2024 Jul 12;100(8):fiae103. doi: 10.1093/femsec/fiae103. PMID: 39039015; PMCID: PMC11302951.

Victoria M. Fulfer, Susanne Menden-Deuer. Heterotrophic Dinoflagellate Growth and Grazing Rates Reduced by Microplastic Ingestion. Front. Mar. Sci., 12 August 2021, Sec. Marine Pollution. https://doi.org/10.3389/fmars.2021.716349

Wu Y, Guo P, Zhang X, Zhang Y, Xie S, Deng J. Effect of microplastics exposure on the photosynthesis system of freshwater algae. J Hazard Mater. 2019 Jul 15;374:219-227. doi: 10.1016/j.jhazmat.2019.04.039.

Zhang C, Chen X, Wang J, Tan L. Toxic effects of microplastic on marine microalgae Skeletonema costatum: Interactions between microplastic and algae. Environ Pollut. 2017 Jan;220(Pt B):1282-1288. doi: 10.1016/j.envpol.2016.11.005.

CHAPTER III

Title: Limited Effects of Bacteria-Sized Microplastics on Coastal Baltic Microbial Dynamics

Uroosa[1,2], Aleksandar Stanojković[1], Sohrab Khan[1], Marcin Białowąs[1], Magdalena Jakubowska-Lehrmann[1], Kasia Piwosz[1*].

1 National Marine Fisheries Research Institute, ul. Kołłątaja 1, 81-332 Gdynia, Poland.

2 Institute of Oceanology, Polish Academy of Sciences, Powstańców Warszawy 55, 81-712 Sopot, Poland

* Corresponding author: kpiwosz@mir.gdynia.pl

Abstract

The impact of microplastics (MPs) on marine ecosystems remains poorly understood, particularly regarding how particle effects interact with natural microbial succession. We investigated how bacteria-sized polyethylene (PE) and polystyrene (PS) microplastics influence a natural coastal Baltic microbial food web over a five-day incubation using amplicon sequencing and genome-resolved metagenomics. Incubation time was the primary driver of change across bacterial, eukaryotic, and bacterial metagenome-assembled genome (MAG) datasets, whereas microplastics caused limited community-level effects. Natural succession shifted the food web toward late-stage organic matter recycling and a dominance of bacterivorous grazers. Out of 118 reconstructed bacterial MAGs, none of the dominant taxa responded to microplastic exposure. However, PE induced a narrow, polymer-specific response by enriching three low-abundance bacterial MAGs, including an *Arcticibacterium*-affiliated genome that uniquely carried an alkane-1-monooxygenase hydrocarbon-oxidation homolog. Gene mining confirmed that putative plastic-processing traits were structured by time rather than particle exposure. Overall, short-term exposure to bacteria-sized PE and PS caused limited disruption to microbial community structure, as natural food-web dynamics overrode broad particle effects. These findings demonstrate that microplastic impacts must be evaluated against baseline ecological succession while highlighting specific low-abundance candidate taxa for future functional validation

Key words: Microplastics, Microbiome, Metagenomics, Succession

1. Introduction

Microplastics have become a persistent component of marine pelagic habitats, not only as visible debris but as a continuum of particles whose ecological behaviour changes as they fragment, weather, and enter smaller size classes. Global plastic production, waste leakage, and diverse land- and sea-based inputs have generated a long-lived source of buoyant and suspended particles to the ocean (Jambeck et al., 2015; Geyer et al., 2017; Osman et al., 2023), while polymer chemistry, additives, density, crystallinity, and ageing regulate transport, fragmentation, surface reactivity, and persistence (Salehi et al., 2024). This matters for microbial ecology because the smallest microplastics approach the dimensions of planktonic cells and prey particles. In semi-enclosed seas such as the Baltic, where stratification, haloclines, and coastal retention can prolong particle residence, microplastics may remain embedded within the same microscale environment in which bacteria, protists, and dissolved organic matter interact (Gewert et al., 2017; Zhou et al., 2021; Mishra et al., 2022).

Microplastic effects on the pelagic microbial loop is crucial because it converts dissolved organic carbon into biomass, which then supports higher levels of the marine food web. Bacteria form the prey base for heterotrophic nanoflagellates (HNFs), which regulate bacterial abundance and diversity, recycle nutrients, and determine how efficiently bacterial carbon is retained or respired (Azam et al., 1983; Piwosz and Pernthaler, 2010). Recent work has sharpened this view by showing that dominant marine HNFs are adapted to natural planktonic bacterial abundances and differ strongly in functional responses and grazing strategies (Rodriguez-Martinez et al., 2022). Natural flagellate assemblages also show coordinated gene-expression dynamics during bacterivory, with phagotrophic activity linked to digestive enzymes such as peptidases and glycoside hydrolases (Obiol et al., 2023). Thus, HNFs are not interchangeable bacterial consumers;

they are physiologically and taxonomically structured grazers whose responses depend on prey abundance, prey quality, and the particles they encounter.

The microbial prey community is vulnerable to disturbance because HNFs feeding is selective and mechanistically constrained. Capture depends on microscale hydrodynamics, surface forces, prey motility, size, and digestibility (Monger and Landry, 1990; Boenigk et al., 2001). Bacterial taxa can be grazed unevenly, and protists can reshape bacterial communities through selective removal or avoidance, as shown in both heterotrophic and mixotrophic flagellate systems (Simek et al., 2013; Ivankovic et al., 2023). Because prey selection is strongly influenced by physical characteristics such as size and surface properties, particles that resemble bacterial cells may also interact with HNF feeding mechanisms. Although microplastics provide no nutritional value, bacteria-sized particles can still be encountered, captured, and ingested by grazers. Thus, bacteria-sized microplastics can act as non-living prey analogues that dilute edible prey and alter handling, vacuole processing, and grazer selectivity.

Polystyrene (PS) has received the greatest experimental attention. PS nano- and microplastics can inhibit bacterial growth and physiology in culture (Sun et al., 2018), induce dysbiosis and predicted functional shifts in surrounding seawater communities (Ye et al., 2021), and affect phytoplankton physiology and aggregation (Zhang et al., 2017; Wu et al., 2019). Protistan grazers can also ingest microplastics. Microzooplankton predation on microplastics may redirect particles through the microbial loop (Geng et al., 2021), while heterotrophic dinoflagellates that ingest PS beads show reduced grazing, growth, and secondary production (Fulfer and Menden-Deuer, 2021).

Polyethylene (PE) is highly abundant in the environment, but its effects on bacteria-HNF interactions remain less directly tested than those of PS. Available PE studies show that this polymer is biologically active as a microbial surface and as a grazer-sized particle: low-density PE

is rapidly colonized by bacteria in coastal sediment microcosms (Harrison et al., 2014), and marine plastic debris, including PE, can host bacterial assemblages distinct from surrounding seawater and natural particles (Dussud et al., 2018a, 2018b). Importantly, small PE beads can also enter protozoan grazing pathways. For instance, a ciliate *Sterkiella* sp. ingested and repackaged ≤5 micrometre PE particles into fecal material (Bermudez et al., 2021). However, this evidence comes mainly from bacterial colonization studies, mixed-polymer mesocosms, or ciliates rather than direct PE-HNF assays. Weathered microplastic mixtures tested in Baltic plankton mesocosms did not negatively affect HNF abundance (Ebbesen et al., 2024), while recent Baltic work found only weak microbial responses to conventional and biodegradable particles (Lora et al., 2024). Thus, PE can plausibly interact with microbial food webs, but its specific effects on HNF abundance, ingestion, and community composition remain insufficiently resolved.

PE and PS provide a useful contrast for this question because both are environmentally common but differ in density, surface properties, and environmental behaviour. PE is among the most abundant polymers in marine litter and is readily colonized by microbial biofilms (Harrison et al., 2014; Oberbeckmann et al., 2016), whereas PS is widely used in experimental ecotoxicology because it is available as size-defined spheres and has repeatedly shown biological effects in microbial and planktonic assays (Sun et al., 2018; Ye et al., 2021). Recent mesocosm studies have tested mixed-polymer additions or PS-based treatments and reported responses ranging from altered planktonic ecosystem functioning to weak microbial effects (Ebbesen et al., 2024; Montoya et al., 2024; Lora et al., 2024). However, these designs do not directly separate bacteria-sized PS, PE, and non-plastic particle effects on natural bacteria-HNF coupling, leaving this comparison unresolved.

Here, we used a natural coastal Baltic microbial community to test whether bacteria-sized PS and PE microplastics alter bacteria-HNF coupling. We compared PS and PE with size-matched glass particles to distinguish polymer-associated responses from general physical particle effects. We quantified bacterial and HNF abundances and assessed bacterial and eukaryotic community composition using 16S and 18S rRNA gene amplicon data. Genome-centric metagenomic analyses of the bacterial fraction were used to examine shifts in microbial population dynamics, functional pathways, and the distribution of genes associated with microplastics processing. We expected similar responses across plastic and glass treatments if physical particle interference dominated and divergent PS, PE or glass responses if polymer-specific effects were important.

2. Materials and Methods

2.1 Experimental design

We tested three particle treatments and an untreated control: 2 μm PS spheres (Polysciences, Polybeads microspheres, Cat. No. 19518-500), 1-4 μm PE beads (Cospheric, CPMS-0.96), and 1-4 μm silica microspheres used as a non-plastic particle control (Bangs Laboratories, Inc., Cat. No. SSD5000). Final particle concentrations were 5.34×10^9 PS spheres mL-1, 5.54×10^9 PE beads mL-1, and 5.28×10^9 silica spheres mL-1, corresponding to the targeted 1:1 particle:bacteria abundance ratio. In addition, the particle-free control was prepared in triplicate (Fig. 1).

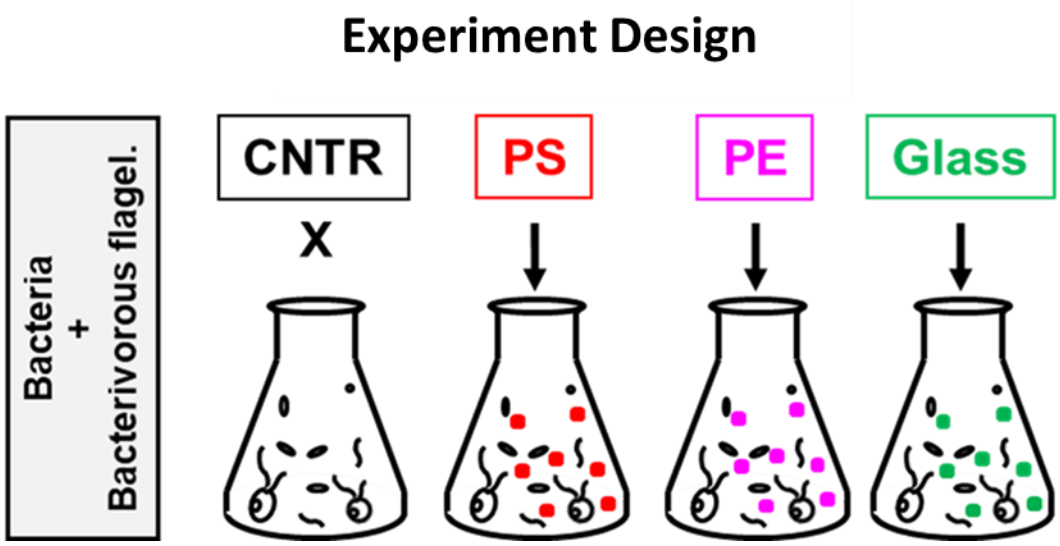

Figure. 1 Schematic representation of the experimental design, including the control and treatments including polystyrene (PS), polyethylene PE and glass (G) microspheres used to assess their effects on microbial communities.

2.2 Setting up the experiment

Eighty liters of surface seawater were collected from a coastal station (54°31'05.2''N; 18°33'21.5''E) in the Gulf of Gdańsk (southern Baltic Sea, Poland) into containers thoroughly cleaned with sanitizing detergent, 10% bleach, and MilliQ water, and rinsed three times with the sampled water. The water was prefiltered on-site through a 10 µm mesh plankton net and transported to the laboratory within 30 minutes. Further fractionation through 10 µm polycarbonate filters (diameter 142 mm, Millipore) was done using an autoclaved gravity filtration apparatus made of stainless steel (Sartorius) that was sterilized with boiling MilliQ water each time the filter was exchanged. Seventy two liters of filtered water were distributed into twelve 10-litre glass bottles (six liters per bottle). Afterwards, the bottles were closed with silica plugs and put into the

water bath at *in situ* temperature (±15°C, room temperature). Bottles were incubated in the dark. The content of each bottle was continuously aerated to maintain water movement and prevent sedimentation of microspheres. The air was delivered via sterile 0.2 µm syringe filters and autoclaved aeration stones that were exchanged after each sampling.

The filtered water was used for the analysis of the total bacterial and HNFs abundance, as well as microbial community composition at time T1(0h) as described below. Subsequent samples were collected from the experimental bottles into sterile glass bottles under a fume hood every 24 h for a total of five days T1(0h), T2 (24h), T3(48h), T4(72h), T5 (96 h). This time has been found optimal to measure microbial responses at both single species (Geng et al. 2021) and community level (Šimek et al., 2013).

2.2 Abundance of Bacteria and Heterotrophic Nanoflagellates

Three ml of water sampled for bacterial abundance was fixed with 150 µl of prefiltered 40% formalin (Final concentration: fc = 2%). The fixed samples were then filtered onto black-stained polycarbonate filters (PC; 25 mm, 0.2 µm) and stained with 4'-6-diamidino-2-phenylindole (DAPI; 1 µg ml^{-1}). For HNF, 25 ml of sample water was fixed with neutral Lugol solution (fc = 1%) and particle-free formalin (fc = 2%), followed by decolorization with 3% $Na_2S_2O_3$ (Sherr BF et al., 1987). The fixed samples were then filtered onto black-stained polycarbonate filters (PC; 25 mm, 0.8 µm) that were then air-dried and stained with 4'-6-diamidino-2-phenylindole (DAPI; 1 µg ml^{-1}). 100 bacterial or HNFs cells were enumerated from randomly selected fields of view at 1000× magnification using epifluorescence microscopy (Nikon upright microscope Eclipse 80i) equipped with an Hg-lamp with UV/blue light filter for DAPI.

Differences in growth rates were assessed with a Kruskal-Wallis test at a significance level alpha = 0.05. Post-hoc Dunn's test with Benjamini-Hochberg correction for multiple testing was

conducted to identify differences between the treatments. For this analysis, a significance level of alpha = 0.1 was assumed.

2.3 Control of contamination

We took necessary precautions to prevent any contamination during the experiment and analyses. Processes were performed under a fume hood when needed to lessen cross-contamination, particularly to avoid the air-borne plastic particles. No plastic materials were used in the filtration set-up and other laboratory procedures. Working surfaces and necessary equipment were continually rinsed with MilliQ, followed by 70% alcohol and additionally decontamination solution (1% NaOCl, 1% NaOH, 1% detergent) in case of DNA extraction. In addition, the fume hood used for DNA extraction was sterilized using a UV lamp. To control for contamination during the sample collection and processing, blank controls consisting of filtered sterile MilliQ water were collected alongside the samples for DNA extraction. Although no DNA was detected, these blank controls were included in library preparation and sequencing, where amplification failed, confirming the absence of contamination during biomass collection and DNA extraction (Khan et al., 2025).

2.4 DNA extraction and metagenome sequencing

A liter of water was collected into sterile glass bottles. Two half-liter water samples were filtered onto mixed-cellulose-esters filters (47 mm, 0.22 µm, Millipore, Darmstadt, Germany), placed into sterile 2 ml cryotubes, flash-frozen in liquid nitrogen and stored at -80°C. DNA was extracted using our custom, optimized protocol combining the GeneMATRIX Soil DNA Purification Kit (Eurx, Gdansk, Poland) and GeneMAGNET PCR Clean-Up Beads (Eurx, Cat. ES3401). The extracted DNA samples were stored at -80°C. The quality and concentration of the extracted DNA were assessed with gel electrophoresis, NanoDrop One (Thermo Scientific), and QubitFlex

Fluorometer (Invitrogen, CAT.Q33327) using Qubit™ 1X dsDNA High Sensitivity (HS) Assay Kit.

Extracted DNA samples were sent to Novogene (Cambridge, UK) for sequencing on the Illumina NovaSeq 6000 platform (2x250 bp paired-end mode). The V3-V4 regions of 16S rRNA genes were amplified for bacterial community (Bolyen E et al., 2019; Fadeev Eduard et al., 2021), and the V6-V8 fragment of 18S rRNA gene was sequenced for eukaryotic community (Meike et al., 2022).

For metagenomics sequencing was performed for 34 samples spanning the three experimental sampling points (T1, T3, and T5).

2.5 Amplicon sequence analysis

Demultiplexed sequence data underwent quality control and pre-processing using the DADA2 pipeline within the R environment, version 4.3.2 (Callahan BJ et al.,2016). The initial dataset comprised an average of ± 52362 reads per sample for 16S and ± 52259 reads per sample for 18S. These reads were then filtered and trimmed using the filterAndTrim function with parameters set to maxN = 0, maxEE = c(2,2), and truncQ = 2, as implemented in the DADA2 package (v1.12.1) within the R/Bioconductor framework. Amplicon sequence variants (ASVs) were then inferred, and chimeric sequences were removed using the 'consensus' method (Callahan BJ et al., 2017). The final dataset included an average of ± 46716 reads per sample for 16S and ± 41592reads per sample for 18S.

Taxonomic assignment of the ASVs was carried out using the *assignTaxonomy* function in DADA2, leveraging curated, reference databases: SILVA version 138.1 for bacterial 16S rRNA gene sequences (Pruesse E et al., 2007; Quast C et al.,2012) and PR2 version 5.0.0 for 18S rRNA

gene sequences (Guillou et al., 2012). Community composition bar plots were generated using ggplot2 v3.4.3 (Ginestet C, 2011).

2.6 Amplicon data analysis

Amplicon data were analyzed using phyloseq v1.46.0 (McMurdie PJ et al.,2013), and non-eukaryotic/non-bacterial and unclassified sequences (NSs) at each taxonomic level were filtered out, retaining only eukaryotic and bacterial data.

To account for differences in sequencing depth, samples were rarefied 1000 times to the minimum read count (using rrarify, vegan, R). The resulting abundance tables were averaged to generate a representative abundance matrix. Samples with fewer than 10,000 reads were excluded, and taxa were aggregated at the genus level (using tax_glom) to facilitate diversity comparisons. Sequences unassigned at the genus level were grouped based on the phylogenetic analysis as described above. Final data were visualized using ggplot2 v3.4.3 (Ginestet C, 2011).

All multivariate statistical analyses for amplicon data were conducted using PRIMER (v7.1.17) software (Clarke and Gorley, 2015) along with the PERMANOVA+ add-on (v1.0.7) with 9999 permutations (Anderson et al., 2008). The effects of the factors 'Time' and 'Polymer type' on microbial community composition were tested using PERMANOVA, with significance set at $p < 0.005$. To visualize similarities among communities in response to exposure to various microsphere types and concentrations, nMDS based on Bray-Curtis similarities of fourth root-transformed Eukaryotic/Bacterial ASV relative abundance data was used to assess changes in community composition across time points and treatment concentrations. (Clarke and Gorley, 2015).

2.7 Metagenome assembly and binning

Raw sequencing reads were quality-filtered and trimmed using Trimmomatic v0.39 (Bolger et al., 2014) to remove adapter sequences and low-quality bases. Read quality before and after filtering was assessed with MultiQC v1.19 (Ewels et al., 2016). The quality-controlled paired-end reads were assembled de novo using MEGAHIT v1.2.9 (Li et al., 2015), and the assembly metrics were calculated with QUAST v5.3.0 (Gurevich et al., 2013). Open reading frames from each contig from 34 assemblies were predicted with Prodigal v2.6.3 (Hyatt et al., 2010) and the -meta parameter. The metagenomic reads were mapped to the contigs with bwa-mem2 v2.2.1 (Li, 2013) and SAMtools v1.13 (Li et al., 2009), and then genomic binning was performed with MaxBin2 v2.2.7 (Wu et al., 2014) and MetaBAT2 v2.12 (Kang et al., 2019). Bins obtained from the two binners were integrated using a consensus binning tool, DAS_Tool v1.1.7 (Sieber et al., 2018). For each MAG, completeness and contamination were determined using checkm2 v1.1.0 (Chklovski et al., 2023). For downstream analyses, all MAGs with completeness less than 50% were excluded. To reduce potential contamination of MAGs, they were decontaminated with MDMcleaner v0.8.7 (Vollmers et al., 2022) using an MDMcleaner reference database v1 (Vollmers, 2021; https://zenodo.org/records/5698995#.YkylqjVCRhE). The quality of decontaminated bins was checked with checkm2 and the lineage_wf parameter. To create a non-redundant set of MAGs across samples, all reconstructed MAGs were pooled together, and dereplication was performed at the strain level with Galah v0.4.2 (https://github.com/wwood/galah) at 99% ANI identity and selecting only MAGs with > 70% completeness and < 10% contamination.

2.8 Taxonomic profiling and phylogeny

The taxonomy of each MAG was assigned with GTBD-Tk v2.1.1 (Chaumeil et al., 2020) against the GTDB r207 v2 database using the classify_wf parameter. All MAGs were functionally annotated with prokka v1.14.6 (Seemann, 2014), and amino acid sequences were used for multiple sequence alignment (MSA). An MSA based on single-copy orthologs was constructed with Orthofinder v2.5.5 (Emms & Kelly, 2019). The phylogenetic relationships between MAGs were inferred using the maximum likelihood approach with IQ-TREE v2.4 (Minh et al., 2020). ModelFinder (Kalyaanamoorthy et al., 2017) identified Q.pfam+I+G4 as the best-fitting substitution model, and branch support was assessed with 2000 ultrafast bootstrap replications.

2.9 Genome annotations and relative abundances of MAGs

The coverage percentage, relative abundance, and read count of the dereplicated MAGs in each assembly were computed by read mapping to the corresponding metagenome assembly with CoverM v0.7.0 (Aroney et al., 2025). The following arguments were used: coverm genome relative_abundance mean count –min-read-percent-identity 0.95 –min-read-aligned-percent 0.75 –trim-min 0.1 and –trim-max 0.9. To determine differentially abundant MAGs between each treatment and timepoint, DeSeq2 (Love et al., 2014) was employed in R v4.4.3 (R Core Team, 2024). The P values were adjusted using the Benjamini-Hochberg false discovery rate, and observations with adjusted $P < 0.05$ and log2 fold change (log2FC) > 1 were considered differentially abundant, the latter corresponding to a 2-fold difference between the treatments.

EnrichM v0.6.8 (https://github.com/geronimp/enrichM) and the function ‘annotate’ used DIAMOND v2.1.24 (Buchfink et al., 2015) to blast MAG protein sequences against the EnrichM database, which incorporates a KO-annotated Uniref100 database. The EnrichM ‘classify’ function was used to find genes and pathways enriched in particular treatment and timepoint based

on statistical findings from Fisher's exact test. KeggDecoder v1.3 (Graham et al., 2018) was used to determine the completeness of pathways within MAGs as well as pathways associated with genes that were enriched at a particular timepoint.

Putative plastic-degrading enzymes of MAGs were searched against the PlasticDB database (available at https://plasticdb.org/downloaddata, Gambarini et al., 2022) with blastp (≥30 % amino acid similarity and ≥70 % alignment). This database comprises amino acids for a total of 329 enzymes, covering various plastic types, such as PE, PS, polyamide (PA), polyethylene terephthalate (PET), polyethylene glycol (PEG), and polylactic acid (PLA), low-density polyethylene (LDPE), and polyurethane (PU). Relatively low thresholds were applied to capture potentially distant homologs and estimate the potential of bacteria to utilize microplastics as a carbon source.

2.10 Data for enzymes putatively linked to plastic biodegradation

To identify the abundance shifts of plastic-degrading enzymes across the treatments, predicted protein sequences of metagenome assemblies were searched against the PlasticDB database. Hits were filtered with a percent identity ≥40, e-value <1e-05, bitscore ≥ 60, and query coverage ≥70. Annotated genes were then extracted from all assemblies with seqkit v2.10 (Shen et al., 2016) and merged to make plastic gene catalogues. To make a non-redundant set of genes related to specific plastic, gene products were clustered at 95% sequence similarity using CD-HIT v4.8.1 (Fu et al., 2012) with -aS 0.8. Gene abundance quantification was computed by mapping paired-end reads from each sample against the gene catalogue using CoverM. Hits to a sequence are weighted based on the sequence target length and further normalized to produce reads aligned to the reference assembly per kilobase per million reads (RPKM). Differences in abundances of plastic degradation

enzymes over timepoints and treatments were performed with analysis of variance (ANOVA), followed by post hoc pairwise comparisons with the package emmeans v2.0.3 (Lenth et al., 2019).

3. Results

3.1 Microbial community growth

Heterotrophic nanoflagellates' abundance changed over time and the temporal dynamics differed among treatments (Fig. 2a). HNFs abundance initially increased from T1 to T3 in the control and particle-amended treatments. After T3, HNFs abundance remained relatively stable around T4 and then decreased by T5 in the PS and PE treatments, whereas it increased or remained higher in the control and glass treatments. Based on these temporal patterns, three growth phases were defined for HNF abundance: Phase 1 (T1-T3), Phase 2 (T3-T4), and Phase 3 (T4-T5; Fig. S1).

The presence of particles significantly affected HNFs growth rates during Phase 1 or Phase 2 according to Kruskal-Wallis tests ($p<0.05$, Dunn tests did not identify significant pairwise differences between treatments. During Phase 3, growth rates differed among treatments (Kruskal-Wallis, $p = 0.04$), with a significant difference between the glass and PE treatments (Dunn test, $p = 0.02$). No other pairwise comparisons were significant. However, growth rates calculated over the whole duration of the experiment (T1-T5) differed among treatments (Kruskal-Wallis, $p = 0.02$), with a significant difference between the glass and PS treatments (Dunn test, $p = 0.03$).

Bacterial abundance also changed over time, with an initial increase between T1 and T2 in all treatments (Fig. 2b). Thereafter, bacterial dynamics differed among treatments, although no consistent treatment-specific pattern was observed. Four bacterial growth phases were defined from the abundance trajectories: Phase 1 (T1-T2), Phase 2 (T2-T3), Phase 3 (T3-T4), and Phase 4 (T4-T5) (Fig. S2).

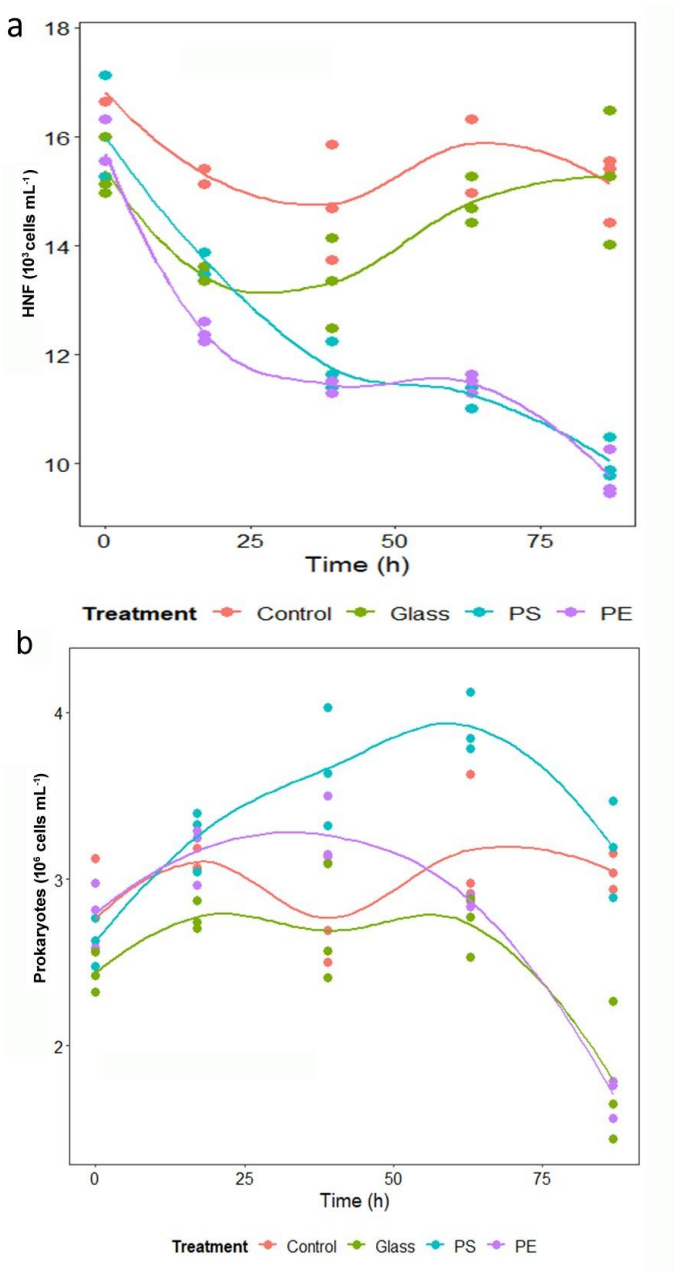

Figure. 2. Temporal dynamics of microbial abundance across Control, PS, PE and Glass treatments over the incubation period. (a) Heterotrophic nanoflagellate (HNFs) abundance and (b) prokaryotic abundance measured at five sampling time points (T1–T5). Lines represent changes in abundance over time across treatments.

Particle addition did not significantly affect bacterial growth rates during Phase 1 ($p = 0.10$). Significant overall treatment effects were detected during Phase 2 (Kruskal-Wallis, $p = 0.02$), Phase 3 ($p = 0.03$), and Phase 4 ($p = 0.03$); however, most Dunn pairwise comparison tests were not significant. The only significant pairwise difference was observed between the control and PE treatments during Phase 4 (Dunn test, $p = 0.03$). However, no pairwise significance was found between T1 and T5.

3.2 Changes in eukaryotic community composition

Eukaryotic community composition changed significantly over the course of the experiment, based on PERMANOVA analysis of 18S rRNA gene amplicon data ($p < 0.005$; Fig. 3a; Table S1).

Pairwise PERMANOVA comparisons showed significant differences between all time points (Table S1), indicating a strong temporal restructuring of the eukaryotic community. In contrast, no significant differences were detected between treatments at individual time points ($p > 0.005$), suggesting that incubation time had a stronger effect on eukaryotic community composition than particle type.

At the division level, Stramenopiles, along with Alveolata, Haptophyta, and Rhizaria, initially dominated the eukaryotic community across all treatments (Fig. 4a). Over time, Stramenopiles increased in relative abundance and became the dominant group by T5, reaching approximately 75% of total eukaryotic reads. Within Stramenopiles, diatoms *Chaetoceros* and *Cyclotella* dominated at the beginning of the experiment, whereas heterotrophic nanoflagellates, including *Paraphysomonas* and *Spumella*, increased toward the later time points (Fig. 4b).

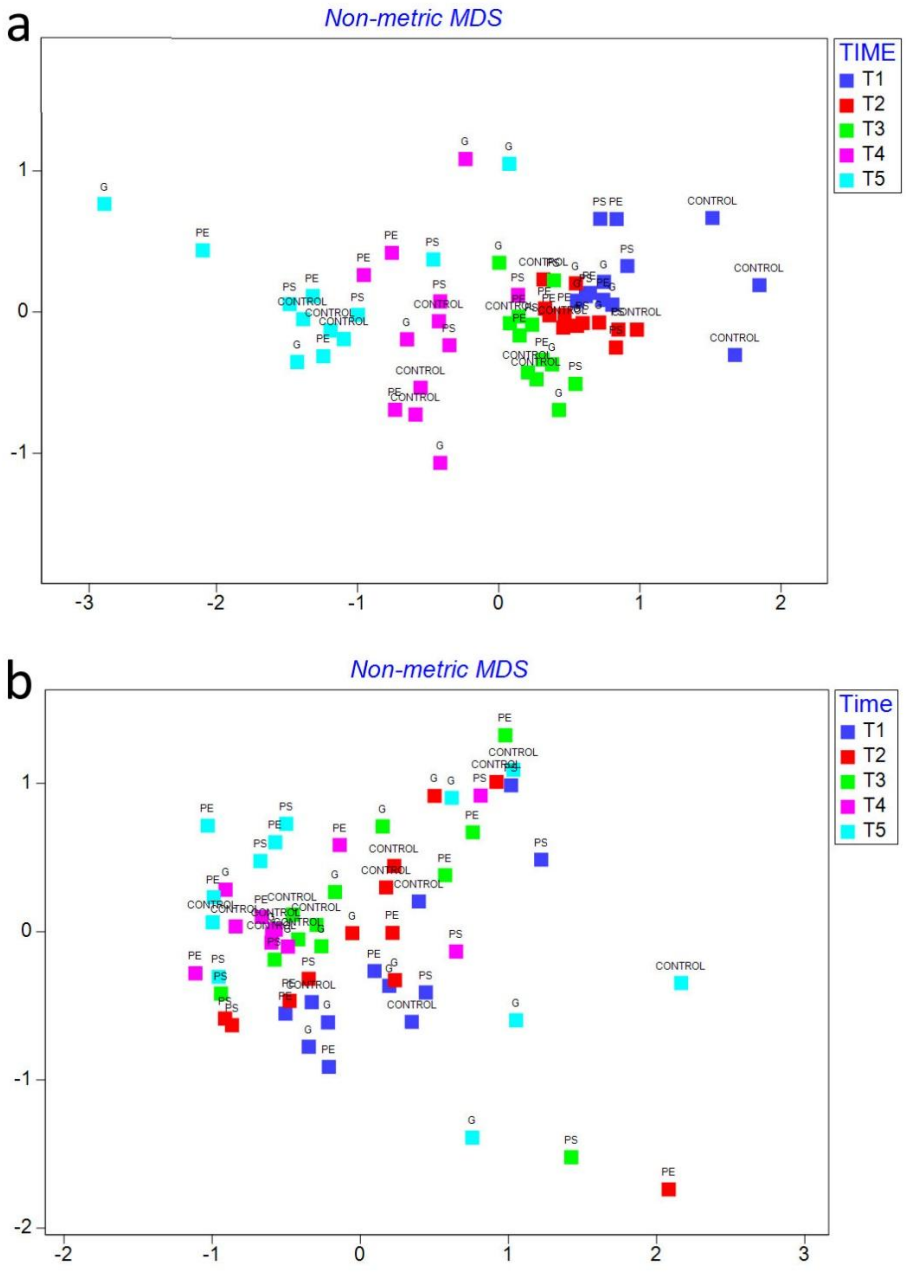

Figure. 3 Non-metric multidimensional scaling (NMDS) ordination showing temporal changes in community composition across Control, PS, PE, and Glass (G) treatments over the incubation period (T1–T5). (a) Eukaryotic community composition based on 18S rRNA gene amplicon data. (b) Bacterial community composition based on 16S rRNA gene amplicon data. Differences in community structure across time and treatments were assessed using PERMANOVA analysis.

Alveolata represented a substantial fraction of the eukaryotic community at T1, contributing up to approximately 40% of reads, but declined strongly by T5 in all treatments (Fig. 4a). Within Alveolata, *Karlodinium* dominated throughout the experiment, contributing approximately 80-90% of alveolate reads, while *Urotricha* increased slightly at later time points, particularly at T4 and T5 (Fig. 4c).

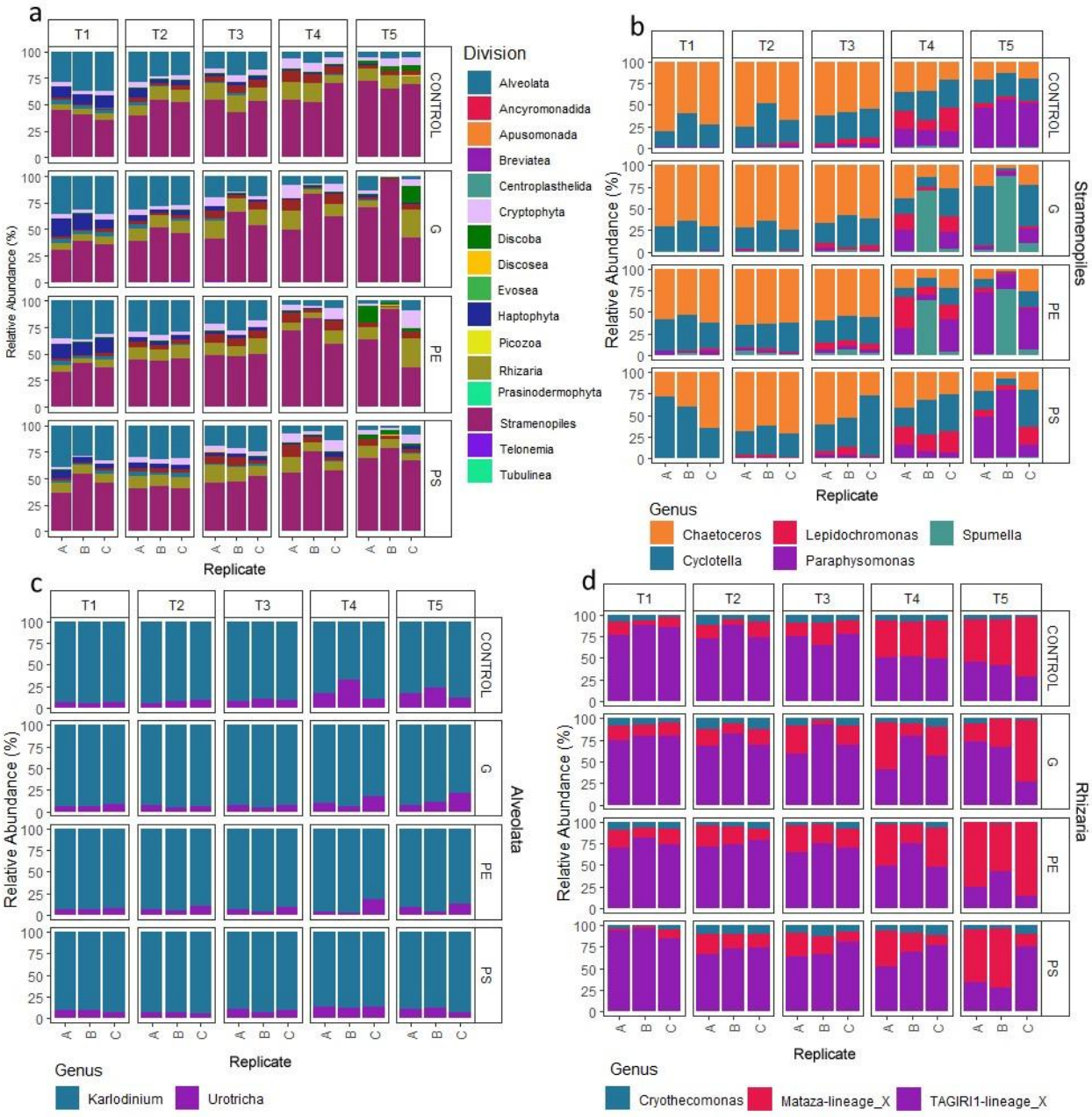

Figure. 4 Temporal changes in the relative abundance of dominant eukaryotic taxa across Control, Glass, PE, and PS treatments over the incubation period (T1–T5). (a) Relative abundance of major eukaryotic divisions. (b) Relative abundance of dominant stramenopile genera. (c) Relative abundance of dominant alveolate genera. (d) Relative abundance of dominant rhizarian genera. Community composition is shown for three biological replicates (A–C) within each treatment at each sampling time point.

Haptophyta decreased over time and were nearly absent at later time points, with *Chrysochromulina* as the dominant detected genus. Rhizaria showed an opposite temporal pattern, increasing in relative abundance around T3 and contributing approximately 25-30% of total reads at this time point (Fig. 4d). Within Rhizaria, TAGIRI-lineage_X dominated during the early and middle stages of the experiment, whereas Mataza-lineage_X became more prominent by T5.

3.3 Changes in bacterial community composition

Bacterial community composition also changed over time, based on PERMANOVA analysis of 16S rRNA gene amplicon data (Fig. 3b; Table S1). Pairwise comparisons showed significant differences between several time points, particularly between T1 and later sampling points, and between T2 and T5. However, no significant differences were detected between particle treatments at individual time points. Thus, as observed for the eukaryotic community, bacterial community composition was mainly structured by incubation time rather than by particle type.

Across treatments, the bacterial community was dominated by Pseudomonadota, Bacteroidota, and Actinobacteriota, which together accounted for most bacterial reads (Fig. 5a). Although treatment-specific differences were weak, the relative abundance of the dominant phyla changed over time.

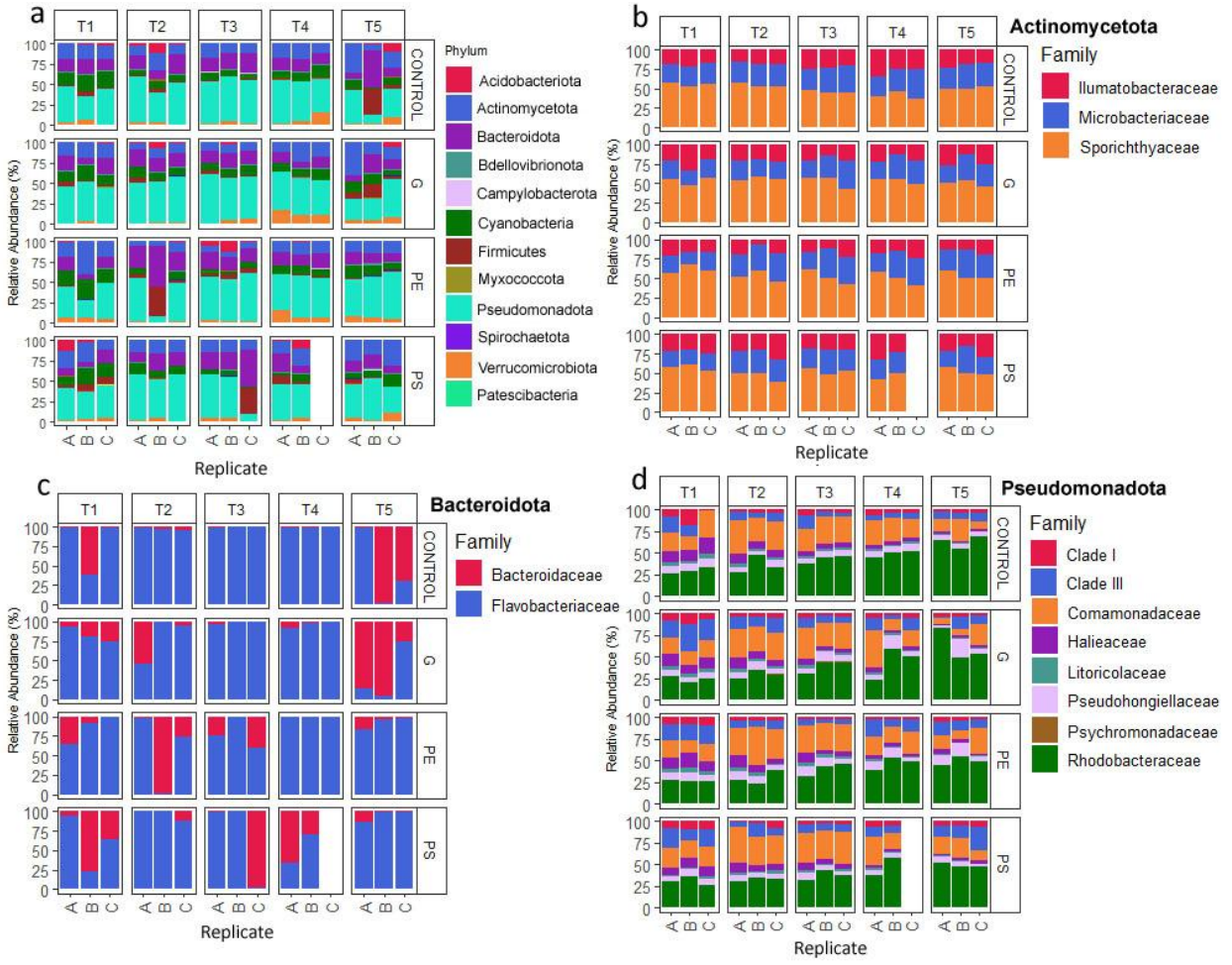

Figure. 5 Temporal changes in bacterial community composition across Control, Glass, PE, and PS treatments over the incubation period (T1–T5). (a) Relative abundance of dominant bacterial phyla. (b) Relative abundance of dominant families within Actinomycetota. (c) Relative abundance of dominant families within Bacteroidota. (d) Relative abundance of dominant families within Pseudomonadota.

Actinobacteriota generally decreased until T3 and then increased again toward T5, particularly in the glass and PE treatments, while remaining more stable in the control and PS treatments. Within

Actinobacteriota, Sporichthyaceae, Microbacteriaceae, and Ilumatobacteraceae were the dominant families, together accounting for most actinobacterial reads (Fig. 5b). Sporichthyaceae was especially abundant in the control, PS, and glass treatments, contributing approximately 50-60% of actinobacterial reads across several time points. However, no clear treatment-specific shift among the dominant actinobacterial families was observed.

Bacteroidota showed a temporal pattern broadly opposite to Actinomycetota, increasing until approximately T3 and then decreasing toward the end of the experiment (Fig. 5a). Flavobacteriaceae was the dominant family in most samples (Fig. 5c), while Bacteroidaceae increased in some later samples, particularly at T5 in the control and glass treatments, although this pattern was not consistent across all replicates.

Proteobacteria remained abundant throughout the experiment and generally increased or remained stable over time, except in some control and glass samples at T5 (Fig. 5a). Rhodobacteraceae and Comamonadaceae were the main contributing families within Pseudomonadota (Fig. 5d). Rhodobacteraceae increased toward T5 in most treatments, whereas Comamonadaceae was more abundant at intermediate time points, especially T2 and T3, before declining by T5.

3.4 MAG diversity and community representation

Shotgun Illumina sequencing yielded a total of 148.3 Gb of raw paired-end reads, with 1,108 million raw reads and 32.6 million paired-end reads per sample on average. After quality filtering and trimming, 132.9 Gb of data and 979 million paired-end reads remained, corresponding to an average of 28.8 million reads per sample (range 12.3 – 49 million). Assembly with MEGAHIT produced an average of 454,181.7 contigs per sample, of which 142,406 were larger than 1000 bp in length. The average proportion of mapped reads was 87.5%, with an average assembly coverage of 12.4x (range 8 – 17x).

The binning workflow reconstructed 2,371 MAGs. Dereplication at 99% ANI yielded 118 non-redundant medium-quality MAGs (completeness >70% and contamination <10%), including 56 high-quality MAGs (completeness >90% and contamination <5%). The MAGs had an average genome size of 2.67 Mb (range 0.89-7.3Mb), average completeness of 88% (range 70.1-100%), and contamination of 1.97% (range 0-8.5%).

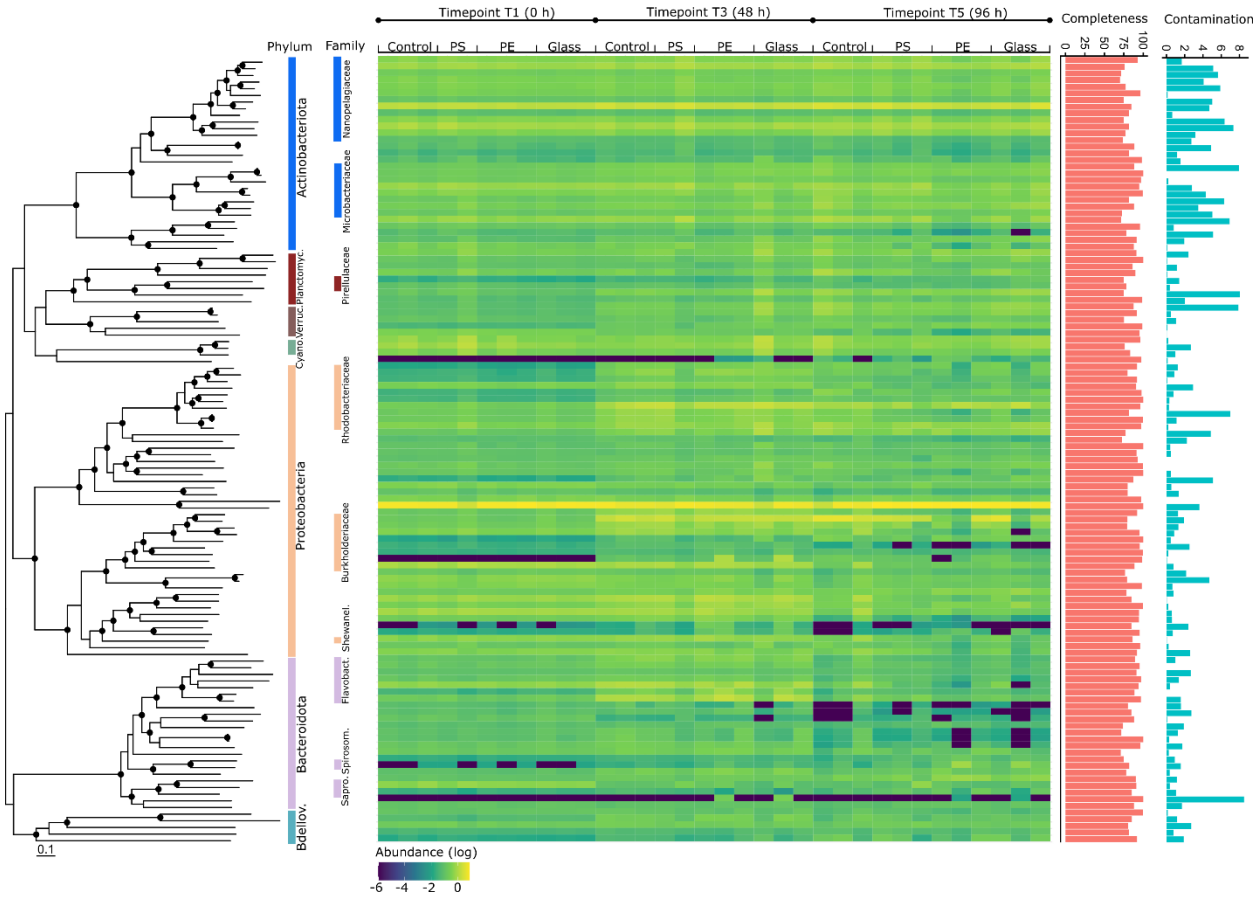

Figure. 6 Phylogenomic tree and relative abundance patterns of metagenome-assembled genomes (MAGs) recovered across Control, PS, PE, and Glass treatments at three sampling time points (T1, T3, and T5). The phylogenomic reconstruction is based on 27,430 aligned amino acid sites and includes 118 non-redundant medium- to high-quality MAGs classified into eight bacterial

phyla. The heatmap shows log-transformed MAG abundance across samples, while bar plots indicate genome completeness and contamination estimates for each MAG.

Phylogenomic reconstruction based on 27,430 aligned amino acid sites resolved MAGs into eight bacterial phyla (Figure. 6), dominated by Proteobacteria (44 MAGs), Actinobacteria (29 MAGs), and Bacteroidota (23 MAGs), followed by Planctomycetota (8 MAGs), Verrucomicrobiota (5 MAGs), Cyanobacteria (3 MAGs), Myxococcota (1 MAG), and Bdellovibrionota (5 MAGs). Notably, 82 MAGs (69%) could not be attributed to a described species, indicating that a substantial proportion of the recovered genomes represent previously uncharacterized microbial diversity.

3.5 Temporal succession shapes MAG abundance and differential responses

A total of 20 MAGs exceeded 1% relative abundance in at least one treatment (Figure. 6), spanning five phyla (Actinobacteriota, Bacteroidota, Cyanobacteria, Planctomycetota, and Proteobacteria). However, none of these abundant MAGs showed significant enrichment in response to either microplastic treatment (log2FC < 1), consistent with the amplicon-based analyses.

Differential abundance analysis identified only three MAGs significantly enriched in the PE treatment relative to the control (log2FC ≥ 1, adjusted $P < 0.05$). These belonged to the family Spirosomaceae (two MAGs, including one assigned to the genus *Acricibacterium*) and the family Shewanellaceae (genus *Shewanella*). These MAGs encoded 22 and 11 putative genes, respectively, associated with the processing of PEG, PLA, PET, and PS (Figure. 7). The enrichment of these MAGs in the PE treatment suggests that taxa with a broad plastic- and polymer-degradation potential may be selectively favored in the presence of PE particles, although the overall treatment effect remained weak.

Across all 118 MAGs, 18 (15.3%) and 8 MAGs (6.8%) encoded homologs linked to PE and PS processing, respectively. MAGs harboring putative PE-processing genes (alkane hydroxylases, laccases, copper oxidases) were predominantly assigned to Alpha- and Gammaproteobacteria, while those containing PS-processing genes (alkane-1-monooxygenase) belonged to the class Bacteroidia.

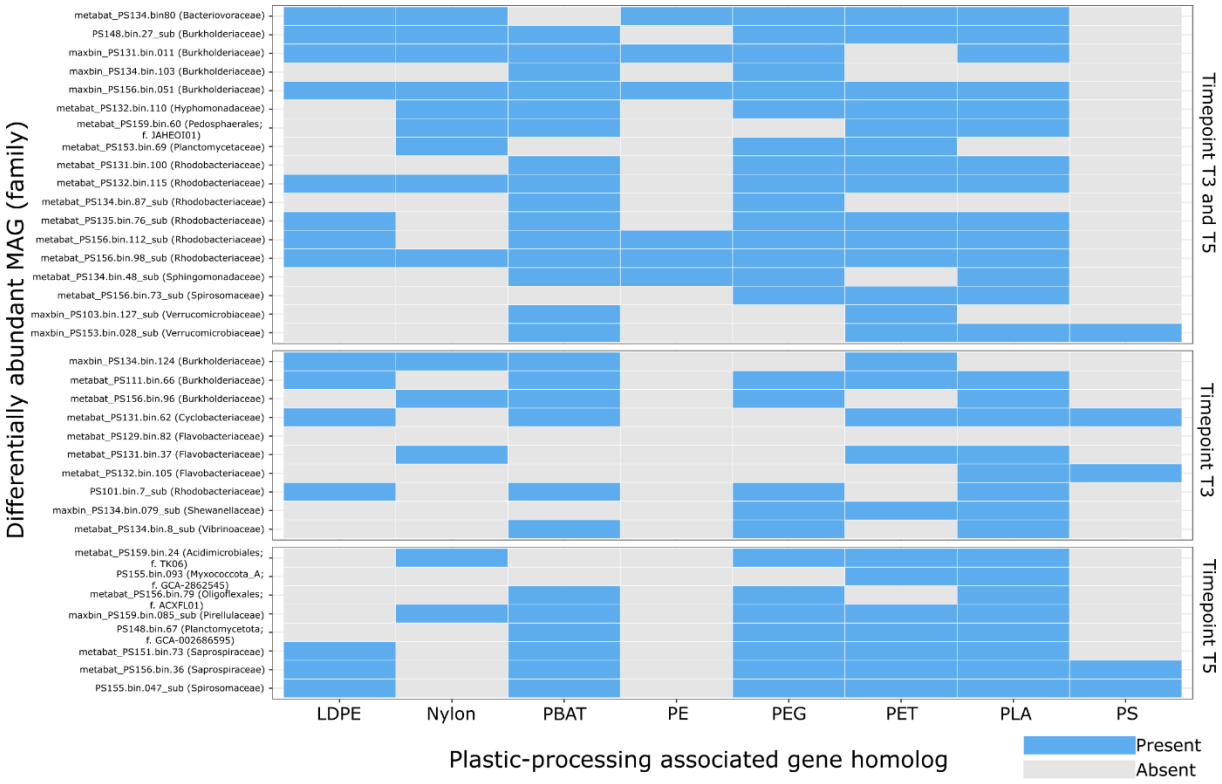

Figure. 7 Presence and absence of genes putatively involved in processing of microplastics across differentially abundant MAGs at T3 and T5.

In contrast to the limited treatment-specific effects, temporal variation strongly shaped the community composition. A total of 28 MAGs were differentially abundant at T3 (including 10

unique to this timepoint), whereas 25 MAGs were differentially abundant at T5 (including 8 unique MAGs; log2FC ≥ 1, adjusted $P < 0.05$). These findings indicate that microbial succession over time, rather than exposure to PE or PS particles, was the primary driver of changes in community composition. The considerably larger number of temporally responsive MAGs compared with treatment-responsive MAGs further supports the amplicon results that natural community dynamics outweighed the effects of MP exposure during the experimental incubation time.

To investigate whether temporal shifts in community composition were accompanied by functional changes, MAGs enriched at T3 and T5 were subjected to KEGG Orthology enrichment analysis. Enriched pathways were broadly similar between the two timepoints, although several metabolic pathways displayed higher completeness at T5, suggesting ongoing functional succession within the microbial community (Supplimentary Figure. 4). In particular, MAGs enriched at T5 contained a higher representation of genes associated with the amino acid metabolism (e.g., M00079 – keratan sulfate degradation, M00077 – chondroitin sulfate degradation, M00087 – beta-oxidation). In contrast, MAGs differentially abundant at T3 showed greater representation of pathways related to carbohydrate metabolism (M00151 and M00156 – cytochrome c oxidase, M00118 – glutathione biosynthesis), stress response (M00970 – proline degradation, M00985 – sulfide oxidation), and secretion (M00597 – anoxygenic photosystem II, M00595 – sulfur oxidation) (Figure. 8). This indicates a shift in dominant metabolic processes during the incubation period from oxidative stress and mixed nutrient utilization to resource specialization and recycling organic matter during the incubation period.

3.5 Key putative plastic-processing enzymes across metagenomes

To assess whether microplastic exposure influenced the distribution and potential activity of enzymes linked to plastic processing, genome mining was performed against the PlasticDB database across all metagenomic assemblies. The abundance patterns of putative plastic-processing enzymes showed limited treatment-specific responses. Enzymes associated with the processing of LDPE, PE, PEG, PET, PLA, PS, and PU exhibited a strong temporal structure across the experiment (ANOVA, R^2 = 0.36-68, $p < 0.001$). In contrast, only enzymes associated with nylon processing (i.e., hydrolases and polyamidases) differed significantly in abundance between the control and PE treatment at T5 (ANOVA, $R^2 = 0.30$, $p < 0.01$).

4. Discussion

The central outcome of this experiment is that the microbial community responded more strongly to incubation time than to the addition of PE or PS particles. Rather than producing clearly separated plastic-specific communities, the treatments were embedded within a broader temporal reorganization of bacterial, eukaryotic, and genome-resolved community structure. This is important because short-term microplastic experiments can easily cloud particle effects with natural succession in confined seawater. Rapid changes in prokaryotic populations have been reported in marine succession incubations (Haro-Moreno et al., 2019), and natural heterotrophic flagellate assemblages also show coordinated changes during bacterivory incubations (Obiol et al., 2023). Thus, the dominant time effect was not merely experimental background variation, but reflected rapid ecological succession within the confined microbial food web.

This time-driven interpretation is also consistent with the biology of bacteria-HNF coupling. Heterotrophic nanoflagellates respond to prey abundance, prey quality, and prey identity, and their

grazing can restructure bacterial communities selectively rather than uniformly (Monger and Landry, 1990; Boenigk et al., 2001; Simek et al., 2013). Dominant marine HNFs are adapted to natural bacterial prey fields and may differ in their grazing strategies and functional responses (Rodriguez-Martinez et al., 2022). In the present experiment, PE and PS did not produce a coherent growth response across phases; instead, the abundance patterns suggest that grazer-prey dynamics continued to develop through the incubation (Fig. S1 and S2). Thus, bacteria-sized particles may have interacted with this system, but they did not override the intrinsic succession of the microbial food web.

The amplicon data reinforced this interpretation. Multivariate analysis confirmed that eukaryotic and bacterial communities changed significantly over time (Fig. 5a), whereas treatment effects at individual time points were not significant. In the eukaryotic fraction, the strongest temporal signal was the increase of Stramenopiles, including the later increase of the heterotrophic nanoflagellates *Paraphysomonas* and *Spumella* (Fig. 3a,b). These bacterivorous taxa are important components of the microbial loop and can contribute to bacterial mortality and nutrient regeneration through grazing (Boenigk & Arndt, 2002; Jürgens & Güde, 1994; Weisse, 1997). Alveolata and Haptophyta declined over the incubation period, although this decrease is likely expected given that the experiment was conducted under dark conditions, which would disadvantage autotrophic taxa. However, this pattern should be interpreted cautiously from a taxonomic perspective rather than as a simple functional shift, particularly because Alveolata comprises autotrophic, mixotrophic, and heterotrophic lineages. Thus, the eukaryotic data primarily reflects protistan community turnover, with an increasing relative importance of bacterivorous heterotrophic nanoflagellates (HNFs) at later time points.

The observed bacterial succession may partly reflect changing resources and grazing pressure during the dark incubation. Bacteroidota increased until T3, consistent with the ability of many members of this phylum to use high-molecular-weight organic matter from phytoplankton-derived detritus or other labile organic matter, before declining toward T5 (Teeling et al., 2012; Pontiller et al., 2022). In contrast, Actinobacteriota decreased initially but recovered during the later stages, when HNF abundance was highest (Fig. 4a). Because HNF grazing can selectively favor small or grazing-resistant bacterial taxa, including some Actinobacteriota, this pattern may indicate increasing top-down control on bacterial community composition (Pernthaler, 2005; Mukherjee et al., 2024). The continued dominance of Proteobacteria, particularly Rhodobacteraceae, may reflect their capacity to respond rapidly to dissolved organic substrates released through cell lysis, grazing, and remineralization (Buchan et al., 2014). Overall, these patterns support temporal succession in community composition during incubation, but they do not represent a shift from primary production because the bottles were incubated in the dark and no primary-production measurements were made.

Although no significant treatment effect was detected at the community level, polymers were not biologically irrelevant. Differentially abundant MAGs in the PE treatment relative to the control represented members of the Spirosomaceae and Shewanellaceae families. While these taxa were present in the amplicon dataset, they represented low-abundance members of the community, suggesting that PE selected for a narrow subset of responsive bacteria. All three MAGs encoded homologs associated with metabolic pathways involved in processing of synthetic polymers, including PEG, PET, and PLA (Figure. 6). Interestingly, *Arciticbacterium* (Spirosomaceae) MAG uniquely contained an alkane-1-monooxygenase homolog, an enzyme involved in alkane oxidation that has been proposed as an important component of PE and PS biodegradaton pathways

(Gyun Yoon et al., 2012). Although the presence of this gene does not demonstrate the ability to degrade PE, it suggests a potential capacity of this MAG to utilize compounds derived from PE degradation. Notably, the lack of a corresponding enrichment in the PS treatment indicates that this response could be driven by polymer-specific surface properties or chemical traits unique to PE, rather than particle attachment.

Among the PE-responsive MAGs, the *Arcticibacterium*-affiliated Spirosomaceae genome is particularly noteworthy. Members of Bacteroidota-related particle-attached lineages are often involved in the transformation of complex organic matter, especially during microbial succession on labile substrates (Teeling et al., 2012; Pontiller et al., 2022). Its enrichment in the PE treatment may therefore reflect access to surface-derived or dissolved organic compounds rather than direct plastic degradation. However, this MAG uniquely encoded an alkane-1-monooxygenase homolog, an enzyme family involved in the initial oxidation of alkane-like hydrocarbons and often considered relevant when assessing polyethylene biodegradation capacity (Meiyerani et al., 2024; Gambarini et al., 2022; Zrimec et al., 2021). This signal does not demonstrate PE degradation during the experiment, but it identifies *Arcticibacterium* as a candidate taxon for future validation. Cultivation, transcriptomics, enzyme assays, or stable-isotope probing would be needed to test whether this organism can actively process PE-derived compounds (Pérez-García et al., 2025; Przygoda-Kuś et al., 2025).

Genome mining across all metagenomic assemblies revealed that the abundance of plastic-associated enzyme homologs was influenced by temporal scale rather than polymer treatment, apart from nylon-associated hydrolases and polyamidases (Supplimentary Figure. 5). The increased prevalence of these genes at T5 may therefore reflect temporal shifts in community composition and metabolic potential, favoring organisms capable of utilizing a broader range of

complex organic compounds as environmental conditions and resource availability shift over the course of incubation. Overall, these results indicate that temporal ecological processes influence the distribution of plastic-associated metabolic traits stronger than short-term exposure to microplastics.

Across the MAGs that exhibited differential abundance among treatments, homologs of enzymes associated with processing of PEG, PLA, PET, and PBAT were detected across a broad range of taxa (Figure 7). The widespread occurrence of dehydrogenases, esterases, proteases, and carboxylesterases may reflect their involvement in general metabolic functions or in the utilization of naturally occurring compounds with structural similarities to synthetic polymers. In contrast, the more restricted distribution of PE- and PS-associated homologs, including alkane monooxygenase and alkane hydroxylases, suggests that the capacity to interact with these polymers may be limited to a narrower set of bacterial taxa. In this context, the PE-enriched *Arcticibacterium* MAG provides a focused candidate for future validation, because it combines treatment responsiveness with a hydrocarbon-oxidation marker. However, the presence of homologous genes does not imply that an organism can utilize microplastics, as many enzymes implicated in plastic degradation have broad substrate specificities and may also act on natural substrates (Gambarini et al., 2022; Pérez-García et al., 2025). Consequently, metagenomic studies provide only a initial step, and genomic evidence should be followed with cultivation, transcriptomics, enzyme assays, or stable-isotope probing to determine whether candidate taxa actively process PE-derived compounds.

The functional shifts further support community succession as the dominant driver of change rather than direct plastic utilization. Enrichment of carbohydrate metabolism, stress-response, and secretion-related pathways at the intermediate time point (T3) may reflect an early stage of

community restructuring, characterized by rapid resource exploitation and metabolic flexibility across multiple bacterial lineages. Similar temporal dynamics have been observed within the marine plastisphere, where colonization and surface-bound community restructuring over time can alter localized biogeochemical cycles (Pinnell et al., 2022). By T5, enrichment of amino acid metabolism pathways points toward the recycling and utilization of more complex forms of microbial organic matter. This later functional signal may also be linked to the increasing contribution of HNFs, as shown with amplicon data, whose grazing can selectively remove bacterial prey, favour grazing-resistant taxa, and release dissolved or particulate organic matter through digestion and excretion, thereby reshaping both bacterial community composition and substrate availability (Pernthaler, 2005; Šimek et al., 2013; Mukherjee et al., 2024). Dominance of Saprospiraceae MAGs at T5 is consistent with this interpretation, because members of this family are often associated with degradation of proteinaceous substrates and other complex organic matter. Thus, the functional patterns observed here are interpreted as a consequence of microbial food-web succession, in which bacterial substrate use and protistan grazing jointly shaped the metabolic potential of the community.

Overall, the results suggest that short-term exposure to bacteria-sized PE and PS particles caused limited community-level disruption in this Baltic microbial assemblage. Temporal succession was the dominant organizing force, while polymer-related signals appeared mainly as restricted MAG-level responses and putative functional potential. This does not exclude stronger effects under longer exposure, different particle aging states, higher concentrations, or attached-biofilm conditions. Rather, it shows that in natural microbial communities, microplastic effects must be evaluated against rapid endogenous succession. Future experiments combining free-living and particle-attached fractions with metatranscriptomics, metaproteomics, chemical polymer analyses,

or stable-isotope probing would be needed to test whether the detected genetic potential is expressed and whether polymer-derived carbon is actually incorporated into microbial biomass.

Conclusion

Our results show that short-term exposure to bacteria-sized PE and PS microplastics caused limited community-level disruption in a natural coastal Baltic microbial assemblage. Across bacterial, eukaryotic, and genome-resolved datasets, temporal succession during incubation was the dominant organizing process, outweighing broad treatment-specific effects of plastic particles. Nevertheless, the PE treatment produced narrow MAG-level responses, including enrichment of an *Arcticibacterium*-affiliated Spirosomaceae genome carrying an alkane-1-monooxygenase homolog, suggesting that specific low-abundance taxa may respond to polymer-associated microhabitats or dissolved compounds. The detection of putative plastic-processing enzyme homologs indicates metabolic potential, but does not demonstrate active plastic degradation. Overall, these findings suggest that bacteria-sized microplastics did not override endogenous microbial food-web dynamics over the timescale tested, but may selectively influence particular bacterial taxa and functional traits. Future work should combine particle-attached and free-living fractions with transcriptomic, cultivation, enzyme-activity, and isotope-based approaches to determine whether candidate taxa actively process polymer-derived carbon.

Supplementary Data

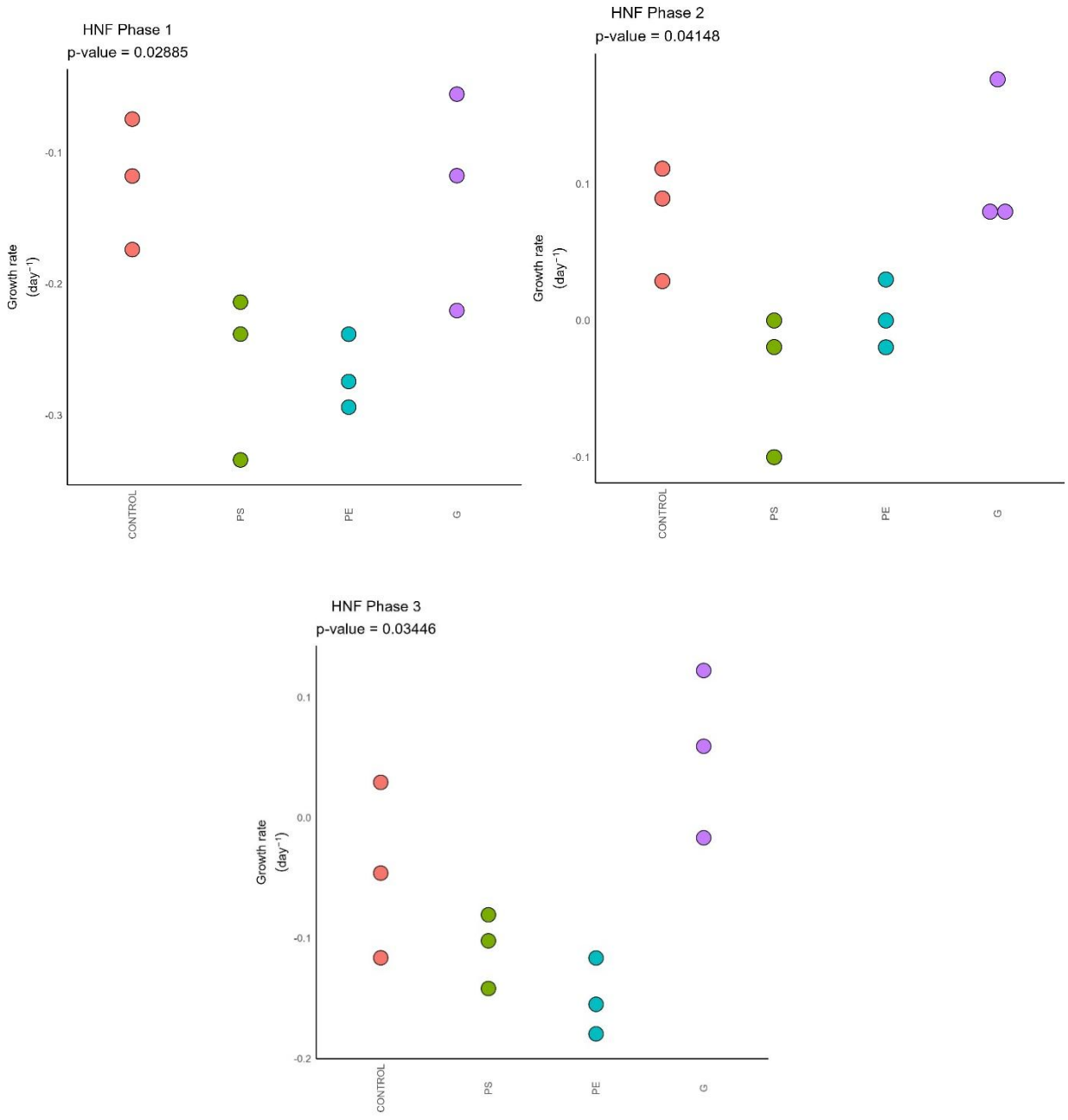

Figure S1. Figure X. HNF growth rates (day⁻¹) across Control, PS, PE, and G treatments during three HNF growth phases: Phase 1 (T1-T3), Phase 2 (T3-T4), and Phase 3 (T4-T5), defined from abundance trajectories.

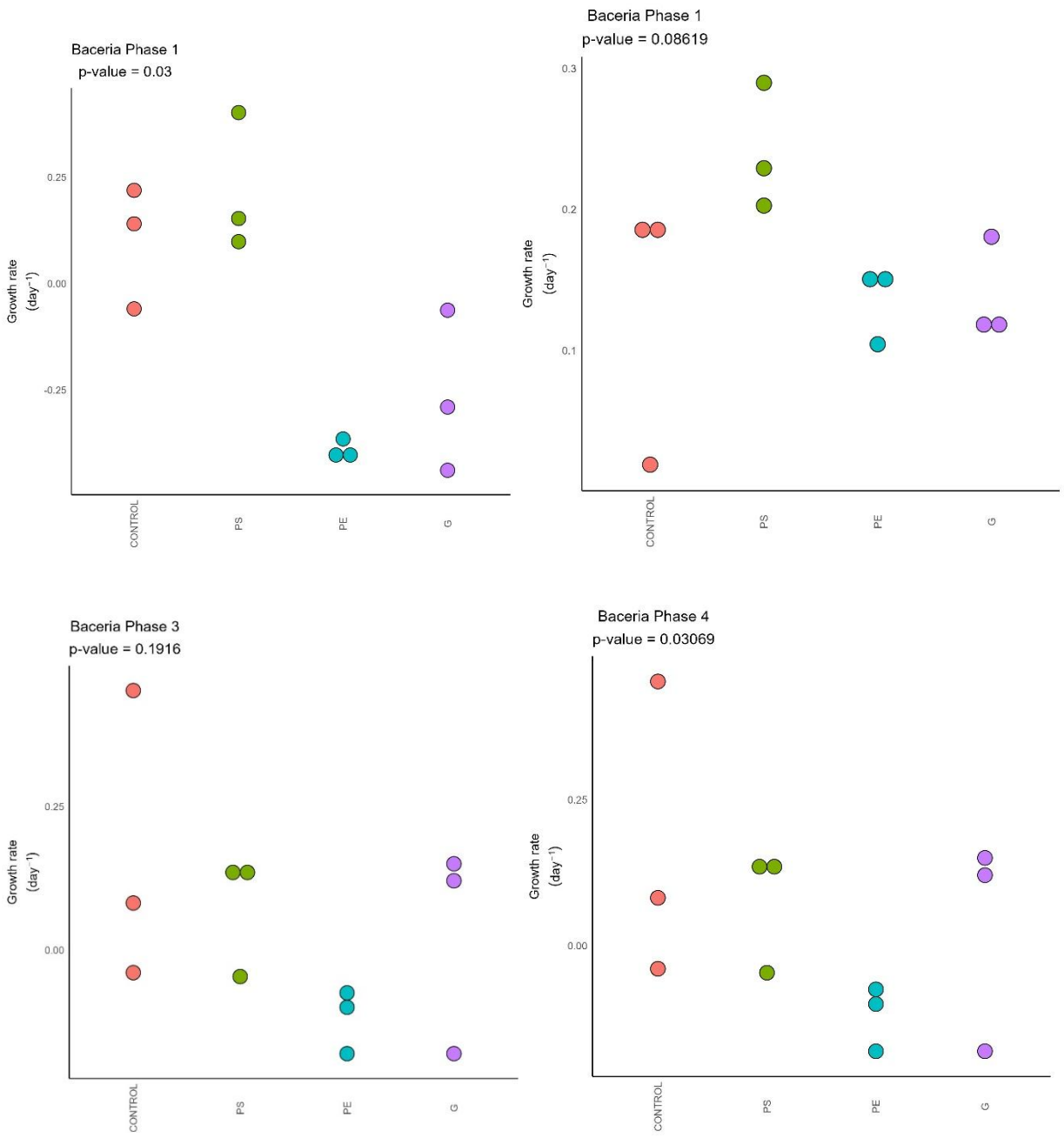

Figure S2. Bacterial growth rates (day⁻¹) across Control, PS, PE, and G treatments during four bacterial growth phases: Phase 1 (T1–T2), Phase 2 (T2–T3), Phase 3 (T3–T4), and Phase 4 (T4–T5). Statistical differences among treatments within each phase were assessed using Kruskal–Wallis tests followed by Dunn's pairwise comparisons.

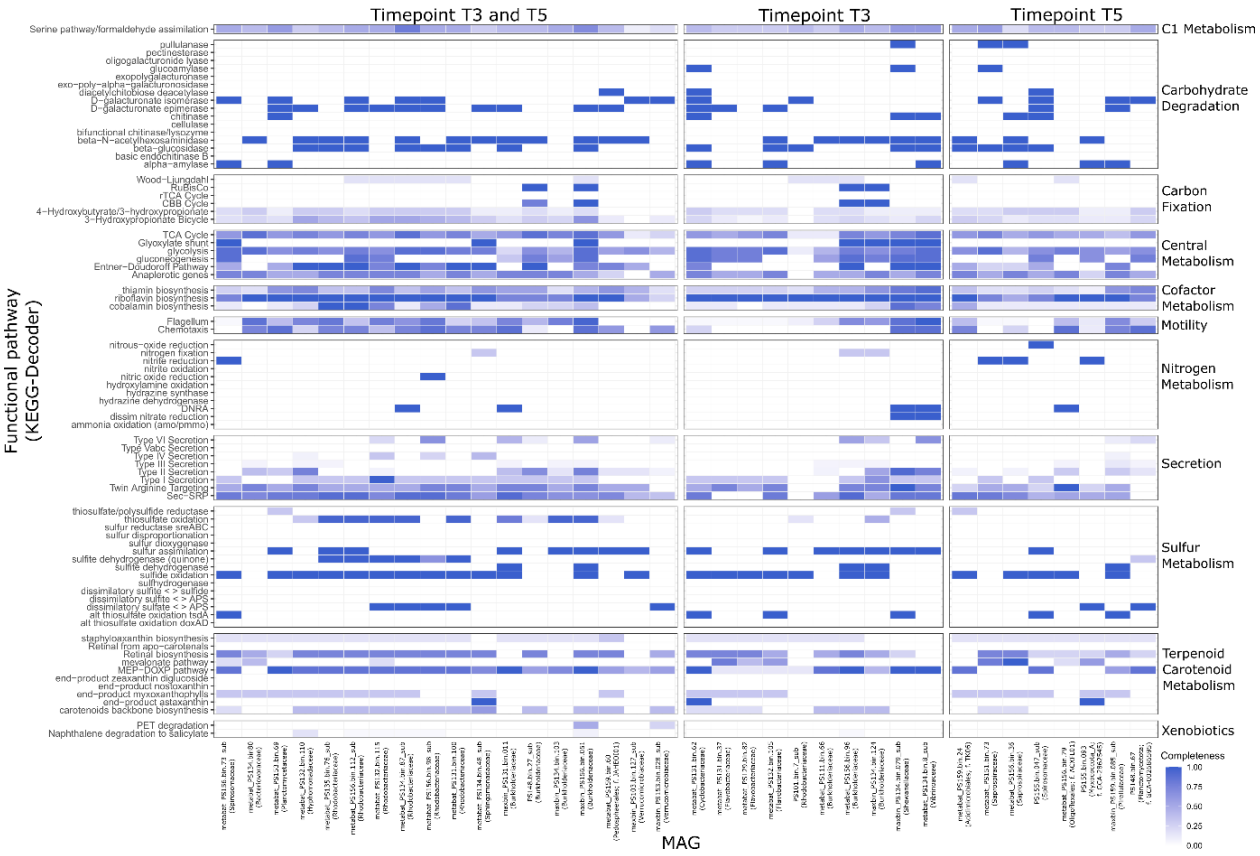

Figure S3. Completeness of selected pathways across differentially abundant MAGs at timepoints T3 and T5.

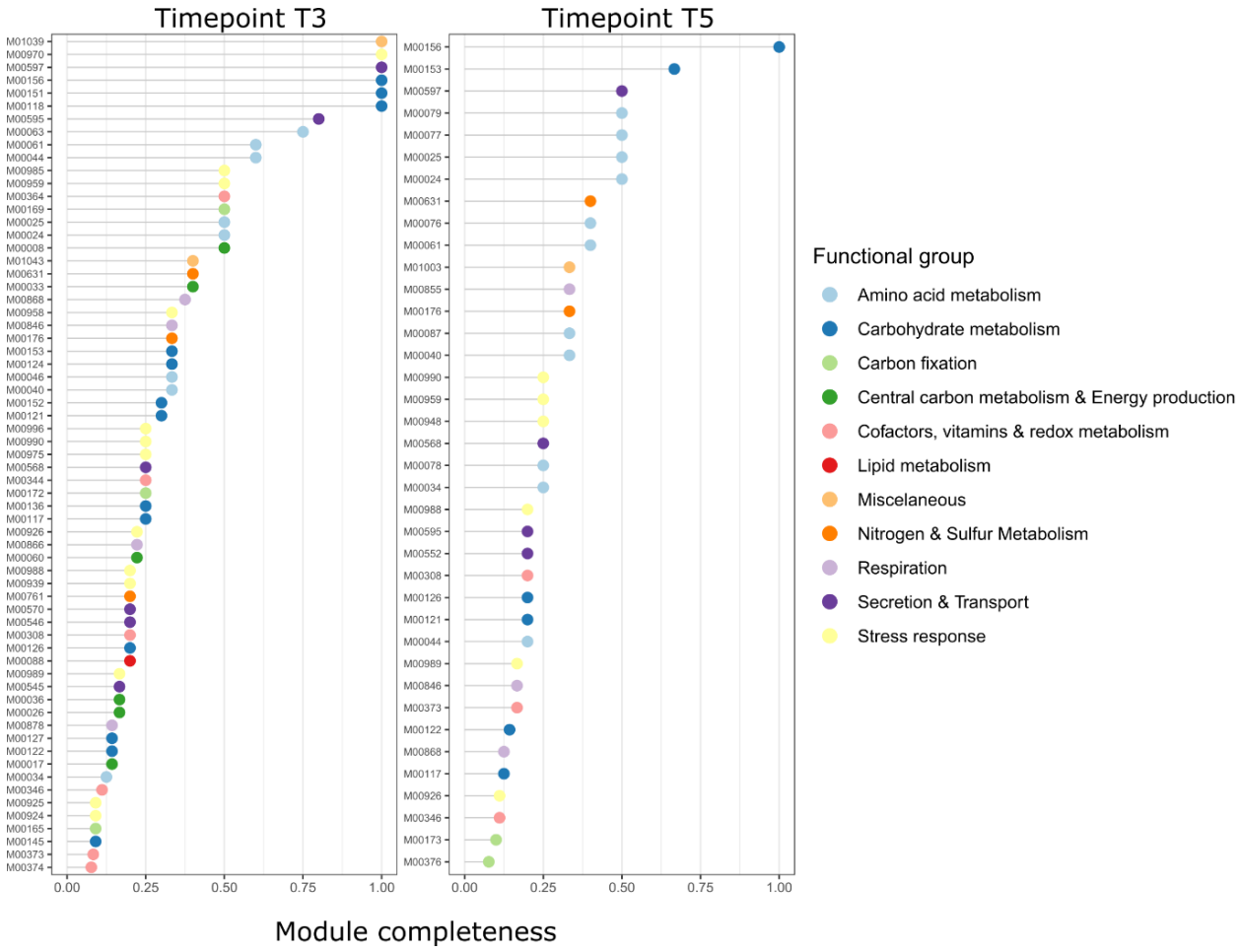

Figure S4. Completeness of modules significantly enriched at T3 and T5.

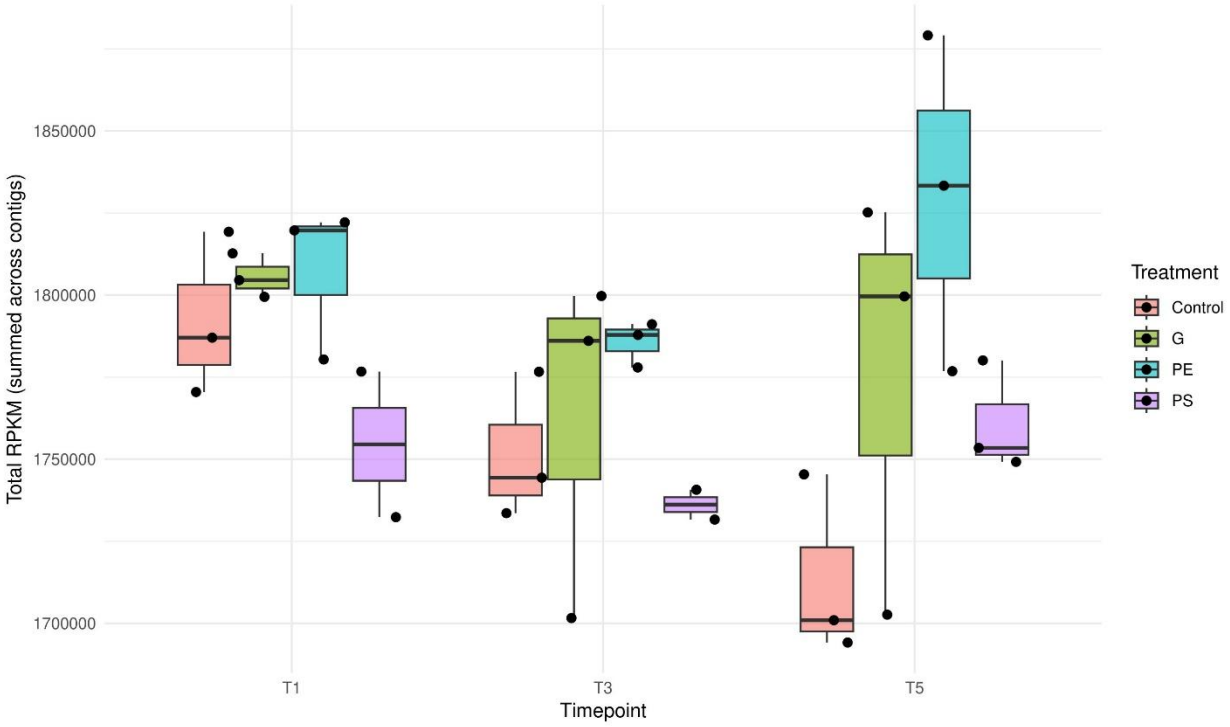

Figure S5. Temporal changes in the abundance of putative nylon-processing genes (hydrolases and polyamidases) across treatments, expressed as RPKM values. A significant treatment effect was observed between the control and PE treatment (ANOVA, R2 = 0.30, p < 0.01).

References

Anderson, M. J., Gorley, R. N., & Clarke, K. R. (2008). PERMANOVA+ for PRIMER: Guide to software and statistical methods. PRIMER-E.

Azam, F., Fenchel, T., Field, J. G., Gray, J. S., Meyer-Reil, L. A., & Thingstad, F. (1983). The ecological role of water-column microbes in the sea. Marine Ecology Progress Series, 10, 257-263.

Bermúdez, J. R., Metian, M., Oberhänsli, F., Taylor, A., & Swarzenski, P. W. (2021). Preferential grazing and repackaging of small polyethylene microplastic particles (≤5 μm) by the ciliate Sterkiella sp. Marine Environmental Research, 166, 105260. https://doi.org/10.1016/j.marenvres.2021.105260

Boenigk J, Arndt H. Bacterivory by heterotrophic flagellates: community structure and feeding strategies. Antonie Van Leeuwenhoek. 2002 Aug;81(1-4):465-80. doi: 10.1023/a:1020509305868. PMID: 12448743.

Boenigk, J., Matz, C., Jürgens, K., & Arndt, H. (2001). Confusing selective feeding with differential digestion in bacterivorous nanoflagellates. Journal of Eukaryotic Microbiology, 48(4), 425-432.

Bolger, A. M., Lohse, M., & Usadel, B. (2014). Trimmomatic: A flexible trimmer for Illumina sequence data. Bioinformatics, 30(15), 2114-2120. https://doi.org/10.1093/bioinformatics/btu170

Bolyen, E., Rideout, J. R., Dillon, M. R., Bokulich, N. A., Abnet, C. C., Al-Ghalith, G. A., Alexander, H., Alm, E. J., Arumugam, M., Asnicar, F., et al. (2019). Reproducible, interactive, scalable and extensible microbiome data science using QIIME 2. Nature Biotechnology, 37, 852-857. https://doi.org/10.1038/s41587-019-0209-9

Buchan A, LeCleir GR, Gulvik CA, González JM. Master recyclers: features and functions of bacteria associated with phytoplankton blooms. Nat Rev Microbiol. 2014 Oct;12(10):686-98. doi: 10.1038/nrmicro3326.

Buchfink, B., Xie, C., & Huson, D. H. (2015). Fast and sensitive protein alignment using DIAMOND. Nature Methods, 12, 59-60. https://doi.org/10.1038/nmeth.3176

Callahan, B. J., McMurdie, P. J., Rosen, M. J., Han, A. W., Johnson, A. J. A., & Holmes, S. P. (2016). DADA2: High-resolution sample inference from Illumina amplicon data. Nature Methods, 13, 581-583. https://doi.org/10.1038/nmeth.3869

Chaumeil, P.-A., Mussig, A. J., Hugenholtz, P., & Parks, D. H. (2020). GTDB-Tk: A toolkit to classify genomes with the Genome Taxonomy Database. Bioinformatics, 36(6), 1925-1927. https://doi.org/10.1093/bioinformatics/btz848

Chistoserdova, L. (2011). Modularity of methylotrophy, revisited. Environmental Microbiology, 13(10), 2603-2622. https://doi.org/10.1111/j.1462-2920.2011.02464.x

Chklovski, A., Parks, D. H., Woodcroft, B. J., & Tyson, G. W. (2023). CheckM2: A rapid, scalable and accurate tool for assessing microbial genome quality using machine learning. Nature Methods, 20, 1203-1212.

Christaki, U., Genitsaris, S., Monchy, S., Li, L. L., Rachik, S., Breton, E., & Sime-Ngando, T. (2017). Parasitic eukaryotes in a meso-eutrophic coastal system with marked Phaeocystis globosa blooms. Frontiers in Marine Science, 4, Article 416. https://doi.org/10.3389/fmars.2017.00416

Clarke, K. R., & Gorley, R. N. (2015). PRIMER v7: User manual/tutorial. PRIMER-E.

Davidov, K., Itzahri, S., Sinberger, L. A., & Oren, M. (2025). Unveiling microbial succession dynamics on different plastic surfaces using WGCNA. PLOS ONE.

Di Pippo F, Bocci V, Amalfitano S, Crognale S, Levantesi C, Pietrelli L, Di Lisio V, Martinelli A, Rossetti S. Microbial colonization patterns and biodegradation of petrochemical and biodegradable plastics in lake waters: insights from a field experiment. Front Microbiol. 2023 Dec 6;14:1290441. doi: 10.3389/fmicb.2023.1290441. PMID: 38125574; PMCID: PMC10731271.

Dussud, C., Hudec, C., George, M., Fabre, P., Higgs, P., Bruzaud, S., Delort, A.-M., Eyheraguibel, B., Meistertzheim, A.-L., Jacquin, J., Cheng, J., Callac, N., Odobel, C., Rabouille, S., & Ghiglione, J.-F. (2018b). Colonization of non-biodegradable and biodegradable plastics by marine microorganisms. Frontiers in Microbiology, 9, 1571. https://doi.org/10.3389/fmicb.2018.01571

Dussud, C., Meistertzheim, A. L., Conan, P., Pujo-Pay, M., George, M., Fabre, P., Coudane, J., Higgs, P., Elineau, A., Pedrotti, M. L., Gorsky, G., & Ghiglione, J. F. (2018a). Evidence of niche partitioning among bacteria living on plastics, organic particles and surrounding seawaters. Environmental Pollution, 236, 807-816.

Ebbesen, L. G., Strange, M. V., Gunaalan, K., Paulsen, M. L., Herrera, A., Nielsen, T. G., Shashoua, Y., Lindegren, M., & Almeda, R. (2024). Do weathered microplastics impact the planktonic community? A mesocosm approach in the Baltic Sea. Water Research, 255, 121500.

Emms, D. M., & Kelly, S. (2019). OrthoFinder: Phylogenetic orthology inference for comparative genomics. Genome Biology, 20, 238. https://doi.org/10.1186/s13059-019-1832-y

Ewels, P., Magnusson, M., Lundin, S., & Käller, M. (2016). MultiQC: Summarize analysis results for multiple tools and samples in a single report. Bioinformatics, 32(19), 3047-3048. https://doi.org/10.1093/bioinformatics/btw354

Fu, L., Niu, B., Zhu, Z., Wu, S., & Li, W. (2012). CD-HIT: Accelerated for clustering the next-generation sequencing data. Bioinformatics, 28(23), 3150-3152. https://doi.org/10.1093/bioinformatics/bts565

Fulfer, V. M., & Menden-Deuer, S. (2021). Heterotrophic dinoflagellate growth and grazing rates reduced by microplastic ingestion. Frontiers in Marine Science, 8, 716349. https://doi.org/10.3389/fmars.2021.716349

Gambardella, C., Basili, M., Castelli, F., Miroglio, R., Manini, E., Quero, G. M., Almeda, R., Regoli, F., Faimali, M., & Garaventa, F. (2025). Early biofilm colonization on traditional and biodegradable plastics in the Baltic Sea using a mesocosm approach. Marine Environmental Research.

Gambarini, V., Pantos, O., Kingsbury, J. M., Weaver, L., Handley, K. M., & Lear, G. (2022). PlasticDB: A database of microorganisms and proteins linked to plastic biodegradation. Database, 2022, baac008. https://doi.org/10.1093/database/baac008

Geng, X., Wang, J., Zhang, Y., & Jiang, Y. (2021). How do microplastics affect the marine microbial loop? Predation of microplastics by microzooplankton. Science of the Total Environment, 758, 144030. https://doi.org/10.1016/j.scitotenv.2020.144030

Gewert, B., Ogonowski, M., Barth, A., & MacLeod, M. (2017). Abundance and composition of near surface microplastics and plastic debris in the Stockholm Archipelago, Baltic Sea. Marine Pollution Bulletin, 120(1-2), 292-302.

Geyer, R., Jambeck, J. R., & Law, K. L. (2017). Production, use, and fate of all plastics ever made. Science Advances, 3(7), e1700782. https://doi.org/10.1126/sciadv.1700782

Graham, E. D., Heidelberg, J. F., & Tully, B. J. (2018). Potential for primary productivity in a globally-distributed bacterial phototroph. ISME Journal, 12, 1861-1866.

Guillou, L., Bachar, D., Audic, S., Bass, D., Berney, C., Bittner, L., Boutte, C., Burgaud, G., de Vargas, C., Decelle, J., et al. (2012). The Protist Ribosomal Reference database (PR2): A catalog of unicellular eukaryote small sub-unit rRNA sequences with curated taxonomy. Nucleic Acids Research, 41(D1), D597-D604. https://doi.org/10.1093/nar/gks1160

Gurevich, A., Saveliev, V., Vyahhi, N., & Tesler, G. (2013). QUAST: Quality assessment tool for genome assemblies. Bioinformatics, 29(8), 1072-1075. https://doi.org/10.1093/bioinformatics/btt086

Haro-Moreno, J. M., Rodriguez-Valera, F., & López-Pérez, M. (2019). Prokaryotic population dynamics and viral predation in a marine succession experiment using metagenomics. Frontiers in Microbiology, 10, 2926. https://doi.org/10.3389/fmicb.2019.02926

Harrison, J. P., Schratzberger, M., Sapp, M., & Osborn, A. M. (2014). Rapid bacterial colonization of low-density polyethylene microplastics in coastal sediment microcosms. BMC Microbiology, 14, 232. https://doi.org/10.1186/s12866-014-0232-4

Hyatt, D., Chen, G.-L., Locascio, P. F., Land, M. L., Larimer, F. W., & Hauser, L. J. (2010). Prodigal: Prokaryotic gene recognition and translation initiation site identification. BMC Bioinformatics, 11, 119. https://doi.org/10.1186/1471-2105-11-119

Ihara, H., Hori, T., Aoyagi, T., Takasaki, M., & Katayama, Y. (2017). Sulfur-oxidizing bacteria mediate microbial community succession and element cycling in launched marine sediment. Frontiers in Microbiology, 8, 152. https://doi.org/10.3389/fmicb.2017.00152

Ivanković, M., Ptacnik, R., & Bengtsson, M. M. (2023). Top-down structuring of freshwater bacterial communities by mixotrophic flagellates. ISME Communications, 3, 89.

Jambeck, J. R., Geyer, R., Wilcox, C., Siegler, T. R., Perryman, M., Andrady, A., Narayan, R., & Law, K. L. (2015). Plastic waste inputs from land into the ocean. Science, 347(6223), 768-771. https://doi.org/10.1126/science.1260352

Jeong, M., Kim, J. I., Nam, S. W., & Shin, W. (2021). Molecular Phylogeny and Taxonomy of the Genus Spumella (Chrysophyceae) Based on Morphological and Molecular Evidence. Frontiers in Plant Science, 12, Article 758067. https://doi.org/10.3389/fpls.2021.758067

Jürgens, K., & Güde, H. (1994). The potential importance of grazing-resistant bacteria in planktonic systems. Marine Ecology Progress Series, 112, 169–188. https://doi.org/10.3354/meps112169

Kalyaanamoorthy, S., Minh, B. Q., Wong, T. K. F., von Haeseler, A., & Jermiin, L. S. (2017). ModelFinder: Fast model selection for accurate phylogenetic estimates. Nature Methods, 14, 587-589. https://doi.org/10.1038/nmeth.4285

Kang, D. D., Li, F., Kirton, E., Thomas, A., Egan, R., An, H., & Wang, Z. (2019). MetaBAT 2: An adaptive binning algorithm for robust and efficient genome reconstruction from metagenome assemblies. PeerJ, 7, e7359. https://doi.org/10.7717/peerj.7359

Kavagutti VS, Bulzu PA, Chiriac CM, Salcher MM, Mukherjee I, Shabarova T, Grujčić V, Mehrshad M, Kasalický V, Andrei AS, Jezberová J, Seďa J, Rychtecký P, Znachor P, Šimek K, Ghai R. High-resolution metagenomic reconstruction of the freshwater spring bloom. Microbiome. 2023 Jan 26;11(1):15. doi: 10.1186/s40168-022-01451-4

Khan S, Klaudia W, Joanna C, Krzysztof R, Lidia N, Anetta A, Tanja S, Indarnil M, Karel S, Aneta J, Mariusz Z, Kasia P. High-Temporal Resolution of Microbial Food Web Dynamics and Structure During Phytoplankton Blooms in the Baltic Sea." Environmental Microbiology 27, no. 11 (2025): e70190.

Klein, V. J., Irla, M., Gil López, M., Brautaset, T., & Fernandes Brito, L. (2022). Unravelling formaldehyde metabolism in bacteria: Road towards synthetic methylotrophy. Microorganisms, 10(2), 220. https://doi.org/10.3390/microorganisms10020220

Li, D., Liu, C.-M., Luo, R., Sadakane, K., & Lam, T.-W. (2015). MEGAHIT: An ultra-fast single-node solution for large and complex metagenomics assembly via succinct de Bruijn graph. Bioinformatics, 31(10), 1674-1676. https://doi.org/10.1093/bioinformatics/btv033

Li, H. (2013). Aligning sequence reads, clone sequences and assembly contigs with BWA-MEM. arXiv. https://arxiv.org/abs/1303.3997

Li, H., Handsaker, B., Wysoker, A., Fennell, T., Ruan, J., Homer, N., Marth, G., Abecasis, G., & Durbin, R. (2009). The Sequence Alignment/Map format and SAMtools. Bioinformatics, 25(16), 2078-2079. https://doi.org/10.1093/bioinformatics/btp352

Lindeque PK, Cole M, Coppock RL, Lewis CN, Miller RZ, Watts AJR, Wilson-McNeal A, Wright SL, Galloway TS. Are we underestimating microplastic abundance in the marine environment? A comparison of microplastic capture with nets of different mesh-size. Environ Pollut. 2020 Oct;265(Pt A):114721. doi: 10.1016/j.envpol.2020.114721. Epub 2020 May 3. PMID: 32806407.

Lora, U., Schenone, L., Forn, I., Peters, F., Piiparinen, J., Kaartokallio, H., Lehtiniemi, M., & Sala, M. M. (2024). Weak effects of conventional and biodegradable microplastics on marine microbial communities. Frontiers in Marine Science, 11, 1502825.

Love, M. I., Huber, W., & Anders, S. (2014). Moderated estimation of fold change and dispersion for RNA-seq data with DESeq2. Genome Biology, 15, 550. https://doi.org/10.1186/s13059-014-0550-8

McMurdie, P. J., & Holmes, S. (2013). phyloseq: An R package for reproducible interactive analysis and graphics of microbiome census data. PLOS ONE, 8(4), e61217. https://doi.org/10.1371/journal.pone.0061217

Meiyerani, R., Estuningsih, S., & Agussalim, A. (2024). Degradation of polyethylene plastic by bacteria isolated from seawaters in coastal and estuarine marine ecosystems. Journal of Marine Research and Bioflux, 17(2), 2065–2074.

Mindolina, Y. V., Selivanova, E. A., Ignatenko, M. E., Krasnova, E. D., Voronov, D. A., & Plotnikov, A. O. (2022). Taxonomic Composition of Protist Communities in the Coastal Stratified Lake Kislo-Sladkoe (Kandalaksha Bay, White Sea) Revealed by Microscopy. Diversity, 15(1), 44. https://doi.org/10.3390/d15010044

Minh, B. Q., Schmidt, H. A., Chernomor, O., Schrempf, D., Woodhams, M. D., von Haeseler, A., & Lanfear, R. (2020). IQ-TREE 2: New models and efficient methods for phylogenetic inference in the genomic era. Molecular Biology and Evolution, 37(5), 1530-1534. https://doi.org/10.1093/molbev/msaa015

Mishra, A., Buhhalko, N., Lind, K., Lips, I., Liblik, T., Väli, G., & Lips, U. (2022). Spatiotemporal variability of microplastics in the Eastern Baltic Sea. Frontiers in Marine Science, 9, 875984.

Monger, B. C., & Landry, M. R. (1990). Direct-interception feeding by marine zooflagellates: The importance of surface and hydrodynamic forces. Marine Ecology Progress Series, 65, 123-140.

Montoya, D., Rastelli, E., Casotti, R., Manna, V., Trano, A. C., Balestra, C., Santinelli, C., Saggiomo, M., Sansone, C., Corinaldesi, C., Montoya, J. M., & Brunet, C. (2024). Microplastics alter the functioning of marine microbial ecosystems. Ecology and Evolution, 14, e70041. https://doi.org/10.1002/ece3.70041

Mukherjee I, Grujčić V, Salcher MM, Znachor P, Seďa J, Devetter M, Rychtecký P, Šimek K, Shabarova T. Integrating depth-dependent protist dynamics and microbial interactions in spring succession of a freshwater reservoir. Environ Microbiome. 2024 May 8;19(1):31. doi: 10.1186/s40793-024-00574-5.

Oberbeckmann, S., Osborn, A. M., & Duhaime, M. B. (2016). Microbes on a bottle: Substrate, season and geography influence community composition of microbes colonizing marine plastic debris. PLOS ONE, 11(8), e0159289.

Osman, A. I., Hosny, M., Eltaweil, A. S., Omar, S., Elgarahy, A. M., Farghali, M., Yap, P.-S., Wu, Y.-S., Nagandran, S., Batumalaie, K., et al. (2023). Microplastic sources, formation, toxicity and remediation: A review. Environmental Chemistry Letters, 21, 2129-2169. https://doi.org/10.1007/s10311-023-01593-3

Pernthaler J. Predation on prokaryotes in the water column and its ecological implications. Nat Rev Microbiol. 2005 Jul;3(7):537-46. doi: 10.1038/nrmicro1180.

Pinnell, L. J., Conkle, J. L., & Turner, J. W. (2022). Microbial succession during the degradation of bioplastic in coastal marine sediment favors sulfate reducing microorganisms. Frontiers in Marine Science, 9, Article 945822. https://doi.org/10.3389/fmars.2022.945822

Piwosz, K., & Pernthaler, J. (2010). Seasonal population dynamics and trophic role of planktonic nanoflagellates in coastal surface waters of the Southern Baltic Sea. Environmental Microbiology, 12(2), 364-377.

Pontiller B, Martínez-García S, Joglar V, Amnebrink D, Pérez-Martínez C, González JM, Lundin D, Fernández E, Teira E, Pinhassi J. Rapid bacterioplankton transcription cascades regulate organic matter utilization during phytoplankton bloom progression in a coastal upwelling system. ISME J. 2022 Oct;16(10):2360-2372. doi: 10.1038/s41396-022-01273-0.

Pruesse, E., Quast, C., Knittel, K., Fuchs, B. M., Ludwig, W., Peplies, J., & Glöckner, F. O. (2007). SILVA: A comprehensive online resource for quality checked and aligned ribosomal RNA sequence data compatible with ARB. Nucleic Acids Research, 35(21), 7188-7196. https://doi.org/10.1093/nar/gkm864

Przygoda-Kuś, P., Kosiorowska, K. E., Urbanek, A. K., & Mirończuk, A. M. (2025). Current approaches to microplastics detection and plastic biodegradation. Molecules, 30, 2462. https://doi.org/10.3390/molecules30112462

Pérez-García, P., et al. (2025). Microbial plastic degradation: Enzymes, pathways, challenges, and perspectives. Microbiology and Molecular Biology Reviews.

Quast, C., Pruesse, E., Yilmaz, P., Gerken, J., Schweer, T., Yarza, P., Peplies, J., & Glöckner, F. O. (2012). The SILVA ribosomal RNA gene database project: Improved data processing and web-based tools. Nucleic Acids Research, 41(D1), D590-D596. https://doi.org/10.1093/nar/gks1219

R Core Team. (2024). R: A language and environment for statistical computing. R Foundation for Statistical Computing.

Rodríguez-Martínez, R., Vaqué, D., Forn, I., & Massana, R. (2022). Dominant marine heterotrophic flagellates are adapted to natural planktonic bacterial abundances. Environmental Microbiology, 24, 198-210.

Salehi, M., Pincus, L. N., Deng, B., & Peters, C. A. (2024). Microplastics: From intrinsic properties to environmental fate. Environmental Engineering Science.

Seemann, T. (2014). Prokka: Rapid prokaryotic genome annotation. Bioinformatics, 30(14), 2068-2069. https://doi.org/10.1093/bioinformatics/btu153

Shen, W., Le, S., Li, Y., & Hu, F. (2016). SeqKit: A cross-platform and ultrafast toolkit for FASTA/Q file manipulation. PLOS ONE, 11(10), e0163962. https://doi.org/10.1371/journal.pone.0163962

Sherr, B. F., Sherr, E. B., & Fallon, R. D. (1987). Use of monodispersed, fluorescently labeled bacteria to estimate in situ protozoan bacterivory. Applied and Environmental Microbiology, 53(5), 958-965.

Sieber, C. M. K., Probst, A. J., Sharrar, A., Thomas, B. C., Hess, M., Tringe, S. G., & Banfield, J. F. (2018). Recovery of genomes from metagenomes via a dereplication, aggregation and scoring strategy. Nature Microbiology, 3, 836-843. https://doi.org/10.1038/s41564-018-0171-1

Sun, J., Steindler, L., Thrash, J. C., Halsey, K. H., Smith, D. P., Carter, A. E., Landry, Z. C., & Giovannoni, S. J. (2011). One carbon metabolism in SAR11 pelagic marine bacteria. PLOS ONE, 6(8), e23973. https://doi.org/10.1371/journal.pone.0023973

Sun, X., Chen, B., Li, Q., Liu, N., Xia, B., Zhu, L., & Qu, K. (2018). Toxicities of polystyrene nano- and microplastics toward marine bacterium Halomonas alkaliphila. Science of the Total Environment, 642, 1378-1385.

Teeling H, Fuchs BM, Becher D, Klockow C, Gardebrecht A, Bennke CM, Kassabgy M, Huang S, Mann AJ, Waldmann J, Weber M, Klindworth A, Otto A, Lange J, Bernhardt J, Reinsch C, Hecker M, Peplies J, Bockelmann FD, Callies U, Gerdts G, Wichels A, Wiltshire KH, Glöckner FO, Schweder T, Amann R. Substrate-controlled succession of marine bacterioplankton populations induced by a phytoplankton bloom. Science. 2012 May 4;336(6081):608-11. doi: 10.1126/science.1218344.

Vuillemin, A., Coskun, Ö. K., & Orsi, W. H. (2022). Microbial activities and selection from surface ocean to subseafloor on the Namibian continental shelf. Applied and Environmental Microbiology, 88(8), Article e00216-22. https://doi.org/10.1128/aem.00216-22

Weisse, T. (1997). Growth and production of heterotrophic nanoflagellates in a meso-eutrophic lake. Journal of Plankton Research, 19(6), 703–722. https://doi.org/10.1093/plankt/19.6.703

Wu, Y., Guo, P., Zhang, X., Zhang, Y., Xie, S., & Deng, J. (2019). Effect of microplastics exposure on the photosynthesis system of freshwater algae. Journal of Hazardous Materials, 374, 219-227.

Wu, Y.-W., Simmons, B. A., & Singer, S. W. (2014). MaxBin: An automated binning method to recover individual genomes from metagenomes using an expectation-maximization algorithm. Microbiome, 2, 26.

Ye, G., Zhang, X., Yan, C., Lin, Y., & Huang, Q. (2021). Polystyrene microplastics induce microbial dysbiosis and dysfunction in surrounding seawater. Environment International, 156, 106724. https://doi.org/10.1016/j.envint.2021.106724

Zhang, C., Chen, X., Wang, J., & Tan, L. (2017). Toxic effects of microplastic on marine microalgae Skeletonema costatum: Interactions between microplastic and algae. Environmental Pollution, 220, 1282-1288.

Zhou, Q., Tu, C., Yang, J., Fu, C., Li, Y., & Waniek, J. J. (2021). Trapping of microplastics in halocline and turbidity layers of the semi-enclosed Baltic Sea. Frontiers in Marine Science, 8, 761566. https://doi.org/10.3389/fmars.2021.761566

Zrimec, J., Kokina, M., Jonasson, S., Zorrilla, F., & Zelezniak, A. (2021). Plastic-degrading potential across the global microbiome correlates with recent pollution trends. mBio, 12(5), e02155-21. https://doi.org/10.1128/mBio.02155-21

Šimek, K., Kasalický, V., Jezbera, J., Hornák, K., Nedoma, J., Hahn, M. W., Bass, D., Jost, S., & Boenigk, J. (2013). Differential freshwater flagellate community response to bacterial food quality with a focus on Limnohabitans bacteria. The ISME Journal, 7, 1519-1530.

Thesis Summary

Microplastic pollution is now recognized as a persistent pressure on marine ecosystems, but its effects on the smallest components of pelagic food webs remain insufficiently understood. While many studies have focused on larger organisms, the smallest microplastic particles overlap in size with bacteria and other microbial prey. This makes them especially relevant for pelagic microbial food webs, where bacteria and heterotrophic nanoflagellates play central roles in carbon transfer, nutrient recycling, and the regulation of microbial community structure. This thesis investigated how bacteria-sized microplastics affect the structure and functioning of pelagic microbial food webs, with particular focus on bacteria, heterotrophic nanoflagellates, and methodological challenges associated with detecting very small particles.

The first part of the thesis addressed a key analytical problem: the reliable detection of small microplastics. Because particles below 5 micrometres are difficult to detect using standard approaches, an optimized Nile Red staining protocol was developed for microplastics smaller than 5 micrometres, with emphasis on particles of 2 micrometres or less. The protocol was tested using polystyrene and polyethylene particles, together with inorganic controls. Under optimized filtration and staining conditions, 1 and 2 micrometre polystyrene particles and 2 micrometre polyethylene particles showed strong and consistent fluorescence signals, while glass particles and biological material did not stain. Formalin fixation, commonly used for preserving microbial samples, improved fluorescence brightness and signal-to-noise ratio without compromising selectivity. This study therefore provided a simple, cost-effective, and practical method for detecting small microplastics in preserved marine samples, forming an important methodological foundation for studying their ecological effects.

The second part of the thesis provided the first experimental assessment of how bacteria-sized polystyrene particles affect natural Baltic microbial food webs. A five-day microcosm experiment tested three concentrations of 1.1 micrometre polystyrene particles and compared them with size-matched glass particles to separate polymer-specific effects from the physical effects of suspended particles. Using bacterial and HNF abundance measurements, respiration estimates, and 16S and 18S rRNA gene amplicon sequencing, this chapter showed that HNF growth declined in a concentration-dependent manner, with the strongest effects in the highest polystyrene and glass treatments. Because similar responses occurred in both plastic and inert particle treatments, the results indicate that the physical presence of particles, rather than polystyrene toxicity alone, was the main driver of reduced HNF growth. Bacterial abundance and respiration were not significantly affected, suggesting that the decline in HNFs was not caused by reduced prey availability. Instead, bacteria-sized particles may have interfered with feeding by reducing prey encounter efficiency, increasing handling costs, or occupying food vacuoles without providing nutritional value.

The community analyses in Chapter 2 showed that eukaryotic communities changed mainly over time, with shifts from initially dominant phototrophic or mixotrophic groups toward heterotrophic taxa, including bacterivorous flagellates. Bacterial communities were comparatively stable. These findings demonstrated that high concentrations of bacteria-sized particles can rapidly suppress key microbial grazers and potentially alter carbon transfer within the microbial loop. However, because this chapter relied mainly on amplicon sequencing, it described taxonomic community shifts but could not resolve genome-level functional potential or identify which bacterial populations might carry genes associated with plastic-related metabolism.

Chapter 3 therefore extended Chapter 2 in two important ways. First, it compared two environmentally relevant polymers, polystyrene and polyethylene, under the same experimental

conditions and at the same bacteria: particle ratio, while retaining glass particles as a non-plastic particle control. Second, it added genome-resolved metagenomics to move beyond community composition and examine bacterial population dynamics, metagenome-assembled genomes, and putative genes associated with plastic-processing pathways. In this way, Chapter 3 tested whether the limited community-level responses observed in Chapter 2 were specific to polystyrene or reflected a broader response to bacteria-sized particles, while also asking whether polymer-specific effects could be detected at finer genomic and functional levels.

In Chapter 3, microbial abundance and community composition again changed strongly over time. HNF abundance increased initially and later declined in the plastic treatments, while bacterial abundance showed variable but not clearly treatment-specific dynamics. Both bacterial and eukaryotic community composition were shaped mainly by incubation time rather than particle type. Eukaryotic communities showed temporal restructuring, including an increase in Stramenopiles and bacterivorous genera such as Paraphysomonas and Spumella. Bacterial communities were dominated by Pseudomonadota, Bacteroidota, and Actinobacteriota with temporal shifts among dominant families but no strong polymer-specific separation.

Genome-resolved analyses added a finer layer of interpretation. A total of 118 medium to high quality metagenome-assembled genomes were recovered, many of which could not be assigned to described species, highlighting the unexplored microbial diversity in Baltic coastal waters. Most abundant MAGs did not show strong treatment-specific enrichment. However, three low-abundance MAGs affiliated with Spirosomaceae and Shewanellaceae were enriched in the polyethylene treatment and contained homologs of genes associated with processing synthetic polymers or related compounds. Across all MAGs, putative genes linked to polyethylene and polystyrene processing were detected, but their abundance patterns were influenced more by time

than by polymer treatment. These results suggest that short-term exposure to bacteria-sized PE and PS particles did not cause broad community-level disruption, but PE may selectively favour a narrow subset of bacteria with potential polymer-associated metabolic traits.

Overall, this thesis demonstrates that the ecological effects of bacteria-sized microplastics on pelagic microbial food webs are subtle, size-dependent, and strongly mediated by physical interactions and natural microbial succession. By first establishing a robust methodological basis for detecting the smallest microplastic particles, this work subsequently reveals that bacteria-sized polystyrene and inert particles can suppress heterotrophic nanoflagellate (HNF) growth through physical particle effects. Expanding upon this framework through a comparison of polystyrene and polyethylene, the research utilizes metagenomics to detect finer bacterial and functional responses. Together, these findings show that while short-term exposure to bacteria-sized microplastics may not drastically restructure entire microbial communities, it significantly affects key microbial grazers and reveals narrow, polymer-associated responses among specific bacterial populations. Ultimately, this thesis contributes to a more mechanistic understanding of how small microplastics influence microbial food-web structure, grazing interactions, and carbon flow at the base of marine ecosystems.

References

Azam, F., Fenchel, T., Field, J. G., Gray, J. S., Meyer-Reil, L. A., and Thingstad, F. (1983). The ecological role of water-column microbes in the sea. Marine Ecology Progress Series, 10, 257-263.

Barrows, A. P. W., Neumann, C. A., Berger, M. L., and Shaw, S. D. (2017). Grab vs. neuston tow net: a microplastic sampling performance comparison and possible advances in the field. Analytical Methods, 9, 1446-1453.

Boenigk, J., Matz, C., Jurgens, K., and Arndt, H. (2001). Confusing selective feeding with differential digestion in bacterivorous nanoflagellates. Journal of Eukaryotic Microbiology, 48, 425-432.

Carpenter, E. J., and Smith, K. L. (1972). Plastics on the Sargasso Sea surface. Science, 175, 1240-1241.

Cornwall, The plastic eaters. Science 373, 36-39 (2021).

Cozar, A.; Marti, E.; Duarte, C.M.; Garcia-de-Lomas, J.; van Sebille, E.; Ballatore, T.J.; Eguiluz, V.M.; Gonzalez-Gordillo, J.I.; Pedrotti, M.L.; Echevarria, F.; et al. The Arctic Ocean as a dead end for floating plastics in the North Atlantic branch of the Thermohaline Circulation. Sci. Adv. 2017, 3.

Dawson AL, Kawaguchi S, King CK, Townsend KA, King R, Huston WM, Bengtson Nash SM. Turning microplastics into nanoplastics through digestive fragmentation by Antarctic krill. Nat Commun. 2018 Mar 8;9(1):1001. doi: 10.1038/s41467-018-03465-9. PMID: 29520086; PMCID: PMC5843626.

Di Mauro, R., Kupchik, M. J., and Benfield, M. C. (2017). Abundant plankton-sized microplastic particles in shelf waters of the northern Gulf of Mexico. Environmental Pollution, 230, 798-809.

Eerkes-Medrano, D., Thompson, R. C., and Aldridge, D. C. (2015). Microplastics in freshwater systems: a review of the emerging threats, identification of knowledge gaps and prioritisation of research needs. Water Research, 75, 63-82.

Eriksen, M.; Mason, S.; Wilson, S.; Box, C.; Zellers, A.; Edwards, W.; Farley, H.; Amato, S. Microplastic pollution in the surface waters of the Laurentian Great Lakes. Mar. Pollut. Bull. 2013, 77, 177–182.

Erni-Cassola, G., Gibson, M. I., Thompson, R. C., and Christie-Oleza, J. A. (2017). Lost, but found with Nile Red: a novel method for detecting and quantifying small microplastics. Environmental Science & Technology, 51, 13641-13648.

Fouilland, E., and Mostajir, B. (2010). Revisited phytoplanktonic carbon dependency of heterotrophic bacteria in freshwaters, transitional, coastal and oceanic waters. FEMS Microbiology Ecology, 73, 419-429.

Frias, J. P. G. L., and Nash, R. (2019). Microplastics: finding a consensus on the definition. Marine Pollution Bulletin, 138, 145-147.

Fulfer, V. M., and Menden-Deuer, S. (2021). Heterotrophic dinoflagellate growth and grazing rates reduced by microplastic ingestion. Frontiers in Marine Science, 8, 716349.

Galgani, L., Engel, A., Rossi, C., Donati, A., and Loiselle, S. A. (2018). Polystyrene microplastics increase microbial release of marine chromophoric dissolved organic matter in microcosm experiments. Scientific Reports, 8, 14635.

Geng, X., Wang, J., Zhang, Y., and Jiang, Y. (2021). How do microplastics affect the marine microbial loop? Predation of microplastics by microzooplankton. Science of the Total Environment, 758, 144030.

Gewert, B., Ogonowski, M., Barth, A., and MacLeod, M. (2017). Abundance and composition of near surface microplastics and plastic debris in the Stockholm Archipelago, Baltic Sea. Marine Pollution Bulletin, 120, 292-302.

Geyer, R., Jambeck, J. R., and Law, K. L. (2017). Production, use, and fate of all plastics ever made. Science Advances, 3, e1700782.

Graca, B., Szewc, K., Zakrzewska, D., Dolega, A., and Szczerbowska-Boruchowska, M. (2017). Sources and fate of microplastics in marine and beach sediments of the Southern Baltic Sea: a preliminary study. Environmental Science and Pollution Research International, 24, 7650-7661.

Hartmann, N. B., Huffer, T., Thompson, R. C., Hassellov, M., Verschoor, A., Daugaard, A. E., et al. (2019). Are we speaking the same language? Recommendations for a definition and categorization framework for plastic debris. Environmental Science & Technology, 53, 1039-1047.

Ivankovi?, M., Ptacnik, R., and Bengtsson, M. M. (2023). Top-down structuring of freshwater bacterial communities by mixotrophic flagellates. ISME Communications, 3, 93.

Jambeck, J. R., Geyer, R., Wilcox, C., Siegler, T. R., Perryman, M., Andrady, A., et al. (2015). Plastic waste inputs from land into the ocean. Science, 347, 768-771.

Kaile, N., Lindivat, M., Elio, J., Thuestad, G., Crowley, Q. G., and Hoell, I. A. (2020). Preliminary results from detection of microplastics in liquid samples using flow cytometry. Frontiers in Marine Science, 7, 552688.

Khoaele, K. K., Gbadeyan, O. J., Chunilall, V., & Sithole, B. (2023). The Devastation of Waste Plastic on the Environment and Remediation Processes: A Critical Review. Sustainability, 15(6), 5233. https://doi.org/10.3390/su15065233

Kirstein, I. V., Kirmizi, S., Wichels, A., Garin-Fernandez, A., Erler, R., Loder, M., and Gerdts, G. (2016). Dangerous hitchhikers? Evidence for potentially pathogenic Vibrio spp. on microplastic particles. Marine Environmental Research, 120, 1-8.

Kukulka, T., Proskurowski, G., Moret-Ferguson, S., Meyer, D. W., and Law, K. L. (2012). The effect of wind mixing on the vertical distribution of buoyant plastic debris. Geophysical Research Letters, 39, L07601.

Law, K.L.; Thompson, R.C. Microplastics in the seas. Oceans 2014, 345, 144–145.

Lebreton, L., Slat, B., Ferrari, F., Sainte-Rose, B., Aitken, J., Marthouse, R., et al. (2018). Evidence that the Great Pacific Garbage Patch is rapidly accumulating plastic. Scientific Reports, 8, 4666.

Lindeque, P. K., Cole, M., Coppock, R. L., Lewis, C. N., Miller, R. Z., Watts, A. J. R., et al. (2020). Are we underestimating microplastic abundance in the marine environment? Environmental Pollution, 265, 114721.

Lora, U., Schenone, L., Forn, I., Peters, F., Piiparinen, J., Kaartokallio, H., et al. (2024). Weak effects of conventional and biodegradable microplastics on marine microbial communities. Frontiers in Marine Science, 11, 1502825.

MacLeod M, Arp HPH, Tekman MB, Jahnke A. The global threat from plastic pollution. Science. 2021 Jul 2;373(6550):61-65. doi: 10.1126/science.abg5433. PMID: 34210878.

Maes, T., Jessop, R., Wellner, N., Haupt, K., and Mayes, A. G. (2017). A rapid-screening approach to detect and quantify microplastics based on fluorescent tagging with Nile Red. Scientific Reports, 7, 44501.

Meyers, N., Catarino, A. I., Declercq, A. M., Brenan, A., Devriese, L., Vandegehuchte, M., et al. (2022). Microplastic detection and identification by Nile Red staining: towards a semi-automated, cost- and time-effective technique. Science of the Total Environment, 823, 153441.

Mishra, A., et al. (2022). Spatiotemporal variability of microplastics in surface waters of the eastern Baltic Sea. Frontiers in Marine Science, 9, 875984.

Monger, B. C., and Landry, M. R. (1990). Direct-interception feeding by marine zooflagellates: the importance of surface and hydrodynamic forces. Marine Ecology Progress Series, 65, 123-140.

Montoya, D., Rastelli, E., Casotti, R., Manna, V., Trano, A. C., Balestra, C., Santinelli, C., Saggiomo, M., Sansone, C., Corinaldesi, C., Montoya, J. M., and Brunet, C. (2024). Microplastics alter the functioning of marine microbial ecosystems. Ecology and Evolution, 14, e70041. https://doi.org/10.1002/ece3.70041

Nalecz-Jawecki, G., Chojnacka, J., Wawryniuk, M., and Drobniewska, A. (2021). Influence of nano- and small microplastics on ciliated protozoan Spirostomum ambiguum. Water, 13, 2857.

Oberbeckmann, S., Osborn, A. M., and Duhaime, M. B. (2016). Microbes on a bottle: substrate, season and geography influence community composition of microbes colonizing marine plastic debris. PLOS ONE, 11, e0159289.

Obiol, A., L?pez-Escard?, D., Salomaki, E. D., Wi?niewska, M. M., Forn, I., S?, E., Vaqu?, D., Kol?sko, M., and Massana, R. (2023). Gene expression dynamics of natural assemblages of heterotrophic flagellates during bacterivory. Microbiome, 11, 134.

Piwosz, K., Ameryk, A., Wdowka, K., Mordec, M., Uroosa, Chuvakova, A., Khan, S., and Lacaran, J. V. (2025). Vertical distribution of heterotrophic nanoflagellates in the Baltic Proper. Oceanologia, 67, 67101.

Piwosz, K., and Pernthaler, J. (2010). Seasonal population dynamics and trophic role of planktonic nanoflagellates in coastal surface waters of the Southern Baltic Sea. Environmental Microbiology, 12, 364-377.

PlasticsEurope. (2025). Plastics the Fast Facts 2025: Global and European plastics production and economic indicators. PlasticsEurope AISBL.

Prata, J. C., Reis, V., Matos, J. T. V., da Costa, J. P., Duarte, A. C., and Rocha-Santos, T. (2019). A new approach for routine quantification of microplastics using Nile Red and automated software (MP-VAT). Science of the Total Environment, 690, 1277-1283.

Reddy, M.S.; Basha, S.; Adimurthy, S.; Ramachandraiah, G. Description of the small plastics fragments in marine sediments along the Alang-Sosiya ship-breaking yard, India. Estuar. Coast. Shelf Sci. 2006, 68, 656–660.

Reisser, J., Slat, B., Noble, K., du Plessis, K., Epp, M., Proietti, M., et al. (2015). The vertical distribution of buoyant plastics at sea: an observational study in the North Atlantic Gyre. Biogeosciences, 12, 1249-1256.

Rodr?guez-Mart?nez, R., Vaqu?, D., Forn, I., and Massana, R. (2022). Dominant marine heterotrophic flagellates are adapted to natural planktonic bacterial abundances. Environmental Microbiology, 24, 2421-2434.

Romera-Castillo, C., Pinto, M., Langer, T. M., Alvarez-Salgado, X. A., and Herndl, G. J. (2018). Dissolved organic carbon leaching from plastics stimulates microbial activity in the ocean. Nature Communications, 9, 1430.

Salehi, M., Pincus, L. N., Deng, B., and Peters, C. A. (2024). Microplastics: From intrinsic properties to environmental fate. Environmental Engineering Science, 41, 719-739.

Shim, W. J., Song, Y. K., Hong, S. H., and Jang, M. (2016). Identification and quantification of microplastics using Nile Red staining. Marine Pollution Bulletin, 113, 469-476.

Simek, K., Kasalicky, V., Jezbera, J., Hornak, K., Nedoma, J., Hahn, M. W., et al. (2013). Differential freshwater flagellate community response to bacterial food quality with a focus on Limnohabitans bacteria. ISME Journal, 7, 1519-1530.

Sun, X., Chen, B., Li, Q., Liu, N., Xia, B., Zhu, L., and Qu, K. (2018). Toxicities of polystyrene nano- and microplastics toward marine bacterium Halomonas alkaliphila. Science of the Total Environment, 642, 1378-1385.

ten Hietbrink, S., Materic, D., Holzinger, R., Groeskamp, S., and Niemann, H. (2025). Nanoplastic concentrations across the North Atlantic. Nature, 643, 412-416.

Tranvik, L. J., Porter, K. G., and Sieburth, J. M. (1989). Occurrence of bacterivory in Cryptomonas, a common freshwater phytoplankter. Oecologia, 78, 473-476.

Uroosa, and Piwosz, K. (2026). Systematic optimization of Nile Red staining parameters for the reliable detection of microplastics <= 2 micrometres. Frontiers in Marine Science, 13, 1818345.

Uurasjärvi, E., Pääkkönen, M., Setälä, O., Koistinen, A., and Lehtiniemi, M. (2020). Microplastics accumulate to thin layers in the stratified Baltic Sea. Environmental Pollution, 268, 115700. https://doi.org/10.1016/j.envpol.2020.115700

Wu, Y., Guo, P., Zhang, X., Zhang, Y., Xie, S., and Deng, J. (2019). Effect of microplastics exposure on the photosynthesis system of freshwater algae. Journal of Hazardous Materials, 374, 219-227.

Yang, H., Chen, G., & Wang, J. (2021). Microplastics in the Marine Environment: Sources, Fates, Impacts and Microbial Degradation. Toxics, 9(2), 41. https://doi.org/10.3390/toxics9020041

Ye, G., Zhang, X., Yan, C., Lin, Y., and Huang, Q. (2021). Polystyrene microplastics induce microbial dysbiosis and dysfunction in surrounding seawater. Environment International, 156, 106724.

Zettler, E. R., Mincer, T. J., and Amaral-Zettler, L. A. (2013). Life in the plastisphere: microbial communities on plastic marine debris. Environmental Science & Technology, 47, 7137-7146.

Zhang, C., Chen, X., Wang, J., and Tan, L. (2017). Toxic effects of microplastic on marine microalgae Skeletonema costatum: interactions between microplastic and algae. Environmental Pollution, 220, 1282-1288.

List of Papers and Authors' Contributions

1. **Uroosa** and Piwosz K (2026). Systematic optimization of Nile Red staining parameters for the reliable detection of microplastics ≤ 2 µm. *Front. Mar. Sci. 13:1818345. doi: 10.3389/fmars.2026.1818345.* U: Conceptualization, Data curation, Formal Analysis, Investigation, Validation, Visualization, Writing original draft. **Estimated percentage contribution: 90%.**
2. **Uroosa**, Sohrab Khan, Marcin Białowąs, Magdalena Jakubowska-Lehrmann, Barbara Urban-Malinga, Cristian Villena Alemany, Kasia Piwosz. (Manuscript under review in Frontiers in Marine Science). U: Conceptualization, Methodology, Investigation, Formal analysis, Writing original draft and Visualization. **Estimated percentage contribution: 70%.**
3. **Uroosa**, Aleksandar Stanojković, Sohrab Khan, Marcin Białowąs, Magdalena Jakubowska-Lehrmann, Kasia Piwosz. Limited Effects of Bacteria-Sized Microplastics on Coastal Baltic Microbial Food-Web Dynamics. (in preparation). U: Conceptualization, Methodology, Investigation, Formal analysis (Amplicon, 16S 18S), Writing original draft and Visualization. **Estimated percentage contribution: 50%.**

Co-author agreement

I, Dr hab. Katarzyna Piwosz, prof. MIR-PIB, supervisor of this thesis, co-author all the three publications, fully acknowledge the contribution of Uroosa to these manuscripts.

Katarzyna Piwosz

I, Dr. Aleksandar Stanojković co-author of paper 3, fully acknowledge the contribution of Uroosa to this manuscript.

Aleksandar Stanojković

I, MSc Marcin Białowąs, co-author of paper 2 and 3, fully acknowledge the contribution of Uroosa to this manuscript.

Marcin Białowąs

I, Dr. Magdalena Jakubowska-Lehrmann co-author of paper 2 and 3, fully acknowledge the contribution of Uroosa to this manuscript.

Magdalena Jakubowska-Lehrmann

I, Dr. Sohrab Khan co-author of papers 2 and 3, fully acknowledge the contribution of Uroosa to this manuscript.

Sohrab Khan

I, Dr hab. Barbara Urban-Malinga, prof. MIR-PIB co-author of paper 2, fully acknowledge the contribution of Uroosa to this manuscript.

Barbara Urban-Malinga

I, Dr. Cristian Villena Alemany co-author of paper 2, fully acknowledge the contribution of Uroosa to this manuscript.

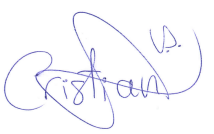

Cristian Villena Alemany